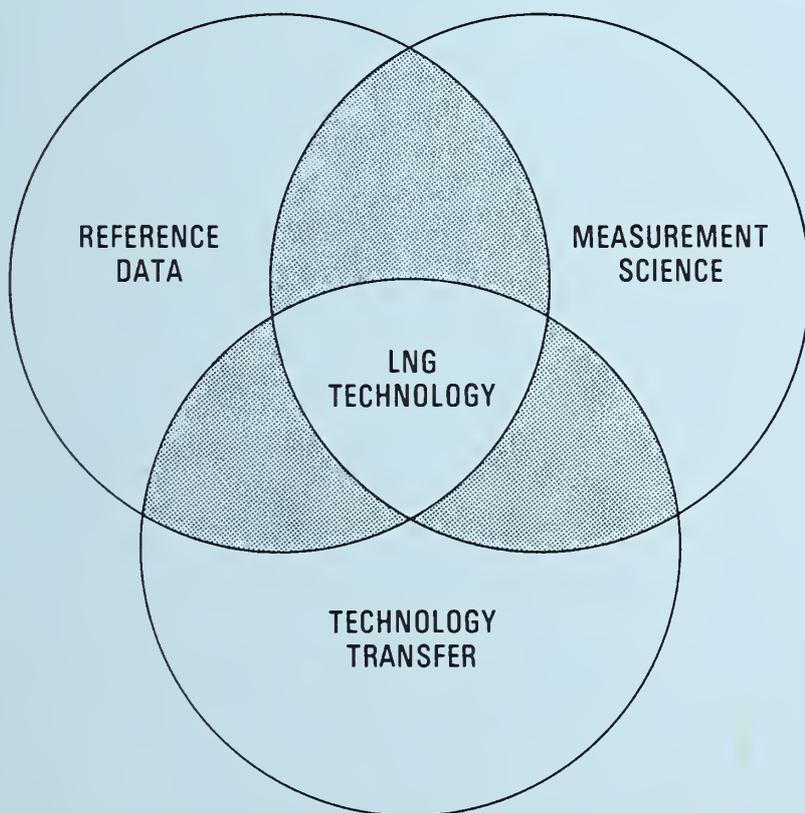NBSIR 78 - 894

U-257-10

LIQUEFIED NATURAL GAS RESEARCH

at the

NATIONAL BUREAU OF STANDARDS

PROGRESS REPORT FOR THE PERIOD
1 January - 30 June 1978

D.E. Diller, Editor

THERMOPHYSICAL PROPERTIES DIVISION, NATIONAL ENGINEERING LABORATORY,
NATIONAL BUREAU OF STANDARDS, BOULDER, COLORADO

NBSIR 78 - 894

LIQUEFIED NATURAL GAS RESEARCH
at the
NATIONAL BUREAU OF STANDARDS

D.E. Diller, Editor

Thermophysical Properties Division
National Engineering Laboratory
National Bureau of Standards
Boulder, Colorado 80303

Progress Report for the Period
1 January - 30 June 1978

ABSTRACT

Thirty-one cost centers, supported by six other agency sponsors in addition to NBS, provide the basis for liquefied natural gas (LNG) research at NBS. During this six-month reporting period the level of effort was over 20 man-years/year with funding expenditures of over $500,000. This integrated progress report, to be issued in January and July, is designed to:

1) provide all sponsoring agencies with a semiannual report on the activities of their individual programs;

2) inform all sponsoring agencies on related research being conducted at the Thermophysical Properties Division;

3) provide a uniform reporting procedure which should maintain and improve communication while minimizing the time, effort and paperwork at the cost center level.

The contents of this report will augment the quarterly progress meetings of some sponsors, but will not necessarily replace such meetings. Distribution of this document is limited and intended primarily for the supporting agencies. Data or other information must be considered preliminary, subject to change and unpublished, and therefore not for citation in the open literature.

Key words: Cryogenics; liquefied natural gas; measurement; methane; properties; research.

CONTENTS

CONTENTS (Continued)

1. <u>Title</u>. THERMOPHYSICAL PROPERTIES DATA FOR PURE COMPONENTS AND MIXTURES OF LNG COMPONENTS

   <u>Principal Investigators</u>. R. D. Goodwin, H. M. Roder, G. C. Straty, W. M. Haynes, R. D. McCarty, and D. E. Diller

2. <u>Cost Center Number</u>. 7360574, 7360548

3. <u>Sponsor Project Identification</u>. Gas Research Institute Grant No. 5010-362-0019 and American Gas Association, Inc., Project BR-50-10. National Aeronautics and Space Administration, Lewis Research Center, Purchase Order C-78014-C.

4. <u>Introduction</u>. Accurate phase equilibrium, equation of state (PVT), and thermodynamic properties data are needed to design and optimize gas separation and liquefaction processes and equipment, and for mass and heat transfer calculations. Accurate data for the pure components and selected mixtures of hydrocarbon systems will permit developing comprehensive accurate predictive calculation methods which take into account the dependence of the thermophysical properties of mixtures on the composition, temperature, and density.

   This project will provide comprehensive accurate thermophysical properties data and predictive calculation methods for compressed and liquefied hydrocarbon gases and their mixtures to support the development of LNG technology at NBS and throughout the fuel gas industry. It will also serve as the base for a comprehensive mixtures prediction methodology.

5. <u>Objectives or Goals</u>. The objectives of our work are the determination of comprehensive accurate thermophysical properties data and predictive calculation methods for the major pure components (methane, ethane, propane, butanes, and nitrogen) and selected mixtures of liquefied natural gas and hydrocarbon mixtures at temperatures between 80 K and 320 K and at pressures up to 35 MPa (5000 psi). Our goal is to provide a range and quality of data that will be recognized as definitive or standard for all foreseeable low temperature engineering calculations.

6. <u>Background</u>. Liquefied natural gas is expected to supply an increasing percentage of the United States' future energy requirements. It is likely that massive quantities of liquefied natural gas will be imported during the years 1978 - 1990. Ships and importation terminals are being built for transporting, storing, and vaporizing liquefied natural gas for distribution. Accurate physical and thermodynamic properties data for compressed and liquefied natural gas and hydrocarbon mixtures are needed to support these projects. For example, accurate compressibility and thermodynamic properties data are needed to design and optimize liquefaction and transport processes; accurate data for the heating value, which for liquefied natural gas mixtures depends on the total volume, the density, and the composition, are needed to provide a basis for equitable custody transfer. Accurate mixture data prediction methods are needed for use in automated heat transfer calculations.

   Accurate thermodynamic properties data for liquefied gas mixtures must be based on precise compressibility and calorimetric measurements; compressibility data give the dependence of thermodynamic properties on pressure and density (at fixed temperatures); calorimetric data give the dependence of thermodynamic properties on temperature (at fixed pressures and densities). It is impossible, however, to perform enough compressibility and calorimetric measurements directly on multicomponent mixtures to permit accurate interpolation of the data to arbitrary compositions, temperatures and pressures. Instead, thermodynamic properties data for multicomponent mixtures must usually be predicted (extrapolated) from a limited number of measurements on the

pure components and their binary mixtures. This project was initiated to provide the natural gas and aerospace industries with comprehensive accurate data for pure compressed and liquefied methane, the most abundant component in LNG mixtures. We have published National Bureau of Standards Technical Note 653, "Thermophysical Properties of Methane, From 90 to 500 K at Pressures to 700 Bar," by Robert D. Goodwin (April 1974), and National Bureau of Standards Technical Note 684, "Thermophysical Properties of Ethane, From 90 to 600 K at Pressures to 700 Bar," by Robert D. Goodwin, H. M. Roder, and G. C. Straty (August 1976). These reports contain the most comprehensive and accurate tables available for the thermophysical properties of pure gaseous and liquid methane and ethane, and provide an accurate basis for calculating thermophysical properties data for LNG and other hydrocarbon mixtures.

7. Program and Results.

7.1 Propane, PVTx and Dielectric Constant Measurements -- W. M. Haynes

The apparatus for PVT and dielectric constant measurements on propane is now being used for measurements on liquid mixtures of LNG components. The mixtures that have been investigated so far are listed in the report for cost center number 7361574.

To put the apparatus into working order for propane after the mixture measurements are completed, the following tasks need to be performed:

(a) check out the dead weight gauge measurement system,

(b) test the cell to pressures of 35 MPa; this was done before the LNG density program, but has not been checked since the cell has experienced many temperature cycles between 100 and 300 K, and

(c) write computer programs for reduction of the propane data.

The LNG density measurements should be completed within the next two months.

7.2 Calculational Methods -- R. D. McCarty

The developmental work on the extended corresponding states method is continuing. The mapping of the equation of state of one fluid into the equation of state of another, as has been described in previous reports, is continuing. The application of this technique to the prediction of the properties of a mixture has been accomplished in the case of methane-nitrogen mixtures. Initial comparisons between experimental and calculated densities show only minor improvement when the shape factors are obtained by the mapping technique indicating a need to obtain new binary interaction parameters using the new experimental data. This will be accomplished in the near future.

7.3 Propane, Specific Heat Data -- R. D. Goodwin

Experimental specific heats for saturated liquid propane, along the coexistence path, have been determined from the triple-point temperature ($\sim$ 85 K) to 289 K. Specific heats for the compressed liquid at constant molal volume have been determined along isochores at nine different densities ranging from near the triple-point liquid density to about twice the critical-point density (at pressures up to 300 bar). Comparisons with previous experimental- and/or derived-data show agreement within combined uncertainties of about three percent.

The manuscript, "Specific Heats of Saturated and Compressed Liquid Propane," by R. D. Goodwin, has been accepted for publication in the Journal of Research of the National Bureau of Standards, Vol. 83 (5) (Sep-Oct 1978).

7.4 Butane, Preliminary Thermophysical Properties Data -- R. D. Goodwin

The objective is to prepare provisional tables of thermodynamic properties of normal butane, using available physical properties data. In this work we expect to discover those areas of properties data most in need of further experimental measurements.

A "Bibliography of References" on n-butane was prepared June 1, 1977, by the Cryogenic Data Center. Work on the formulation of physical properties, needed for thermal computations, is well under way.

In general, there is an abundance of quite inconsistent data from different laboratories, requiring tedious weightings, selections, and eliminations. There are few data for liquid butanes at LNG temperatures.

Apparently satisfactory formulations have been developed for the virial equation, the saturated liquid densities, specific heats for the saturated liquid below the boiling point, and for the ideal gas thermodynamic functions.

By thermal loops, in a procedure first developed by W. T. Ziegler, we have derived new "data" (where none existed) from the triple- to the boiling-point for vapor pressures, densities of the saturated vapor, and for heats of vaporization. The vapor-pressure equation has been adjusted to include these new data, and a provisional description has been developed for the heats of vaporization up to the critical point.

At this writing, a special difficulty is found with the mass of irregular data for densities of the saturated vapor, in developing a formulation consistent with required behavior, and with that for other substances.

7.5 Pure Nitrogen and Nitrogen-Methane PVTx Property Measurements -- G. C. Straty and D. E. Diller

Gas expansion PVT measurements on pure compressed and liquefied nitrogen have been completed. About 300 measurements were made at 21 densities in the range 11.2 - 28.4 mol/L, 80 - 270 K, 1 - 350 bars. These measurements were made to provide more accurate pure component data for an accurate mathematical model of the PVT properties of nitrogen-methane mixtures.

Twelve isochoric gas-expansion PVT runs have been made on a gravimetrically prepared 50.115 mole % nitrogen-49.885 mole% methane mixture in the T, P, ρ range 82 - 320 K, 2 - 350 bar, 11 - 28.6 mol/L. The measurements are being compared with the extended corresponding states model (R. D. McCarty, NBSIR 77-867 (Oct 1977)), which was previously optimized to saturated liquid density measurements on this mixture at temperatures below 140 K. Differences between calculated and measured densities range from several tenths percent at low temperatures and high densities to several percent near the critical temperature ($\sim$ 161 K) and critical density ($\sim$ 10.5 mol/L). About eight more measurement runs are planned.

8. Problem Areas. None.

9. Funding. January 1 - June 30, 1978.

Man-years expended	0.8
Equipment and/or Services Purchased	3.2K$
Total Reporting Period Cost	69.2K$
Balance Remaining	174.9K$

10. Future Plans.

Objectives and Schedule: Quarter   3   4

Measure, analyze and report PVT and
   dielectric constant data for
   hydrocarbon mixtures and LNG.   ——————————————————⟶

Evaluate and optimize promising
   calculation methods for the
   thermodynamic properties of
   methane-nitrogen mixtures.   ——————————————————⟶

Measure, analyze and report PVT and
   dielectric constant data for propane.   ————

Analyze available thermodynamic data
   for the butanes and develop an
   accurate equation of state.   ——————————————————

4

1. <u>Title</u>. FLUID TRANSPORT PROPERTIES
    <u>Principal Investigator</u>. Howard J. M. Hanley

2. <u>Cost Center Number</u>. 7360124

3. <u>Sponsor Project Identification</u>. NBS-Office of Standard Reference Data

4. <u>Introduction</u>. Methods for predicting the transport properties of fluid mixtures are unreliable and data are scarce. Prediction methods are needed, however, to supply the necessary design data needed to increase efficiency and reduce costs.

5. <u>Objectives or Goals</u>. The long range or continuing goal of the program is to perform a systematic study of the theories and experimental measurements relating to transport properties, specifically the viscosity and thermal conductivity coefficients, of simple mixtures over a wide range of experimental conditions. The specific objectives of the program include: 1) the systematic correlation of the transport properties of simple binary mixtures and the development of prediction techniques, 2) development of a mixture theory for the dilute gas region and the dense gas and liquid regions, 3) extension of the theory and prediction techniques to multicomponent systems, and 4) suggested guidelines for future areas of experimental work.

6. <u>Background</u>. A continuing program has successfully expanded the state-of-the-art of transport phenomena for pure fluids. Information for pure fluids is required as a prerequisite for mixture studies. The theory of transport phenomena has been developed and applied to produce practical numerical tables of the viscosity, thermal conductivity and diffusion coefficients of simple fluids: Ar, Kr, Xe, N_2, O_2, F_2, He, H_2, CH_4,[3] C_2H_6.[4]
    It has been shown that a successful mixture program can emerge from combining the results for pure fluids with mixture equation of state studies. The equation of state work is being carried out by other investigators in this laboratory.

7. <u>Program and Results</u>. A procedure to predict the transport properties of mixtures has been developed via corresponding states.[1-2] The method has been shown to be satisfactory. Current studies include the behavior of the transport coefficients near a critical point of a binary mixture.[2] Tables of transport properties for propane are in press.[5] A compilation of the transport properties of ethylene has been initiated. Theoretical studies on the properties of a $1/r^n$ fluid are in progress.[6]

8. <u>Problem Areas</u>. The lack of suitable experimental mixture transport properties data for comparison purposes is the main problem. Also equation of state (PVT) data for mixtures are needed.

9. <u>Funding</u>. January 1 - June 30, 1978.

Allocation	63.0K$/yr.	
Labor	0.5 MY	30.2K$
Other Costs		3.0K$
Total		33.2K$

10. <u>Future Plans</u>. The corresponding states predictive procedure for mixtures will be more fully developed and expanded in line with the concurrent equation of state studies. We intend to investigate, in particular, the behavior of the transport properties at gas/liquid and liquid/liquid equilibria.

References

1. H. J. M. Hanley, Prediction of the Viscosity and Thermal Conductivity
    Coefficients of Mixtures, Cryogenics, Vol 16, No. 11, 643-51 (Nov 1976);
    H. J. M. Hanley, Prediction of the Thermal Conductivity of Fluid
    Mixtures, Proceedings 7th ASME Conf. on Thermophysical properties;
    H. J. M. Hanley in "Phase Equilibria and Fluid Properties in the
    Chemical Industry," ACS Symp. Series No. 60 (1977).

2. H. J. M. Hanley, Transport Coefficients in the One-Fluid Approximation:
    Behavior in the Critical Region, J. Res. Nat. Bur. Stand. (U.S.) 82,
    18 (1977).

3. H. J. M. Hanley, W. M. Haynes and R. D. McCarty, The Viscosity and
    Thermal Conductivity Coefficients for Dense Gaseous and Liquid Methane,
    J. Phys. Chem. Ref. Data, Vol 6, No. 2, 597-609 (1977).

4. H. J. M. Hanley, K. E. Gubbins and S. Murad, A Correlation of the
    Existing Viscosity and Thermal Conductivity Coefficients of Gaseous and
    Liquid Ethane, J. Phys. Chem. Ref. Data, Vol 6, No. 4, 1167 (1977).

5. H. J. M. Hanley, P. M. Holland, K. E. Gubbins and J. M. Haile, J. Phys.
    Chem. Ref. Data (in press).

6. J. C. Rainwater and H. J. M. Hanley, Chem. Phys. Letts. (in press).

1. <u>Title</u>.   PROPERTIES OF CRYOGENIC FLUIDS
   <u>Principal Investigators</u>.   G. C. Straty, H. M. Roder, L. A. Weber, B. J. Ackerson, and D. E. Diller

2. <u>Cost Center Number</u>.   7360122

3. <u>Sponsor Project Identification</u>.   NBS

4. <u>Introduction</u>.   Accurate thermophysical properties data and predictive calculation methods for cryogenic fluids are needed to support advanced cryogenic technology projects. For example, liquefied natural gas is expected to supply an increasing percentage of the United States' energy requirements through 1990. Liquefaction plants, ships and receiving terminals are being constructed to transport and store natural gas in the liquid state (LNG). Accurate thermophysical properties data for LNG are needed to design low temperature processes and equipment. Accurate data will benefit the energy industries and the consumer by providing for safe and efficient operations and reduced costs. As a logical extension of properties data on LNG, are the data needs for a number of higher temperature industrial fluids such as synthetic natural gas (SNG). SNG mixtures can be characterized as much more complex than natural gas, containing unlike (including highly polar) molecules. Interactions between unlike molecules are not well understood and the accurate data necessary to quantitatively understand the interactions are lacking. The needs for accurate predictive methods for SNG are essentially the same as LNG, i.e., to reduce capital and operating costs and improve energy efficiency.

5. <u>Objectives or Goals</u>.   The objectives of this project are to provide comprehensive accurate thermodynamic, electromagnetic and transport properties data and calculation methods for technically important compressed and liquefied gases (helium, hydrogen, oxygen, nitrogen, methane, ethane, etc.) at low temperatures. In addition we intend to develop the capability to perform accurate PVT measurements on gaseous mixtures and pure components at high pressures and above room temperature. Precise compressibility, calorimetric and other physical property measurements will be performed to fill gaps and reconcile inconsistencies. Definitive interpolation functions, computer programs and tables will be prepared for engineering calculations. The immediate goals of this work are to obtain accurate sound velocity and thermal diffusivity data for compressed and liquefied gases by using laser light scattering spectroscopy techniques; design, construct and performance test a precision PVT apparatus for the region 250 - 900 K with pressures to 35 MPa; and design, construct and performance test a transient hot-wire thermal conductivity apparatus for the region 70 - 350 K with pressures to 80 MPa.

6. <u>Background</u>.   The application of laser light scattering techniques to obtaining thermophysical properties data was initiated to complement and check other measurement methods and to solve measurement problems inherent in more conventional methods. For example, laser light scattering techniques permit measurements of sound velocities for fluids under conditions for which sound absorption is too large to perform ultrasonic measurements; laser light scattering techniques permit measurements of thermal diffusivities under conditions for which convection interferes with measurements of thermal conduction. The feasibility of light scattering experiments to obtain data on binary diffusion coefficients has also been demonstrated.

   Light scattering allows thermal diffusivity measurements in the region where density fluctuations are relatively large, but accuracy drops significantly as you pass outside the extended critical region. To complement the scattering method, thermal conductivity measurements can

7

be made with more conventional techniques such as a hot-wire technique. In the latter method a very small platinum wire is surrounded by the fluid and a voltage pulse is applied to the wire. The temperature of the wire is momentarily raised and the resistance increases. A series of very closely spaced resistance measurements would describe the return of the wire to equilibrium. These resistance vs. time measurements can be related to the rate of heat dissipation in the surrounding fluid and thus the thermal conductivity (provided convection heat transfer is prevented).

The development of accurate mathematical models (equation of state) for fluid mixtures requires accurate PVT data for the pure constituents and binary mixtures of key molecular pairs. Experience with LNG has identified the type and accuracy of the data required. In addition to that, work on SNG at high temperatures is a logical follow-on to the low temperature work on LNG. Typical constituents of raw SNG from coal via the Lurgi process are: water - 50.2%; hydrogen - 20.1%; carbon dioxide - 14.7%; carbon monoxide - 9.2%; methane - 4.7%; ethane - 0.5%; hydrogen sulfide and others - 0.6%.

An apparatus has been assembled for laser light scattering spectroscopy measurements on compressed and liquefied gases (76-300 K, 35 MPa). The apparatus consists of a high pressure optical cell, a cryostat refrigerated by means of liquid nitrogen, an argon ion laser and low-level light detection equipment.

The light scattered from fluctuations in the fluid can be analyzed with either digital autocorrelation techniques for the examination of the very narrow lines associated with scattering from temperature fluctuations (Rayleigh scattering) or with a scanned Fabry Perot interferometer for the measurement of the Doppler frequency shifts associated with the scattering from propagating density (pressure) fluctuations (Brillouin scattering).

Apparatus for photon-counting and digital autocorrelation has been assembled, interfaced with computer facilities and programmed to enable on-line data accumulation and analysis. Initial problems associated with signal modulations from excessive building vibrations have been solved by levitating the apparatus on an air suspension system. A small, highly stable capacitor has also been designed, constructed and installed inside the scattering cell to permit the dielectric constant of the scattering fluid to be determined, which should allow more accurate fluid densities to be obtained for use in the data analysis. Apparatus tests on well characterized, strongly scattering, test fluids have been made to verify data analysis programs.

Extensive thermal diffusivity data have been obtained for methane. Measurements have been made along the coexistence curve, the critical isochore, and critical isotherm. The measurements extend outside the critical region as well as deep into the critical region. In the deep critical region the effect of temperature gradients and impurities have been investigated. Outside the critical region, these effects do not affect measurements beyond experimental accuracy. The range of the measurements extends from 150 K to 230 K and 3 mol/L to 22 mol/L. The inaccuracy of the measurements is about 5% in the critical region, increasing to 10% or greater further away. A detailed analysis of the data and experimental error has been made and a paper[1] reporting the results has been submitted to the Journal of Chemical Physics.

Some preliminary results on a mixture of 70% methane and 30% ethane were obtained very near the vapor-liquid critical point (plait point). The results are interesting in that the thermal conductivity of the mixture does not exhibit a critical anomaly whereas pure methane does exhibit an anomaly in the thermal conductivity as the critical point is approached. The anomalous behavior of pure fluids and nonanomalous

8

behavior of mixtures is qualitatively and quantitatively in agreement with theoretical predictions (see preceding title 'Fluid Transport Properties'). We hope to be able to perform more definitive measurements on hydrocarbon mixtures in the near future.

7. Program and Results. The transient hot-wire apparatus is nearing completion. All parts and electronic equipment have been received. Assembly of the sample cell is nearing completion and programs for acquiring and processing the data have been written and checked out on the Nova minicomputer to be used during the measurements.

No work has started on the high temperature PVT, however an Automatic Systems Laboratory A7 automatically self-balancing thermometry bridge has been ordered as well as two precision quartz pressure transducers. The latter will be placed in the NBS-Pressure Calibration System to test long term stability.

8. Problem Areas. Light scattering has proven to be a valuable tool for obtaining thermal diffusivity data on fluids. This is particularly true in a broad temperature and density range around the critical point, where more conventional experimental methods fail or are severely limited. The intensity of the scattered light however decreases drastically as one moves away from the critical region. Data accuracy in this region becomes limited by the statistical nature of the scattering process and the ability to maintain stability and precise experimental parameters over the extended periods of time necessary for data accumulation.

At the present time no funds are available to begin constructing the new PVT apparatus. It is hoped that partial funding will become available in October, 1978.

9. Funding.   January 1 - June 30, 1978.

Man-years expended	0.2
Equipment and/or Services Purchased	30.7K$
Total Reporting Period Cost	22.0K$
Balance Remaining	18.0K$

10. Future Plans.

Objectives and Schedule: Quarter	3	4
Design, construct and performance test transient hot-wire thermal conductivity apparatus.	⟶	
Design, construct and performance test high temperature-high pressure PVT apparatus		————

Reference

1. B. J. Ackerson and G. C. Straty, Rayleigh Scattering from Methane, J. Chem. Phys. (scheduled for August 1978).

1. Title.   PROPERTIES OF CRYOGENIC FLUID MIXTURES
    Principal Investigators. M. J. Hiza, A. J. Kidnay (part-time), and
    R. C. Miller (part-time).

2. Cost Center Numbers.   7360123, 7360129 and 7364574

3. Sponsor Project Identification.   NBS, NBS (OSRD), AGA, GRI

4. Introduction.   Accurate thermodynamic properties data and prediction
    methods for mixtures of cryogenic fluids are needed to design and
    optimize low temperature processes and equipment. This project provides
    new experimental measurements on equilibrium properties and compilations
    of evaluated equilibrium properties data which are suitable for direct
    technological use or for the evaluation of prediction methods.

5. Objectives or Goals.   The overall objectives of this project are to
    provide critically evaluated data on the phase equilibria and thermo-
    dynamic properties of cryogenic fluid mixtures. The program has been
    divided into the following elements:

    a)   Preparation of a comprehensive bibliography on experimental
         measurements of equilibrium properties for mixtures of selected
         molecular species of principal interest in cryogenic technology.

    b)   Selection and/or development of methods for correlation, evaluation
         and prediction of equilibrium properties data.

    c)   Retrieval and evaluation of experimental data for specific mixture
         systems selected on the basis of theoretical and/or technological
         importance.

    d)   Preparation of guidelines for future research based on the
         deficiencies noted in (a), (b), and (c).

    e)   Performing experimental research to alleviate deficiencies and
         provide a basis for improvement of prediction methods.

6. Background. A physical equilibria of mixtures research project was
    established in the Thermophysical Properties Division in 1959. The
    initial effort, based on a bibliographic search and other considerations,
    was directed toward the acquisition of new experimental data on the
    solid-vapor and liquid-vapor equilibria and physical adsorption properties
    for a limited number of binary and ternary mixtures of components with
    widely separated critical temperatures. Most of the systems studied
    included one of the light hydrocarbon species -- methane, ethane, or
    ethylene (ethene) -- with one of the quantum gases -- helium, hydrogen,
    or neon. The data for these systems led to significant improvements in
    the predictions of physical adsorption equilibrium and a correlation
    for the prediction of deviations from the geometric mean rule for
    combining characteristic energy parameters. In addition, significant
    new information was obtained for interaction third virial coefficients
    which was used in a correlation by one of our consultants, J. M.
    Prausnitz. The approach taken in this work has been as fundamental as
    possible with the intention of having an impact on a broad range of
    mixture problems.

    Recent efforts have been directed toward problems associated with
    systems containing components with overlapping liquid temperature
    ranges, such as nitrogen + methane, methane + ethane, etc.

7. Program and Results. The recent progress is summarized as follows:

a) During this period, reviews were received from the editor of the Journal of Physical and Chemical Reference Data on the paper[1] discussing compilation, evaluation and correlation of liquid-vapor equilibria data for the methane ÷ ethane system. As a result of the comments of one of the three reviewers and one additional question we felt should be answered, a thermodynamic consistency text of each data set via the equal areas test was initiated and a revision of the Barker method program was developed to correct for vapor phase nonidealities with the Peng-Robinson equation of state for comparison with one using the virial equation of state. The results of these additional evaluations will be completed early in the next reporting period and the manuscript will be revised accordingly.

b) A compilation, evaluation, and correlation of the liquid-vapor equilibria for the methane + propane system, similar to that for methane + ethane, was initiated this period. As a result of our experience with the methane + ethane system, and the reaction of the reviewers, we expect the evaluation process to be simplified somewhat.

c) The papers discussing the excess volume model for predicting orthobaric densities of LNG mixtures and the results of the mixture molar volume measurements made at the University of Wyoming will appear in the same issue of Fluid Phase Equilibria. The complete citations are given in the references.[2,3]

8. Problem Areas. None.

9. Funding. January 1 - June 30, 1978.

Man-years expended	0.6
Equipment and/or Services Purchased	2.2K$
Total Reporting Period Cost	48.5K$
Balance Remaining	15.7K$

10. Future Plans.

Objectives and Schedule: Quarter	3	4

Complete thermodynamic consistency tests and comparison of G^E values for different equations of state for methane + ethane. Revise manuscript. ———————→

Compile, evaluate and correlate liquid-vapor equilibria data for methane + propane. ——————————————

Prepare and report graphs of K-values and equilibrium compositions for methane + propane. ————————————————→

11

References

1.　M. J. Hiza, R. C. Miller, and A. J. Kidnay, A Review, Evaluation, and Correlation of the Phase Equilibria, Heat of Mixing, and Change in Volume on Mixing for Liquid Mixtures of Methane + Ethane, J. Phys. Chem. Ref. Data (being revised for publication).

2.　M. J. Hiza, An Empirical Excess Volume Model for Estimating Liquefied Natural Gas Densities, Fluid Phase Equilibria 2, No. 1, 27-38 (1978).

3.　R. C. Miller and M. J. Hiza, Experimental Molar Volumes for Some LNG-Related Saturated Liquid Mixtures, Fluid Phase Equilibria 2, No. 1, 49-57 (1978).

1. Title. DENSITIES OF LIQUEFIED NATURAL GAS MIXTURES
    Principal Investigators. W. M. Haynes, R. D. McCarty and M. J. Hiza

2. Cost Center Numbers.   7361574

3. Sponsor Project Identification.   LNG Density Project Steering
    Committee; American Gas Association, Inc., Project BR-50-11.

4. Introduction. Accurate density measurements and calculational methods
    for liquefied natural gas mixtures are needed to provide a basis for
    custody transfer agreements and for mass, density, and heating value
    gauging throughout the fuel gas industry.

    The basis for the custody transfer of natural gas is its heating value.
    It is difficult to determine and agree on the heating value of extremely
    large volumes of natural gas in the liquid state. For example, methods
    for calculating the heating value of a liquefied natural gas mixture
    require knowing its density, which in turn depends on its composition,
    temperature, and pressure. As the compositions of LNG mixtures vary
    considerably, depending on the sources of the gas and the processing
    conditions, accurate methods are needed for calculating liquid densities
    at arbitrary compositions, temperatures and pressures. The accuracy is
    important because of the extremely large volumes of liquid involved.

5. Objectives or Goals. The objectives of this work are to perform
    accurate (0.1%) and precise (0.02%) measurements of the densities of
    saturated liquid methane, ethane, propane, butanes, nitrogen and their
    mixtures mainly in the temperature range 105 - 140 K, and to test and
    optimize mathematical models for calculating the densities of LNG
    mixtures at arbitrary compositions and temperatures.

6. Background. This project is being carried out at NBS because of the
    realization that equitable custody transfer agreements could be reached
    more readily if the density measurements and the evaluation and develop-
    ment of calculational methods were performed by independent professionals.

    An apparatus incorporating a magnetic suspension technique has been
    developed for absolute density measurements on liquids and liquid
    mixtures, particularly at saturation, for temperatures between 90 and
    300 K. The estimated imprecision of measurement is less than 0.02%
    and the estimated inaccuracy is less than 0.15%.

7. Program and Results.
    7.1 Measurements. During the past six months measurements have been
    performed on the following mixtures:

    $0.85\ CH_4 + 0.15\ C_2H_6$
    $0.93\ CH_4 + 0.07\ nC_4H_{10}$
    $0.85\ CH_4 + 0.05\ C_2H_6 + 0.05\ C_3H_8 + 0.05\ iC_4H_{10}$
    $0.920\ CH_4 + 0.080\ iC_4H_{10}$
    $0.851\ CH_4 + 0.058\ C_2H_6 + 0.048\ C_3H_8 + 0.043\ nC_4H_{10}$
    $0.859\ CH_4 + 0.115\ C_2H_6 + 0.013\ C_3H_8 + 0.005\ iC_4H_{10} + 0.007\ nC_4H_{10}$
    $0.860\ CH_4 + 0.046\ C_2H_6 + 0.048\ C_3H_8 + 0.046\ iC_4H_{10}$
    $0.006\ N_2 + 0.906\ CH_4 + 0.060\ C_2H_6 + 0.022\ C_3H_8 + 0.003\ iC_4H_{10}$
            $+ 0.003\ nC_4H_{10}$
    $0.048\ N_2 + 0.809\ CH_4 + 0.045\ C_2H_6 + 0.050\ C_3H_8 + 0.047\ iC_4H_{10}$

$0.0060 \, N_2 + 0.9007 \, CH_4 + 0.0654 \, C_2H_6 + 0.0220 \, C_3H_8 + 0.0029 \, iC_4H_{10}$
$\qquad + 0.0028 \, nC_4H_{10} + 0.0001 \, iC_5H_{12} + 0.0001 \, nC_5H_{12}$

$0.846 \, CH_4 + 0.079 \, C_2H_6 + 0.051 \, C_3H_8 + 0.025 \, nC_4H_{10}$

$0.014 \, N_2 + 0.859 \, CH_4 + 0.085 \, C_2H_6 + 0.030 \, C_3H_8 + 0.005 \, iC_4H_{10}$
$\qquad + 0.007 \, nC_4H_{10}$

$0.010 \, N_2 + 0.882 \, CH_4 + 0.073 \, C_2H_6 + 0.026 \, C_3H_8 + 0.005 \, iC_4H_{10}$
$\qquad + 0.005 \, nC_4H_{10}$

$0.846 \, CH_4 + 0.082 \, C_2H_6 + 0.048 \, C_3H_8 + 0.013 \, iC_4H_{10} + 0.013 \, nC_4H_{10}$

$0.026 \, N_2 + 0.812 \, CH_4 + 0.085 \, C_2H_6 + 0.049 \, C_3H_8 + 0.027 \, nC_4H_{10}$

$0.9279 \, CH_4 + 0.0721 \, nC_4H_{10}$

$0.783 \, CH_4 + 0.217 \, iC_4H_{10}$

Except for the methane-isobutane binary mixtures, the discrepancies between experimental densities and values predicted using the extended corresponding states method were less than 0.1%.

The next mixtures to be investigated are as follows:

$0.778 \, CH_4 + 0.222 \, nC_4H_{10}$

$0.059 \, N_2 + 0.891 \, CH_4 + 0.050 \, nC_4H_{10}$

8-component mixture containing maximum of 0.5% pentanes

No mixture containing a significant amount of pentanes has been prepared yet for several reasons. Since the mixture must be prepared in steps using several different cylinders, we had to wait until sufficient cylinders were available such that the measurement program would not be interrupted. Also, we wanted time to carefully analyze the procedures for the preparation of such mixtures. We must be sure that the mixture is well characterized. It is expected that a mixture containing 0.5% pentanes will be prepared and its density measured within the next month.

7.2 Calculational Methods. No work on the four models has been done during the reporting period; however, they have been used extensively to compare predicted and newly measured mixture densities. As noted above in this report the disagreement between the densities calculated from the extended corresponding states model and measured values has been less than 0.1% except for two $CH_4 - iC_4H_{10}$ mixtures where the disagreement is from 0.1 to 0.2%.

8. Problem Areas. None.

9. Funding. January 1 - June 30, 1978.

Man-years expended	0.6
Equipment and/or Services Purchased	2.7K$
Total Reporting Period Cost	49.2K$
Balance Remaining	6.7K$

10. Future Plans.

Objectives and Schedule: Quarter   3   4

Complete mixtures measurements.   ——————>

Measure, analyze, and report
  multicomponent mixture data,
  including selected LNG-like   ———————————————————>
  mixtures.

Prepare final calculational
  methods paper.   ———————————————————————>

1. <u>Title</u>. PROGRAM FOR REDUCING THE COST OF LNG SHIP HULL CONSTRUCTION --
   PHASE II SHIP STEEL IMPROVEMENT PROGRAM

   <u>Principal Investigators</u>. H. I. McHenry, M. B. Kasen, and R. P. Reed

2. <u>Cost Center Number</u>.

   2753430 - LNG Ship Hull Materials (Shipyard Contracts)
   2751430 - LNG Ship Construction Materials (Metallurgical Evaluation)
   2752430 - LNG Ship Hull Materials (Fracture Properties)

3. <u>Sponsor Project Identification</u>. Maritime Administration Misc. P. O.
   400-58073.

4. <u>Introduction</u>. Construction of LNG tankers requires the use of fine grain
   normalized steels for the part of the hull structure that is cooled by
   the cargo to temperatures in the range of 255 K (0°F) to 228 K (-50°F).
   Several ABS steels have satisfactory base plate properties but extreme
   care must be exercised during welding to avoid degradation of the steel
   adjacent to weld (the heat affected zone) to a level of toughness below
   U. S. Coast Guard requirements. Significant cost problems are being
   encountered by U. S. shipyards due to the resulting inefficient low-heat-
   input welding procedures that must be employed to meet the fracture
   requirements in the heat affected zone.

   The feasibility of reducing the cost of LNG ship hull construction was
   investigated in Phase I of this project, leading to the Phase II program
   described below.

5. <u>Objective</u>. The objectives of the Phase II program are 1) to have the
   four major plate producers supply three LNG shipyards with production
   heats of ABS steels modified to possess improved transverse fracture
   properties at low temperatures, 2) to have the LNG shipyards evaluate
   these plates by qualifying optimum welding procedures in accordance with
   the USCG requirements, and 3) to provide a metallurgical evaluation of
   factors that influence heat affected zone toughness in the improved
   steels.

6. <u>Background</u>. Early in 1974, the Welding Panel of MarAd's Ship Production
   Committee recommended that a program be conducted to reduce the cost of
   ship hull construction. NBS was requested by MarAd to propose such a
   program to the LNG subcommittee of the Welding Panel at a meeting in
   Boulder in August. In mid-October, MarAd approved the initial phase of
   NBS's recommended program, i.e., to survey the problem and the technology
   available for its solution. On the basis of this survey and as the
   result of a meeting of the Welding Panel in March, 1975, a coordinated
   program involving the LNG shipyards, the steel suppliers, and NBS was
   recommended to MarAd and to the Welding Panel. This program was approved
   and work started in May 1975. Cost-sharing contracts for the evaluation
   of the improved steels were awarded in 1975 to the three participating
   shipyards: Avondale Shipyards, Inc., Newport News Shipbuilding and
   Drydock Co. and General Dynamics-Quincy Shipbuilding Division. A similar
   contract was signed with Lukens Steel Company to evaluate Cb-treated V-
   051 steel with and without sulfide shape control. The three participa-
   ting shipyards and Lukens Steel Co. completed the shipyard evaluation
   phase of the program in 1977. The ABS steels with sulfide shape control
   had excellent toughness and the HAZ toughness was improved, particularly
   for shielded metal arc (SMA) and gas metal arc (GMA) welds. The most
   promising results for high-heat-input welds were obtained with the Cb-
   treated V-051 steel with sulfide shape control.

   Follow-on contracts were awarded to the three participating shipyards to
   further evaluate the most promising ship steels: ABS grades V-051 (Cb,
   SSC), V-062 (SSC), and V-062 (Cb, SSC).

16

7. <u>Program and Results</u>. During this reporting period, most of the work on the follow-on contracts was completed. Six steels were evaluated by one or more shipyards as summarized below:

Steel Type	Thickness (in)	Source	Shipyard Evaluation
V-062 (low S)	1/2, 1	Armco	NNS
V-062 (SSC)	1/2, 1	Armco	NNS, GD/Q
V-062 (Cb, low S)	1/2, 1	Armco	GD/Q, ASI
V-062 (Cb, SSC)	1/2, 1	Armco	GD/Q, ASI
V-051 (Cb, SSC)	1/2, 1	Lukens	NNS, GD/Q, ASI
C-Mn-Mo-Cb	1.2	Climax	NNS, GD/Q

where: NNS - Newport News Shipbuilding, GD/Q - General Dynamics, Quincy Shipbuilding Division, ASI - Avondale Shipyards, Inc.

The results of the NNS evaluation indicated that the V-062 (SSC) and the V-051 (Cb, SSC) had satisfactory HAZ toughness at 222 K (-60°F) providing the weld metal toughness exceeded the 27 J (20 ft lb) requirement. For three-wire SAW welds, the Armco W-18 weld metal with nominally 2% Ni was consistently below 27 J (20 ft lb) and consequently none of the welds were qualified at 222 K (-60°F). For single wire SAW welds, the Rayco 130 weld metal with nominally 1% Ni consistently exceeded 27 J (20 ft lb). In both the 1-wire and 3-wire SAW welds, the same heat input of 67 kJ/cm (161 Btu/in) was used for the final pass. These results indicate that further work on filler metal selection is needed to take advantage of the improved heat input tolerance of the base metals. The NNS tests also indicated that the C-Mn-Mo-Cb pipeline steel had very low HAZ toughness.

The results of the GD/Q evaluation indicated that the V-062 (SSC), V-062 (Cb, low S), V-062 (Cb, SSC) and V-051 (Cb, SSC) steels generally had satisfactory toughness at 222 K (-60°F)(228 K (-50°F) for V-062 (Cb, SSC), 1/2-inch thick) for SMA welds with 8018C-1 electrodes and for SAW welds with Airco AX-90 wire. Exceptions were the 1/2 inch-thick V-062 (Cb, SSC), SMA, vertical and welds made with a twin-wire single-arc process. The GD/Q tests also indicate that the C-Mn-Mo-Cb pipeline steel had very low HAZ toughness.

The results of the ASI investigation indicated that their choice of filler metals resulted in weld metal and sometimes fusion line and 1 mm toughness values that did not exceed 27 J (20 ft lb) at 222 K (-60°F). The ASI filler metals were AWS E-9018-M electrodes for SMA welds and Armco W-19 wire with Linde 709-S flux. ASI plans to conduct additional tests on submerged arc weldments with Linde M1-88 wire.

8. <u>Problem Areas</u>. Low weld metal toughness, particularly in submerged arc welds, is making it difficult to evaluate the V-062 and V-051 base plates.

9. <u>Funding</u>. January 1, 1978 to June 30, 1978

Cost Center	Cost to 6/30/78	Balance
7363430	180K	0
7361430	71K	9K
7362430	64K	16K

10. <u>Future Plans</u>. Work should be completed on the follow-on testing program (Phase II of the Ship Steel Improvement Program) this year. A proposal will be submitted to MarAd to conduct additional tests on filler metals for low temperature service.

1. <u>Title</u>. CUSTODY TRANSFER - LNG SHIPS

   <u>Principal Investigators</u>. W. C. Haight, R. J. Hocken, B. R. Borchardt, R. G. Hartsock, R. C. Veale, J. D. Siegwarth, J. F. LaBrecque, and C. L. Carroll

2. <u>Cost Center Numbers</u>. 7360460, 7361575, 7362575, 7363575, 7310570, 7310571

3. <u>Sponsor Project Identification</u>. LNG Custody Transfer Measurements Supervisory Committee and Maritime Administration Misc. P.O. #400-79005.

4. <u>Introduction</u>. In response to the requests from the U.S. shipbuilding industry, NBS is independently examining the accuracies of LNG tank cargo capacity tables and developing alternative survey techniques.

5. <u>Objectives</u>. The objectives of the program are to develop new techniques for LNG transport tank calibration and to test the accuracy of present calibration techniques as part of an overall study of custody transfer methods aimed at increasing the accuracy of custody transfer measurements.

6. <u>Background</u>. Initial funding by the Maritime Administration (7360460) supported some preliminary tests of calibration of spherical LNG ship tanks. As a result of these measurements, the LNG Custody Transfer Supervisory Committee and the Maritime Administration have funded extension of the work to the membrane tanks and the free standing prismatic tanks now under construction in U.S. shipyards.

7. <u>Program</u>. Techniques for accurately dimensioning prismatic tanks of the membrane type have been developed by the Macrometrology Group at NBS. The technique requires establishing a model of a solid of the same shape as the tank just inside the tank walls using laser planes. Distances from the laser planes to the wall are measured at a larger number of points. The size and shape of the solid defined by the laser planes is measured by a multiple redundant method so the accuracy of the measurement of the dimensions of the solid can also be determined. This technique has been applied to four membrane tanks. Abbreviated surveys have been completed on five additional tanks.

   Two of the free standing prismatic tanks have been tested for distortions resulting from lifting and loading them onto the ships. The distortion detected was not significant relative to the accuracy required of the photogrammetric survey.

   The accuracy and precision of the photogrammetric tank survey method is being tested with length standards. Invar tapes are being employed to give accurate target separations for test lengths near the maximum dimensions of the tank. Of the tanks thus far tested, the accuracy and precision of the photogrammetric measurements of the test target separations indicate this survey technique meets volume accuracy requirements.

8. <u>Problem Areas</u>. None.

9. <u>Funding</u>. January 1 - June 30, 1978.

Man years expended	1.2
Total reporting period cost	$172.0k
Balance remaining	$113.0k

10. <u>Future Plans</u>. Complete the surveys of the membrane tanks and compare the resulting tank capacities with the capacities determined by the primary survey contractor when the latter become available. The laser plane dimensioning technique will be modified to check the capacity of one of the free standing prismatic tanks and to examine hydrostatic distortion effects. Additional test tape measurements are planned for subsequent tanks to look for possible survey distortions and to examine horizontal and vertical calibration factors.

1. Title. HEATING VALUE OF FLOWING LNG
   Principal Investigators. J. A. Brennan

2. Cost Center Number. 7366579

3. Sponsor Project Identification. Pipeline Research Committee (American Gas Association) PR-50-48.

4. Introduction. This project will test instrumentation for making heating value measurements on flowing LNG in actual applications. Information from projects currently underway by Siegwarth (cost center 7367574) on densimeters, by Haynes and Hiza (cost center 7361574) on mixture densities and by Parrish (cost center 7360575) on LNG sampling will be utilized where appropriate to provide state of the art information.

5. Objectives. The objective of this project is to measure total heating value of LNG flowing in a pipeline by the integration of individual measurements of flow, density and specific heating value. Flow measurement requires determination of flowmeter performance in line sizes larger than presently available calibration facilities. Therefore, a secondary objective is to establish appropriate flowmeter scaling laws.

6. Background. The LNG flow facility at NBS was used to evaluate the response and the integration of the individual elements of the heating value measurement. Different compositions of LNG were tested to provide a range of densities and temperatures sufficient to determine any dependencies. Sampling work was combined with the sampling project (cost center 7360575) to better define the important criteria of this phase of the measurement problem.

   Flowmeter scaling work utilizes the cryogenic and water flow facilities at NBS as well as private LNG peak shaving and import facilities.

7. Program and Results. All test instrumentation for the Southern Energy Import Terminal has been installed and the recording equipment connected. The first shipload of LNG arrived during June 1978 but no testing will be attempted until after the terminal has been completely checked out. It will probably be possible to start the actual testing during the third or early fourth quarter of 1978.

8. Problem Areas. The delays in receiving the instrumentation, which was described in the last report, precluded performing all the desired tests in liquid nitrogen before shipment to Southern Energy. Sufficient tests were run to detect equipment failure but not enough to establish overall performance.

9. Funding. January 1 - June 30, 1978.

Man-years expended	.2
Total reporting period costs	$8k
Balance remaining	$22k

10. Future Plans. LNG flow tests will be run when appropriate, consistent with the start-up of the terminal.

1. <u>Title</u>. LNG DENSITY REFERENCE SYSTEM
   <u>Principal Investigators</u>. J. D. Siegwarth and J. F. LaBrecque

2. <u>Cost Center Number</u>. 7367574

3. <u>Sponsor Project Identification</u>. American Gas Association, Inc., Project BR-50-10; National Bureau of Standards, Gas Research Institute.

4. <u>Introduction</u>. A density reference system has been developed to evaluate the ability of commercially available instruments to measure densities of LNG directly. Density is an essential measurement in determining the total energy content of natural gas reservoirs.

5. <u>Objectives</u>. The object of this research is to develop and supply adequate calibration methods and calibration standards to densimeter manufacturers and users for providing traceability of accuracy to field density measurement systems.

6. <u>Background</u>. The density reference system project was initiated in 1973. Since that time the reference system has been designed, constructed, and is now in operation, evaluating commercial density metering systems. Reports describing the density reference system and the results of the tests of four commercial densimeters have been published. These reports are:

   Siegwarth, J. D., Younglove, B. A. and LaBrecque, J. F., Cryogenic fluids density reference system: provisional accuracy statement, Nat. Bur. Stand. (U.S.) Tech. Note 698, 24 pages (1977), and

   Siegwarth, J. D., Younglove, B. A. and LaBrecque, J. F., An evaluation of commercial densimeters for use in LNG, Nat. Bur. Stand. (U.S.) Tech. Note 697, 43 pages (1977).

7. <u>Program and Results</u>. The DRS has been operated with liquid nitrogen fillings several times in the course of testing seven additional Archimedes densimeters. These measurements have not established the accuracy of the DRS as a density standard in liquid nitrogen yet because the temperature was only measured once and the purity of the LN_2 sample was only controlled for that one measurement.

   Tests of the seven Archimedes densimeters in methane and LNG-like mixtures have shown that the accuracy of these densimeters is poorer than indicated by the tests reported in Technical Note 697. This reduced accuracy may result because the instrument calibration is based on measurement in fluids of density and boiling temperature well removed from the density and boiling temperature of LNG. The fault or faults of the densimeter system resulting in reduced accuracy have not yet been positively identified.

   During the course of these tests, modifications of and adjustments to the density reference system have improved its performance. The ΔT in the sample holder is now always below 40 mK and is rarely larger than 20 mK. This reduced ΔT and the addition of pneumatic actuaters to the weight changing mechanism of the DRS densimeter has reduced the 1 σ scatter of the density measurements well below 0.01%.

   Some preliminary redesign work of the sample container is underway. The redesigned sample container will be larger in size and will permit insertion of the densimeters for test without disturbing the insulating vacuum. This design will allow tests of various types and numbers of densimeters with only minor modifications to the DRS.

8. <u>Problem Areas</u>. The recent densimeter tests have shown that LN_2 is not the best choice of a calibration fluid for densimeters to be used in LNG. Better calibration techniques for commercial instruments are needed.

9. <u>Funding</u>.   January 1 - June 20, 1978.

    Man years expended   0.2
    Total reporting period cost $12.0k
    Balance remaining $48.0k

10. <u>Future Plans</u>. The capacity and flexibility of the DRS will be increased.
    With the addition of a separate sample storage dewar, changing the densi-
    meters under calibration will be rapid and the system can be demonstrated
    as a commercially practical calibration system. A transfer standard will
    be sent to Gaz de France, Paris when the calibration problems with the
    Archimedes densimeter are solved. A recent entry to the cryogenic den-
    simeter market has been made available for testing. This instrument is
    a vibrating cylinder type.

1. Title. LNG SAMPLING MEASUREMENT STUDY
   Principal Investigators. W. R. Parrish, R. J. Richards and J. F. LaBrecque.

2. Cost Center Numbers. 7365574.

3. Sponsor Project Identification. A.G.A.-PRC LNG Supervisory Committee.

4. Introduction. Composition is used to determine both the heating value
   and the quantity (through density) of LNG shipments. Thus, any error
   in composition doubles when calculating the total heating value and
   dollar value of a LNG tanker cargo. Compositions are determined by
   sampling LNG, on either a batch or continuous basis, and analyzing the
   vaporized mixture. Although several sampling techniques exist, none
   have received widespread acceptance in the LNG industry. Also, a
   standard technique has not been established for analyzing the vaporized
   sample.

5. Objectives or Goals. The objectives of this work are the same as the
   last reporting period with emphasis on vaporizer and accumulator design.

6. Background. This work was performed because there is a need to
   determine the best means for obtaining the composition of LNG ship-
   ments. Current LNG buying contracts include specifications on when and
   how many liquid samples are to be taken but omit the sampling technique
   to be used. The evaluation of sampling techniques by NBS is expected to
   lead to the acceptance of the most accurate composition determination
   method by all parties involved in LNG custody transfer.

7. Program. Based on the previous work, the two factors preventing develop-
   ment of a general design are sampling rate and vaporizer-accumulator
   design. Test results showed that the precision of the system diminishes
   below a certain sampling rate. Attempts to correlate sampling rate with
   the limited range tested for the other variables failed. However, by
   process of elimination, the most likely factors causing the effect of
   sampling rate on precision are probe size, line size between the probe
   and vaporizer and heat leak. All of these variables are being evaluated
   in a laboratory apparatus, where the operating variables are controlled
   closely and mixtures of known composition are used.

   Laboratory tests demonstrated that, if a simple tube vaporizer is used,
   an accumulator must be used. This is because fractionation occurs during
   vaporization and the accumulator volume provides time for the sample to
   become homogenized again. Laboratory tests indicated that the field sys-
   tem required a larger accumulator than would be expected from laboratory
   results. However, the accumulator residence time should be minimized to
   insure adequate mixing and maintain a reasonable response time. There-
   fore, this project is considering two ways to eliminate the need for the
   accumulator. The first method is to place a static mixing device just
   downstram of the tube vaporizer. If the poorly mixed gas from the vapor-
   izer is not in plug flow, this mixer may remix the components. However,
   it will have no effect if the stream is in plug flow. The second method
   places the static mixing device in the vaporizer. Here the device pro-
   vides both mixing during vaporization and additional heat transfer sur-
   face area. (Previous tests indicated that sampling precision is better
   when the sample is vaporized quickly.)

8. Problem Areas. None.

9. Funding. January 1 - June 30, 1978.
   Man-years expended   .2
   Total reporting period cost $20.3k
   Balance remaining $54.7k

10. Future Plans. The work under cost center 7360575 is complete. However, additional work is being supported by the Pipeline Research Committee, A.G.A., to improve the sample vaporizer design (NBS cost center 7365574). After finishing the laboratory tests, field tests will be made at a yet-to-be-determined site.

1. Title. SURVEY OF CURRENT LITERATURE ON LNG AND METHANE
    Principal Investigator. Neil A. Olien

2. Cost Center Number. 7369574

3. Sponsor Project Identification. Gas Research Institute Grant No.
    5010-362-0019 and American Gas Association, Inc., Project BR-50-10.

4. Introduction. It is important that all NBS personnel working in LNG, as
    well as the AGA and others, keep up with what is going on throughout the
    world in the LNG field. This project is designed to provide the Current
    Awareness and other information services to allow workers to keep
    abreast of new research and other developments.

5. Objectives or Goals. We will publish and distribute each April, July,
    October, and January a listing of all significant papers, reports, and
    patents relating to methane and LNG properties and technology. The
    references will be listed under convenient subject headings. The
    Quarterly will be distributed to all interested AGA member companies and
    be made available to the general public on a subscription basis. In
    addition, LNG related information will be entered into the Cryogenic
    Data Center's Information System for quick retrieval. A continuing
    awareness of the current publication scene is maintained for any new
    periodicals to be reviewed cover-to-cover. Finally we will update and
    make available comprehensive bibliographies on the properties and
    technology of LNG. There are four bibliographies involved: methane
    properties, methane mixtures properties, processes and equipment
    involving methane and LNG, and patents relating to methane and LNG
    technology. These four will be updated annually.

6. Background. In 1969 we made a thorough review of the world's publica-
    tions to determine which periodicals and abstracting services should be
    scanned cover-to-cover to adequately encompass the LNG field. The
    result is that we now scan over 330 primary publications and nearly 25
    secondary publications. Of these, approximately one-third are directly
    related to LNG. In addition, we have increased our coverage of the
    energy field to include hydrogen as a future fuel. Much of this
    information is also pertinent to LNG and as such is listed in our
    LNG-related publications. Our Current Awareness Service has been
    published weekly since 1964 (beginning in 1975 the publication became
    biweekly) and the Liquefied Natural Gas Survey has been published
    quarterly since 1970.

7. Program and Results. Four issues of the LNG Quarterly are prepared each
    year and distributed. There are now 117 subscriptions going to AGA
    Member Companies and 161 to other subscribers.

    The four comprehensive bibliographies mentioned in section 5 have been
    reviewed and shortened, and more selective bibliographies have resulted.
    The latest versions were completed as of January 21, 1977.

    B-1525   THE THERMOPHYSICAL PROPERTIES OF METHANE AND DEUTERO-METHANE
             IN THE SOLID, LIQUID AND GASEOUS PHASES - A SELECTED BIBLI-
             OGRAPHY. Indexed by property, phase and author, 100 pages
             (Jan 1977). ($10.00).

    B-1526   THE THERMOPHYSICAL PROPERTIES OF METHANE MIXTURES - A
             SELECTED BIBLIOGRAPHY. Indexed by property, system and
             author, 166 pages (Jan 1977). ($15.00).

    B-1524   PROCESSES AND EQUIPMENT INVOLVING LIQUEFIED NATURAL GAS AND
             METHANE - A SELECTED BIBLIOGRAPHY. Indexed by subject and
             author, 285 pages (Jan 1977). ($25.00).

B-1527   PATENTS RELATING TO METHANE AND LNG TECHNOLOGY - A SELECTED
          BIBLIOGRAPHY. Indexed by author, 150 pages (Jan 1977).
          ($15.00).

Over the past seven years we have distributed over 500 copies of these
and the comprehensive bibliographies.

The size of these has grown to the extent that their usefulness is
limited, therefore it was decided that they would not be updated and a
series of more specialized bibliographies would be made available. The
following list gives those currently available. Additional topics will
be added as necessary.

B-1528   LIQUEFIED NATURAL GAS STORAGE INCLUDING INSULATION SYSTEMS.
          1181 references, indexed by author and subject, 210 pages
          ($20.00).

B-1529   LIQUEFIED NATURAL GAS PEAKSHAVING AND SATELLITE OPERATIONS.
          221 references, indexed by author, 36 pages ($10.00).

B-1530   LIQUEFIED NATURAL GAS STRATIFICATION AND ROLLOVER. 38 refer-
          ences, indexed by author and subject, 10 pages ($5.00).

B-1531   LIQUEFIED NATURAL GAS SAFETY INCLUDING SPILLS. 368 references,
          indexed by author and subject, 72 pages ($10.00).

B-1532   LIQUEFIED NATURAL GAS PIPELINES AND TRANSFER LINES. 226
          references, indexed by author, 44 pages ($10.00).

B-1533   LIQUEFIED NATURAL GAS SHIPS, BARGES AND OVERWATER TRANSPOR-
          TATION. 805 references, indexed by author, 138 pages ($15.00).

B-1534   LIQUEFIED NATURAL GAS VAPORIZORS INCLUDING COLD UTILIZATION.
          330 references, indexed by author and subject, 58 pages
          ($10.00).

B-1535   LIQUEFIED NATURAL GAS HEAT TRANSFER. 155 references, indexed
          by author, 34 pages ($10.00).

B-1536   LIQUEFIED NATURAL GAS LIQUEFACTION AND REFRIGERATION. 551
          references, indexed by author, 94 pages ($15.00).

B-1537   LIQUEFIED NATURAL GAS ECONOMIC FACTORS. 470 references,
          indexed by author, 84 pages ($15.00).

B-1538   LIQUEFIED NATURAL GAS OVERLAND TRANSPORTATION. 76 references,
          indexed by author, 15 pages ($5.00).

B-1539   LIQUEFIED NATURAL GAS PATENTS. 747 references, indexed by
          author and subject, 119 pages ($15.00).

B-1540   LIQUEFIED NATURAL GAS INSTRUMENTATION. 85 references, indexed
          by author and subject, 23 pages ($5.00).

8.   Problem Areas. None.

9. <u>Funding</u>. January 1 - June 30, 1978.

    Labor   6.8K$
    Other Costs   1.6K$
            Total   8.4K$

            Remaining   7.2K$

10. <u>Future Plans</u>. Issue 78-2 was delivered to the printer the second week
    of July and should be distributed before the end of July.

1. Title. LIQUEFIED NATURAL GAS TECHNOLOGY TRANSFER

   Principal Investigators. Dwain E. Diller, H. M. Ledbetter, and N. A. Olien

2. Cost Centers. 7360403, 7361403, 7360570, 7364574, 7368574, 7360127, 7360461, 7360594

3. Sponsor Project Identification. Maritime Administration, Miscellaneous Purchase Order No. 400-79005; American Gas Association, Inc. Project BR 50-10; Gas Research Institute; American Bureau of Shipping; NBS Office of Standard Reference Data.

4. Introduction. The liquefied natural gas program at the Thermophysical Properties Division of NBS Boulder represents an investment by industry and government agencies of over $5 million over the past six years. This investment was designed to develop reference quality properties data for both fluids and materials and instrumentation and measurement technology for the use of the LNG and related industries. Information developed under this program must be transmitted to the ultimate user in a timely and useful format. The classical publication methods of NBS most certainly provide the scientist and research engineer information in a form most useful to the academic or near academic community. However, as a result of extensive assessments of user requirements, it was found that an additional effective mode for technology transfer would be an LNG Materials and Fluids User's Manual. A complete outline and planned table of contents have appeared in previous semiannual reports. The Maritime Administration of the Department of Commerce and the American Bureau of Shipping have agreed to sponsor the first year's efforts on the materials section, and the American Gas Association, Inc. and the NBS Office of Standard Reference Data have agreed to sponsor the section on fluids and fluid mixtures. The project was begun on April 1, 1976.

5. Objectives. The Liquefied Natural Gas Materials and Fluids User's Manual will provide a method of quick dissemination of property data and related information for the effective generation, utilization and transportation of LNG. The object is to improve technology transfer from the current NBS Thermophysical Properties Division LNG physical measurements program to the users, including federal agencies, the states and industry. For the purpose of this data book, liquefied natural gas is defined as a cryogenic mixture (at less than approximately 150 K) of hydrocarbons, predominantly methane, with less than a total of 20% of the minor components ethane, propane, iso and normal butane, and nitrogen as an inert contaminant. LNG materials will be those associated with the liquefaction, transport and storage of liquefied natural gas.

6. Background. The User's Manual is only one of a number of information dissemination methods used to provide workers in the liquefied natural gas (LNG) industry with properties data of known quality in a format consistent with the requirements of the intended user. In the case of the LNG User's Manual the intended audience is the field engineer, plant manager, ship designer or process engineer interested in a ready reference of assessed quality for data to be used in conceptual design, process monitoring, process analysis, and intercomparisons where precision and accuracy are secondary to specific problem solutions. The hierarchy of accuracy and precision will be defined and traceable through references to scientific and engineering literature.

   Data are classified into three groups by the NBS Thermophysical Properties Division.

   Group 1. Data which have been generated experimentally by NBS, or have been assessed, evaluated or experimentally verified by NBS.

Group 2. Data which have been assessed and evaluated by NBS.

Group 3. Data available in the scientific engineering literature through the NBS Cryogenic Data Center or elsewhere. No NBS evaluation or assessment has been made at this date.

In general, most data included in the LNG user's manual will be from groups 1 and 2. Few new assessments or correlations are anticipated or required for this work.

Data will be presented primarily in graphical form. Tables and analytical expressions will be used only where absolutely necessary. Graphs and charts will be in loose-leaf form for ease of updating and additions. This form will also allow immediate implementation for data already available under the NBS LNG program and will provide a convenient format for the output of data from existing projects. The user's manual will not be a substitute for traditional publications in the scientific literature where measurement science, technique, precision and accuracy are paramount, but will provide the data and references for the necessary assessment by the user.

The publication of both graphical and tabular data will be in a dual system of physical units. These units will be the traditional LNG industry British System of BTU, pound, degree Fahrenheit and the SI system of joule, kilogram and kelvin. It is the intent to give equal weight to each system of units.

7. Program and Results. The first edition of the User's Manual became available for distribution in September 1977. A complete description and ordering information are included as part of this report. About 450 copies have now been distributed to sponsors and purchasers. New orders are currently coming in at the rate of about ten per week.

All materials to be included in the first supplement to the User's Manual have been sent to the printer. The first supplement will contain 31 graphs of revised updated and new material on the properties of structural metals and alloys (aluminums, nickel steels and stainless steels); 40 graphs on thermal insulations (polystyrene foams, polyurethane foams, polyvinyl chloride foams, balsa, perlite, cellular glass and glass fiber); 15 graphs and 3 wall charts on pure LNG components (ethane); and 9 sheets on binary and multicomponent mixtures of LNG components. The first supplement will also contain 46 pages of materials specification tables and 38 pages of additional narrative and other descriptive materials. The first supplement is expected to be ready for distribution by late August 1978.

8. Problem Areas. None.

9. Funding. January 1 - June 30, 1978.

Labor - man-years expended	1.2
Funds expended	81.6K$
Balance remaining (first supplement)	0.0K$
Balance remaining (second supplement)	60.7K$

10. Future Plans. Work on the second supplement is in progress. Propane graphs and thermodynamic property charts are being prepared. Additional graphs on mixtures of LNG components have been scheduled. Graphs on the properties of structural composites and aggregates (with emphasis on concretes) have been proposed. No additional supplements are planned at this time.

LNG MATERIALS AND FLUIDS

A USER'S MANUAL OF PROPERTY DATA IN GRAPHIC FORMAT

The National Bureau of Standards Cryogenics Division is distributing a loose-leaf LNG Materials and Fluids User's Manual. The User's Manual is designed to provide property data and related information for the effective generation, utilization and transport of LNG.

The total edition is planned to include:

— pure fluids data on methane, nitrogen, ethane, propane and iso and normal butane,
— fluid mixtures data involving methane with nitrogen, ethane, propane and iso and normal butane, including commercial LNG compositions,
— LNG materials data on structural metals and alloys, and
— materials data on thermal insulations, joining compounds, structural composite materials and aggregates, polymeric materials, and miscellaneous non-structural materials.

The first edition and expandable binder contains 138 two-color (8½ x 11-inch) charts and six wall charts (22 x 34-inch). This edition's property data are pressure-density-temperature, thermodynamic, transport and electromagnetic properties of pure methane and nitrogen; fluid mixtures of methane with nitrogen; and, the elastic, thermal and mechanical properties of aluminum alloys (3003, 5083 and 6061), stainless steels (304, 304L, 310 and 316), nickel steels (2.25, 3.5, 5 and 9% nickel) and invar. The wall charts are of the thermodynamic properties enthalpy-entropy (H-S), pressure-enthalpy (P-H) and temperature-entropy (T-S) for pure methane and pure nitrogen.

Both British and SI (International System) units are used throughout, easily discernable by printing in separate colors.

The expandable binder allows for future supplements. Purchasers of the first edition will be notified upon completion of addtitional supplements and their respective prices. All charts are printed on a high wet strength lithographic map paper designed for a strong durable life.

Copies of the first edition @ $35 each and additional rolled wall charts @ $1 each may be obtained by forwarding the order form below with payment. For additional information contact LNG Materials and Fluids; National Bureau of Standards; Cryogenics Division; 325 Broadway; Boulder, Colorado 80302.

ORDER FORM		QUANTITY	PRICE
First Edition LNG Materials and Fluids User's Manual	@ $35 ea.	_____	_____
Additional Rolled 22 x 34 Charts:			
Nitrogen thermodynamic data			
Enthalpy-entropy wall chart (H-S)	@ $ 1 ea.	_____	_____
Pressure-enthalpy wall chart (P-H)	@ $ 1 ea.	_____	_____
Temperature-entropy wall chart (T-S)	@ $ 1 ea.	_____	_____
Methane thermodynamic data			
Enthalpy-entropy wall chart (H-S)	@ $ 1 ea.	_____	_____
Pressure-enthalpy wall chart (P-H)	@ $ 1 ea.	_____	_____
Temperature-entropy wall chart (T-S)	@ $ 1 ea.	_____	_____
		TOTAL	_____

Mail form and remittance to:

LNG Materials and Fluids; National Bureau of Standards; Cryogenics Division; 325 Broadway; Boulder, Colorado 80302.

1. <u>Title</u>. OIML JOINT SECRETARIAT ON LNG MEASUREMENTS

   <u>Principal Investigators</u>. Douglas Mann and James A. Brennan, NBS and
   T. L. Hillburn, Phillips Petroleum Company.

2. <u>Cost Center Number</u>. 7361104

3. <u>Sponsor Project Identification</u>. American Gas Association, Inc.,
   NBS-Office of International Standards; and NBS.

4. <u>Introduction</u>. The liquefied natural gas program of the National Bureau
   of Standards Cryogenics Division has, over the past five years, provided
   the gas industry and interested Government agencies with properties data
   on materials and fluids, instrumentation, and measurement assistance in
   the support of commerce in this significant and growing segment of the
   supplementary fossil energy supply. Support of this program by the
   American Gas Association, Inc. and Federal Government agencies such as
   the Maritime Administration (MarAd), NASA, GSA, Federal Power Commission
   and the NBS-Office of Standard Reference Data has provided a basis for
   the national acceptance of the results of the NBS LNG program. Through
   the U.S. membership in the International Organization of Legal Metrology
   there exists, at the present time, an opportunity to extend, interna-
   tionally, the utility of data and measurement practice developed under
   our joint Government/industry program. We have been requested (by OIML
   membership) to establish an LNG Measurement Secretariat within OIML which,
   if implemented, would provide a significant international forum for the
   results of our joint work. It is believed that a joint Secretariat with
   the LNG industry would provide the most effective means of accomplishing
   these objectives.

5. <u>Objectives or Goals</u>. Our objective is to accomplish the following goals
   within the next three years.

   a) To establish U.S. (NBS) thermophysical properties data for LNG as
   the standard data in international usage.

   b) To establish U.S. (NBS) materials property data used in fabrication
   and construction of LNG facilities (liquefiers, storage, transport) as
   the standard data in international usage.

   c) To establish U.S. (NBS) approved measurement technology and
   instrumentation as related to LNG (pressure, temperature, density, liquid
   level, flow) as the standard in international LNG trade. The precedent
   has been established with the successful completion of the joint NBS-CGA
   cryogenic flow measurement program which has resulted in the adoption of
   a cryogenic flow measurement code by the National Conference on Weights
   and Measures. We wish to extend this code on an international basis.

   d) To establish and maintain the leadership of U.S. science, engineering,
   and industry in the research, technology, manufacture and marketing of
   instruments and measurement systems for liquefied natural gas.

6. <u>Background</u>. OIML was founded in 1955 to promote intergovernmental
   cooperation in the field of legal metrology which relates to the com-
   patibility of standards of measurement and the legislation and government
   regulations which may affect such standards of measurement. OIML
   recommends uniform international requirements for scientific and measure-
   ment instruments used in industry and commerce and works out model laws
   and regulations for consideration by member nations; and, in addition,
   serves as a center of documentation and information exchange in legal
   metrology. At present 43 nations are members of this intergovernmental
   organization.

   The United States joined OIML in 1972 (the Senate by resolution of
   August 11, 1972 gave its advice and consent to the accession of the U.S.
   to the convention establishing OIML). The responsibility for managing
   U.S. participation in OIML was assigned to the Department of Commerce

and has since been delegated by the Department to the National Bureau of Standards (NBS). Under the general guidance of the Department of State and the Secretary of Commerce, NBS is directly responsible for formulating and implementing U.S. policy towards OIML. U. S. participation in the organization is deemed important for two reasons: First, to protect and enhance some $1 billion worth of scientific and measurement instruments exported each year by U. S. firms and to ensure equity in the trade of commodities measured by these instruments; and second, to maintain the U.S. as the world leader in the field of metrology.

In the spring of 1975 at a meeting in Paris of the International Committee of Legal Metrology, the French and U.S. representatives discussed the possibility of creating a new Reporting Secretariat No. 13 on "Liquefied Natural Gas (LNG) Measurement". The U. S. representative, W. E. Andrus, Jr. of NBS, agreed to explore the possibility with U. S. industry and interested government agencies. These discussions resulted in a decision to propose a joint Secretariat with the American Gas Association and NBS-Cryogenics Division in order to best accomplish the tasks. These conclusions were reached during several meetings extending through the latter part of 1975 and early 1976. During the summer of 1977, representatives of NBS met with PTB (West Germany) and SIM (France) to discuss the proposed scope and to explore expansion of the effort to include cryogenic fluids in general. Results of those discussions indicate some resistance to including different physical measurements (flow, density, etc.) under a single recommendation for a specific group of fluids.

The proposed plan and scope were presented at the meeting of The Advisory Committee for International Legal Metrology held at NBS-Boulder in September. The committee encouraged NBS to proceed with the present scope and to continue to explore the possible inclusion of other cryogenic fluids.

7. Program and Results. A revised work plan for cryogenic fluids was generated by the technical associates Douglas Mann of NBS and T. L. Hillburn of the Phillips Petroleum Co. representing A.G.A. and API. The scope of the work plan included instrumentation and procedures for the custody transfer measurements of pressure, temperature, density, liquid level, flow and calorific value of liquefied atmospheric and natural (hydrocarbon) gases having pure fluid or mixture normal boiling points of less than 150 K. Recommendations will be limited to establishing total mass and, where applicable, total heating value. Fluids and fluid mixtures considered will be limited to commercially important liquefied atmospheric gases, oxygen, nitrogen and argon and the primary components of liquefied natural gas, methane, ethane, propane, iso- and normal butane and pentane.

The draft work plan is presently under review by the OIML membership and other interested parties. Comments on the plan and an expression of interest as to formation of the first working group are being solicited.

8. Problem Areas. None.

9. Funding. January 1, 1978 - June 30, 1978.

Labor - Man-years expended	0.1
Funds expended	11.0K$
Balance remaining	4.0K$

10. Future Plans. Flow measurement of pure cryogenic fluids will be the first of the recommendations generated under the proposed work plan. This will be accomplished by combining the existing U.S. and European codes for flow measurements. A working group will be formed of interested parties and the first draft of this recommendation should be ready for review by January of 1979.

BIBLIOGRAPHY

NBS Reports and Publications Related to LNG Technology

Which Have Appeared Since January 1977

1. Goodwin, R. D., "Provisional thermodynamic functions for propane from 85 to 700 K at pressures to 700 bar," Nat. Bur. Stand. (U.S.), Interagency Report 77-860 (Jul 1977).

2. Goodwin, R. D., "Specific heats of saturated and compressed liquid propane," J. Res. Nat. Bur. Stand. (U.S.) (in press, 1978).

3. Goodwin, R. D., "On the non-analytic equation of state for propane," Adv. Cryog. Eng. 23, 611 (1978).

4. Tsumura, R. and Straty, G. C., "Speed of sound in saturated and compressed fluid ethane," Cryogenics 17, 193 (1977).

5. Haynes, W. M. and Hiza, M. J., "Measurements of the orthobaric liquid densities of methane, ethane, propane, isobutane and normal butane," J. Chem. Thermodynamics 9, 179 (1977).

6. Hiza, M. J., Haynes, W. M. and Parrish, W. R., "Orthobaric liquid densities and excess volumes for binary mixtures of low molar mass alkanes and nitrogen between 105 and 140 K," J. Chem. Thermodynamics 9, 873 (1977).

7. Hiza, M. J. and Haynes, W. M., "Liquid mixture excess volumes and total vapor pressures using a magnetic suspension densimeter with compositions determined by chromatographic analysis: methane + ethane," in Advances in Cryogenic Engineering, Volume 23 (Plenum, New York, 1978), p. 594.

8. Haynes, W. M., Hiza, M. J. and McCarty, R. D., "Densities of LNG for custody transfer," Proceedings of LNG-5 Conference, Düsseldorf, Germany (Aug 1977).

9. McCarty, R. D., "Comparison of mathematical models for the prediction of LNG densities," Nat. Bur. Stand. (U.S.), Interagency Report 77-867 (Oct 1977).

10. Diller, D. E., "LNG density determination," Hydrocarbon Proc. 56, No. 4, 142 (Apr 1977).

11. Hiza, M. J., "An empirical excess volume model for estimating liquefied natural gas densities," Fluid Phase Equilibria 2, 27 (1978).

12. Miller, R. C. and Hiza, M. J., "Experimental molar volumes for some LNG-related saturated liquid mixtures," Fluid Phase Equilibria 2, 49 (1978).

13. Miller, R. C., Kidnay, A. J. and Hiza, M. J., "Liquid-vapor equilibria in the methane + ethene and methane + ethane systems from 150 to 190 K," J. Chem. Thermodynamics 9, No. 2, 167 (Feb 1977).

14. Hiza, M. J., Miller, R. C. and Kidnay, A. J., "A review, evaluation, and correlation of the phase equilibria, heat of mixing, and change in volume on mixing for liquid mixtures of methane + ethane," J. Phys. Chem. Ref. Data (to be submitted).

15. Hanley, H. J. M., Haynes, W. M. and McCarty, R. D., "Viscosity and thermal conductivity coefficients for dense gaseous and liquid methane," J. Phys. Chem. Ref. Data 6, 597 (1977).

16. Hanley, H. J. M., Gubbins, K. E. and Murad, S., "A correlation of the existing viscosity and thermal conductivity data of gaseous and liquid ethane," J. Phys. Chem. Ref. Data 6, 1167 (1977).

17. Hanley, H. J. M., Holland, P. M., Gubbins, K. E. and Haile, J. M., "A correlation of the viscosity and thermal conductivity data for gaseous and liquid propane," J. Phys. Chem. Ref. Data (in press).

18. Hanley, H. J. M., "Prediction of the thermal conductivity of fluid mixtures," Proceedings 7th ASME Conf. on Thermophysical Properties; Hanley, H. J. M. in Phase Equilibria and Fluid Properties in the Chemical Industry, ACS Symp. Series No. 60 (1977).

19. Hanley, H. J. M., "Transport coefficients in the one-fluid approximation behavior in the critical region," J. Res. Nat. Bur. Stand. (U.S.) 82, 18 (1977).

20. Ackerson, B. J. and Hanley, H. J. M., "The thermal diffusivity of methane in the critical region," Chem. Phys. Letters 53, 596 (1978).

21. Ackerson, B. J. and Straty, G. C., "Rayleigh scattering from methane," J. Chem. Phys. (in press, 1978).

22. Mann, D. B., editor, "LNG materials and fluids user's manual," (Sep 1977), available from the National Bureau of Standards, Boulder, CO 80303.

23. Diller, D. E., "NBS research on LNG thermophysical properties data and custody transfer measurement methods," Proceedings of Symposium on LNG Storage and Handling, Boumerdes, Algeria, April 4-5, 1978.

24. Tobler, R. L. and Reed, R. P., "Fracture mechanics parameters for a 5083-0 aluminum alloy at low temperatures," J. Eng. Mater. Technol. 19, 306 (1977).

25. McHenry, H. I. and Reed, R. P., "Fracture behavior of the heat affected zone in 5% Ni steel weldments," J. Weld. Res. Supp. (Apr 1977).

26. McHenry, H. I., "Fracture mechanics and its applications to cryogenics," in Advances in Cryogenic Engineering, Volume 22 (Plenum, New York, 1977), p. 9-26.

27. Parrish, W. R., Arvidson, J. M. and LaBrecque, J. F., "System is accurate, precise for LNG sampling," Hydrocarbon Processing 57, 114 (1978).

28. Parrish, W. R., Arvidson, J. M. and LaBrecque, J. F., "Evaluation of LNG sampling-measurement systems for custody transfer," Proceedings of American Gas Association Transmission Conference, Montreal, Quebec, Canada, May 8-10, 1978.

29. Parrish, W. R., Arvidson, J. M. and LaBrecque, J. F., "Development and evaluation of an LNG sampling system," Nat. Bur. Stand. (U.S.), Interagency Report 78-887 (in press, 1978).

30. Parrish, W. R., Brennan, J. A. and Siegwarth, J. D., "LNG custody transfer research at the National Bureau of Standards," Proceedings of the American Gas Association Transmission Conference, Montreal, Quebec, Canada, May 8-10, 1978.

31. Giarratano, P. J. and Collier, R. S., "Evaluation of capacitance densitometry for LNG mixtures with low nitrogen composition," Ind. Chem. Eng. Process. Des. Dev. 16, 330 (1977).

32. Siegwarth, J. D., Younglove, B. A. and LaBrecque, J. F., "An evaluation of commercial densimeters for use in LNG," Nat. Bur. Stand. (U.S.), Technical Note 697 (Oct 1977).

33. Siegwarth, J. D., Younglove, B. A. and LaBrecque, J. F., "Cryogenic fluids density reference system: provisional accuracy statement," Nat. Bur. Stand. (U.S.), Technical Note 698 (Nov 1977).

34. Siegwarth, J. D., LaBrecque, J. F. and Younglove, B. A., "Test of densimeters for use in the custody transfer of LNG," Proceedings, International School for Hydrocarbon Measurement, Norman, Oklahoma, April 11-14, 1978.

35. Brennan, J. A., "Better LNG flow measurement sought," Oil and Gas Journal 76, 168 (1978).

36. Collier, R. S., Haber, S., Jackson, R. H. F., LaBrecque, J. F. and Tryon, P. V., "Custody transfer systems for LNG ships; tank survey techniques and sounding tables," Nat. Bur. Stand. (U.S.), Interagency Report (in preparation).

The speed of sound in saturated and compressed fluid ethane has been measured in the temperature range 91 to 323.15 K and at pressures to 35 MPa. These data were combined with newly available PρT data to obtain the isentropic compressibility and the ratio of the specific heats. The quality of the PρT data has been examined by comparison of sound speeds calculated from these data with the measured sound speeds.

Speed of sound in saturated and compressed fluid ethane

R. Tsumura and G.C. Straty

The data presented here were obtained as part of a programme to provide accurate thermodynamic properties data for saturated and compressed fluid ethane to support the development of LNG technology at NBS and throughout the fuel gas industry.

Measurements of the sound speed in saturated liquid ethane have been made from near its triple point temperature to 303 K at frequencies of 1 and 10 MHz. Comparison of the 10 MHz data with those measured at 1 MHz along the saturation boundary indicated no detectable dispersion at higher temperatures. However, as the triple point is approached, an increasing difference in sound speeds measured at 1 MHz and 10 MHz was observed. An interpretation of this apparent dispersion is discussed. Near the critical point, where the attenuation is high, two different techniques were used to measure the sound speed in the saturated liquid. Comparison with other data is made through a new empirical equation which was fitted to the saturated liquid data. This equation has only six parameters and is capable of representing the present experimental data in the entire saturated liquid region within the experimental error. In the compressed fluid, the measurements were carried out along selected isotherms at temperatures from 100 to 323.15 K at pressures to about 35 MPa.

The well-known equations

$$W^2 = \frac{1}{\rho K_s} = \gamma \left(\frac{\partial P}{\partial \rho} \right)_T \qquad (1)$$

which relate the sound speed W to the density ρ, the isentropic compressibility K_s, and the ratio of specific heats γ, have been used together with previously measured pressure, density, and temperature $(P\rho T)$ data[1-3] to determine K_s and γ from the measured sound speed for both saturated and compressed fluid ethane.

Experimental apparatus and procedure

The apparatus was identical to that used previously in this laboratory for measurements on hydrogen,[4] oxygen,[5]

The authors are with the Institute for Basic Standards, Cryogenics Division, National Bureau of Standards, Boulder, Colorado 80302, USA. RT is also with the Consejo Nacional de Ciencia y Tecnologia (CONACYT), Mexico City.   Received 7 January 1977.

fluorine,[6] and methane[7] and has been described in detail. Only a brief summary will be given here.

Two plane parallel x-cut quartz crystals are pressed to the ends of a tubular invar spacer of accurately known length. An electrical pulse to one crystal generates an acoustic pulse which propagates through the fluid. An output signal is obtained from the second crystal and is observed on an oscilloscope. The received signal is generated by the pressure wave in the sample striking the receiving crystal. This pressure wave has travelled the length of the spacer tube in the liquid sample. Successive acoustic signals result from echoes which have made multiple transits through this distance. In the pulse-echo technique used mostly here, the pulse repetition rate is adjusted so the arrival time of a pulse echo at the receiving crystal coincides with that of the succeeding directly received pulse. Under these conditions, the sound speed W is determined by

$$W = 2df \qquad (2)$$

where f is the pulse repetition frequency and d is the length of the tubular spacer. The uncertainty in the sound speed measured in this way is estimated to be less than 0.05, increasing somewhat in the region of high attenuation.

The use of the pulse-echo technique near the critical point is limited because of the large sound attenuation which makes it impossible to detect the pulse echoes. The sound speed can still be measured by a somewhat different technique, however. Even in the absence of echoes the observed signals include the directly received acoustic pulse as well as an electric pulse resulting from electronic cross-talk between input and output circuitry. This electric pulse is received at essentially zero time delay. The position of the acoustic pulse on the oscilloscope depends on its transit time between the crystals and is not affected by a change of the pulse repetition frequency. It is possible to superimpose the electric pulse and the preceding acoustic pulse if the pulse repetition frequency is double the frequency used in pulse-echo technique. The sound speed is then given by

$$W = fd \qquad (3)$$

Since the shape of the electric pulse is different from that of the acoustic pulse, the proper superposition of the electric and acoustic pulse is difficult to recognize. Therefore this

A-1

method of determining the sound speed is, in effect, calibrated against previously determined pulse-echo results.

At some convenient temperature near critical, where pulse-echo results have been obtained, the pulse repetition frequency is adjusted to double that obtained previously. The relative position of an easily recognized peak on both the electric and acoustic pulse is then observed. In subsequent measurements closer to the critical point, using the pulse-electric pulse method, the proper pulse repetition frequency is taken as that frequency which results in the same relative peak positions as observed in the calibration.

The pulse-electric pulse technique was used only at 10 MHz near the critical point. The main source of error in this method is due to errors in adjusting the relative position of the pulses as observed on the oscilloscope screen, but the inaccuracies are estimated to be generally less than 0.06%, increasing to 0.1% very close to the critical point where the large sound attenuation made it difficult to distinguish the acoustic pulse from the noise.

Pressures were measured by reference through differential pressure transducers to oil pressures derived from an oil dead-weight gauge believed accurate to within 0.01%. Temperatures were measured with a platinum resistance thermometer calibrated by the National Bureau of Standards on the IPTS-68. The maximum uncertainty in the measured temperature is estimated to be less than 0.05 K. The ethane used was commercially available research grade with specified minimum purity of 99.98%. This purity was verified by chromatographic analysis.

Results and discussion

The sound speeds in the saturated liquid were fitted to an equation of the form,

$$W(T) = (T_c - T)^\alpha \sum_{i=0}^{n} a_i X^i \qquad (4)$$

where $0 < \alpha < 1$, $X = \ln(T_c - T + 1)$, T_c = critical temperature = 305.33 K. The exponent α was first chosen by trial and error and the coefficients a_i were then found by an unweighted least squares method. The coefficients obtained are as follows:[8]

a_0 = 238.6983990 a_1 = − 95.64244603

a_2 = 39.94268780 a_3 = − 7.318579991

a_4 = 0.7402281555 α = 0.32

Increasing the number of parameters showed no significant improvement in the fit. Measured and calculated values are tabulated together with the percent differences in Table 1. From a comparison between values measured at 10 and 1 MHz above 295 K and from the agreement between the data measured with the different techniques mentioned before no dispersion is indicated.

Equation 4 was used to compare other available data with the present data. Relative percent deviations for saturated liquid are shown in Fig. 1. Poole and Aziz[9] and Vangeel[10] estimated an uncertainty of ± 0.2% for their data. However,
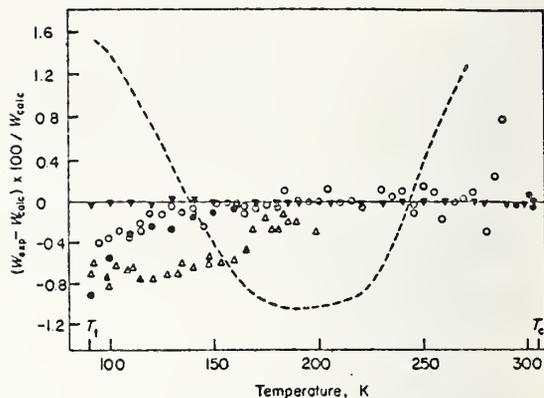
Fig. 1 Deviation plot of sound speeds in saturated liquid ethane compared with values calculated from (4)
▼ ●—this work at 10 and 1 MHz respectively. ○—Vangeel,[9] △—Poole and Aziz,[8] – – –—calculated[1] from volumetric and calorimetric data

their measurements are systematically lower than this work by about 0.6 and 0.4% respectively near the triple point temperature (90.348 K).[11] The fact that Vangeel used the same pulse-echo technique but at a frequency of 2 MHz, suggests that the difference near the triple point could be a dispersion effect. To test this possibility some data were taken at 1 MHz near the triple point and, as is shown in Fig. 1, were, in general, lower than those of Vangeel reaching a difference of 0.9% at 91 K. The apparent dispersion was in the same direction to that encountered by Gammon and Douslin for methane.[12] Although they only took measurements down to 113 K they found it necessary to make a correction to zero frequency of less than 0.025% for their measuring frequency of 1.5 MHz.

To learn more about this apparent dispersion, sound speed measurements were also performed on saturated liquid methane at 1 MHz. The data obtained were smaller than those measured by Straty[7] at 10 MHz but only by about 0.1% at 91 K. At this temperature the acoustic wavelength in methane is similar to that in ethane at about 160 K where the dispersion was also around 0.1%. This similarity suggested the possibility that the apparent dispersion could be independent of the substance depending only on experimental geometry. To verify this interpretation, measurements of sound speed in water were carried out at both 10 and 1 MHz with the same sample holder. The measurements were made near room temperature where the acoustic wavelengths are again similar to those in methane near the triple point. The results showed that the 1 MHz data were again lower by roughly 0.1% than at 10 MHz. These results seem to indicate that this dispersion is identical to that observed by Lastovka and Carome[13] who made an experimental study of the speed of ultrasonic pulses in cylindrical, water-filled, metallic wave guides. They used both the pulse-echo technique and a direct source-to-receiver signal travel time method to test wave guides with inside diameters of 1.27, 2.54, and 3.49 cm. At 5 MHz they found that the measured sound speed in water in the temperature range 23 to 30°C was the same with any of these wave guides and to the free field value (without wave guide). However for frequencies lower than 5 MHz, the sound speed decreased with both the frequency (4, 3, 2, and 1 MHz) and with the diameter of the

A−2

Table 1. Speeds of sound W and derived values of the isentropic compressibility K_s and ratio γ of heat capacities in saturated liquid ethane

Columns 3 and 4 give the values of W calculated from (4) and the percent deviation respectively. e and 1 indicates data measured with pulse-electric pulse technique and at 1 MHz respectively.

T, K		W_{expt}, m s^{-1}	W_{calc}, m s^{-1}	ΔW, %	ρ, mol l^{-1}	K_s, GPa^{-1}	γ
91.0		2002.6	2002.9	−0.013	21.656	0.3829	1.425
95.0		1974.1	1974.4	−0.016	21.511	0.3967	1.438
100.0		1938.7	1938.8	−0.003	21.328	0.4149	1.456
105.0		1902.8	1903.0	−0.010	21.146	0.4344	1.473
110.0		1867.4	1867.1	0.015	20.963	0.4549	1.492
115.0		1831.2	1831.1	0.004	20.779	0.4773	1.510
120.0		1795.0	1795.0	0.000	20.595	0.5012	1.528
125.0		1759.0	1758.8	0.014	20.410	0.5266	1.546
130.0		1722.8	1722.4	0.024	20.224	0.5540	1.563
135.0		1685.9	1685.9	0.002	20.037	0.5839	1.580
140.0		1649.4	1649.2	0.011	19.849	0.6158	1.596
145.0		1612.7	1612.4	0.017	19.660	0.6504	1.612
150.0		1575.5	1575.5	0.001	19.469	0.6882	1.627
155.0		1538.3	1538.4	−0.006	19.276	0.7290	1.642
160.0		1501.1	1501.1	−0.002	19.082	0.7734	1.656
165.0		1463.6	1463.7	−0.006	18.885	0.8220	1.670
170.0		1426.0	1426.1	−0.006	18.687	0.8752	1.684
175.0		1388.1	1388.2	−0.013	18.486	0.9336	1.697
180.0		1350.3	1350.3	0.000	18.282	0.9977	1.710
185.0		1312.1	1312.1	0.000	18.075	1.069	1.723
190.0		1273.6	1273.7	−0.006	17.865	1.148	1.735
195.0		1235.0	1235.0	−0.002	17.651	1.235	1.748
200.0		1196.0	1196.1	−0.011	17.433	1.334	1.761
205.0		1156.9	1157.0	−0.007	17.211	1.444	1.774
210.0		1117.4	1117.5	−0.012	16.984	1.568	1.788
215.0		1077.7	1077.8	−0.009	16.751	1.709	1.802
220.0		1037.7	1037.7	−0.003	16.513	1.871	1.817
225.0		997.2	997.3	−0.011	16.267	2.056	1.834
230.0		956.5	956.5	0.001	16.015	2.270	1.852
235.0		915.2	915.3	−0.006	15.753	2.520	1.872
240.0		873.6	873.5	0.007	15.483	2.815	1.894
245.0		831.3	831.3	0.001	15.201	3.166	1.920
250.0		788.5	788.4	0.008	14.908	3.588	1.949
255.0		745.0	744.9	0.014	14.600	4.104	1.984
260.0		700.7	700.6	0.021	14.275	4.746	2.026
265.0		655.4	655.3	0.020	13.930	5.557	2.078
270.0		608.9	608.9	0.008	13.562	6.613	2.143
275.0		561.0	561.0	−0.005	13.164	8.027	2.226
280.0		511.4	511.4	−0.006	12.728	9.990	2.342
285.0	e	459.4	459.5	−0.015	12.240	12.87	2.507
290.0	e	404.1	404.2	−0.027	11.680	17.43	2.772
295.0	e	343.9	343.9	−0.008	11.003	25.56	3.269
295.0	1	343.9	343.9	−0.008	11.003	25.56	3.269
296.0	e	331.1	331.0	0.030	10.846	27.98	3.429
296.0	1	330.9	331.0	−0.031	10.846	27.99	3.427
297.0	e	317.7	317.7	0.003	10.679	30.85	3.624
297.0	1	317.6	317.7	−0.029	10.679	30.86	3.622
298.0	e	303.9	303.9	−0.011	10.500	34.29	3.867
298.0	1	303.9	303.9	−0.011	10.500	34.30	3.866
299.0	e	289.6	289.6	−0.017	10.306	38.47	4.183
299.0	1	289.7	289.6	0.018	10.306	38.44	4.186
300.0	1	274.8	274.7	0.031	10.093	43.64	4.618
301.0	1	259.1	259.0	0.057	9.854	50.28	5.240
302.0	1	241.9	242.0	−0.054	9.579	59.32	6.203
303.0	1	223.2	223.2	0.009	9.249	72.18	7.966

Table 2. Speed of sounds W and derived values of the isentropic compressibility K_s and ratio γ of heat capacities in compressed fluid ethane

e and I indicates data measured with pulse-electric techniques and at 1 MHz respectively

P, MPa	W, m s^{-1}	ρ, mol l^{-1}	K_s, GPa^{-1}	γ	P, MPa	W, m s^{-1}	ρ, mol l^{-1}	K_s, GPa^{-1}	γ
	T = 100.00 K				25.381	1402.5	18.262	0.9258	1.605
					21.834	1377.9	18.164	0.9643	1.622
31.949	2051.3	21.709	0.3641	1.398	18.326	1352.4	18.061	1.007	1.640
28.495	2040.0	21.670	0.3688	1.403	14.831	1325.7	17.955	1.054	1.660
25.196	2028.8	21.633	0.3735	1.408	14.190	1321.0	17.934	1.063	1.665
21.728	2017.3	21.593	0.3785	1.414	11.523	1299.1	17.848	1.104	1.680
18.427	2005.7	21.555	0.3835	1.419	7.881	1268.2	17.724	1.167	1.703
14.981	1993.6	21.514	0.3889	1.425	4.934	1241.6	17.617	1.225	1.724
11.414	1981.0	21.471	0.3947	1.432					
7.962	1968.4	21.429	0.4005	1.439					
4.122	1954.2	21.381	0.4073	1.447		T = 220.00 K			
					35.977	1361.0	17.881	1.004	1.574
	T = 120.00 K				28.535	1308.1	17.660	1.101	1.609
					21.679	1254.4	17.434	1.212	1.647
36.342	1943.2	21.106	0.4173	1.432	15.513	1200.8	17.208	1.340	1.685
28.584	1914.2	21.006	0.4321	1.449	14.782	1194.2	17.179	1.358	1.691
18.912	1876.1	20.875	0.4526	1.473	10.057	1147.8	16.983	1.486	1.725
14.963	1860.0	20.819	0.4617	1.483	10.029	1147.5	16.982	1.487	1.725
8.105	1831.0	20.719	0.4787	1.503	7.875	1125.4	16.886	1.555	1.745
	T = 140.00 K					T = 240.00 K			
35.565	1819.4	20.451	0.4913	1.477					
28.434	1788.1	20.343	0.5113	1.496	34.279	1242.2	17.163	1.256	1.591
21.457	1756.7	20.231	0.5327	1.517	28.538	1195.8	16.957	1.372	1.622
14.708	1725.2	20.118	0.5554	1.540	21.670	1134.4	16.581	1.549	1.666
7.800	1690.7	19.996	0.5818	1.565	14.733	1063.4	16.357	1.798	1.721
					7.867	980.1	15.974	2.168	1.792
					3.559	917.3	15.684	2.520	1.851
	T = 160.00 K								
35.328	1698.2	19.805	0.5823	1.513		T = 260.00 K			
28.145	1662.8	19.676	0.6113	1.537					
21.806	1629.9	19.556	0.6402	1.560	34.541	1142.5	16.491	1.545	1.595
14.846	1591.7	19.416	0.6761	1.587	31.937	1120.1	16.384	1.618	1.609
8.013	1551.5	19.268	0.7170	1.617	28.478	1087.8	16.229	1.732	1.632
					25.289	1056.6	16.078	1.853	1.655
					22.529	1028.1	15.937	1.974	1.678
					21.770	1019.5	15.896	2.013	1.683
	T = 180.00 K				17.581	971.2	15.657	2.252	1.723
					14.835	936.3	15.482	2.450	1.754
35.697	1583.4	19.170	0.6919	1.541	11.364	887.6	15.236	2.771	1.801
28.615	1543.8	19.021	0.7336	1.567	7.801	830.2	14.942	3.229	1.862
21.600	1502.0	18.862	0.7815	1.596	5.134	780.0	14.684	3.723	1.921
14.716	1457.9	18.693	0.8371	1.628					
11.517	1435.6	18.610	0.8671	1.643					
7.879	1410.3	18.511	0.9033	1.664		T = 280.00 K			
					36.829	1068.5	15.902	1.832	1.584
	T = 200.00 K				34.921	1050.9	15.812	1.905	1.595
					32.035	1023.2	15.669	2.027	1.614
36.754	1475.4	18.551	0.8236	1.557	28.585	987.7	15.484	2.201	1.640
32.140	1446.9	18.438	0.8615	1.575	28.535	987.4	15.481	2.204	1.641
28.520	1423.6	18.346	0.8945	1.591	25.321	952.0	15.293	2.400	1.668

Table 2. Continued

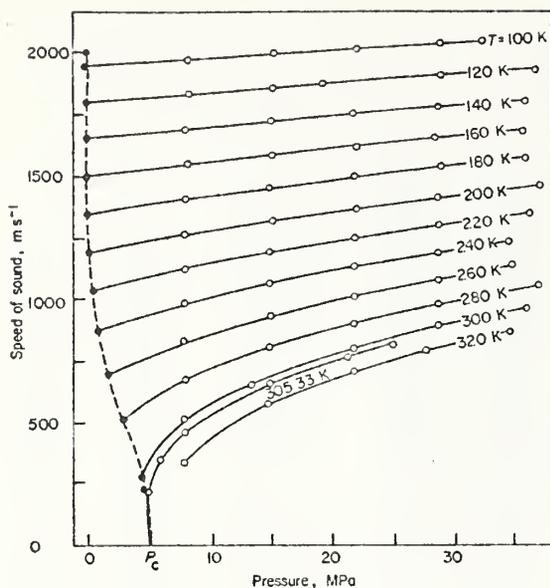| P, MPa	W, m s^{-1}	ρ, mol l^{-1}	K_s, GPa^{-1}	γ	P, MPa	W, m s^{-1}	ρ, mol l^{-1}	K_s, GPa^{-1}	γ
21.684	908.2	15.058	2.678	1.705			$T = 305.33$ K		
21.654	907.7	15.056	2.681	1.704					
18.345	863.9	14.814	3.008	1.746	24.830	821.6	14.205	3.469	1.684
14.752	809.9	14.512	3.494	1.801	21.127	768.9	13.872	4.055	1.736
14.738	809.9	14.510	3.494	1.802	18.210	722.0	13.565	4.704	1.790
11.310	750.2	14.166	4.171	1.874	14.694	656.1	13.113	5.891	1.882
7.824	676.0	13.728	5.302	1.983	11.461 l	581.3	12.567	7.830	2.021
7.804	675.7	13.725	5.308	1.985	11.324	577.8	12.540	7.945	2.029
4.998	598.0	13.253	7.017	2.132	10.156 l	544.8	12.285	9.122	2.109
					8.269 l	480.6	11.759	12.24	2.318
					7.711 e	457.8	11.559	13.73	2.419
					7.427 l	445.1	11.446	14.67	2.481
		$T = 280.00$ K			6.085 l	369.2	10.716	22.76	3.044
					5.701 e	338.7	10.387	27.91	3.442
36.829	1068.5	15.902	1.832	1.584	5.260 l	289.9	9.810	40.35	4.535
34.921	1050.9	15.812	1.905	1.595	5.222 l	284.4	9.738	42.22	4.730
32.035	1023.2	15.669	2.027	1.614	5.088 l	261.7	9.429	51.48	5.799
28.585	987.7	15.484	2.201	1.640	5.052 l	254.2	9.321	55.21	6.292
28.535	987.4	15.481	2.204	1.641	5.023 l	247.5	9.219	58.91	6.834
25.321	952.0	15.293	2.400	1.668	4.996 l	240.6	9.113	63.04	7.500
21.684	908.2	15.058	2.678	1.705	4.930 l	218.2	8.741	79.94	11.008
21.654	907.7	15.056	2.681	1.704					
18.345	863.9	14.814	3.008	1.746					
14.752	809.9	14.512	3.494·	1.801					
14.738	809.9	14.510	3.494	1.802					
11.310	750.2	14.166	4.171	1.874			$T = 320.00$ K		
7.824	676.0	13.728	5.302	1.983					
7.804	675.7	13.725	5.308	1.985	34.482	877.1	14.351	3.012	1.590
4.998	598.0	13.253	7.017	2.132	31.610	844.1	14.145	3.300	1.613
					27.495	792.8	13.811	3.831	1.656
					21.649	707.5	13.225	5.024	1.741
					16.387	610.9	12.500	7.129	1.874
					16.381	610.9	12.499	7.130	1.874
		$T = 300.00$ K			14.707	573.8	12.196	8.282	1.943
35.788	971.1	15.152	2.327	1.586	11.258	479.3	11.346	12.76	2.197
30.764	918.0	14.852	2.657	1.624	9.969	433.6	10.875	16.27	2.392
28.535	892.6	14.704	2.839	1.644	8.588 e	372.5	10.145	23.62	2.811
28.502	892.0	14.702	2.843	1.644	7.802 e	328.1	9.495	32.53	3.342
25.137	850.7	14.457	3.179	1.679	7.348 e	297.2	8.937	42.13	3.911
21.711	804.1	14.174	3.629	1.722					
21.672	803.6	14.170	3.634	1.723					
18.200	750.2	13.836	4.271	1.781					
14.841	690.4	13.444	5.190	1.858					
13.268 l	658.2	13.228	5.803	1.907			$T = 323.15$ K		
11.337 l	614.0	12.919	6.829	1.985	33.170	850.1	14.141	3.254	1.598
11.304	613.3	12.914	6.846	1.988	28.536	793.5	13.772	3.835	1.643
9.547	566.2	12.571	8.252	2.092	25.114	746.6	13.452	4.435	1.686
8.753	541.8	12.389	9.143	2.156	21.665	693.5	13.073	5.289	1.742
7.928 l	513.6	12.172	10.36	2.241	17.178 l	611.3	12.444	7.152	1.853
7.823	509.8	12.142	10.54	2.254	14.694	556.5	11.983	8.961	1.958
7.821	509.8	12.142	10.54	2.255	13.346 l	521.9	11.675	10.46	2.038
7.815	509.6	12.140	10.55	2.256	10.176 l	419.9	10.628	17.74	2.422
7.036 e	478.7	11.895	12.20	2.370	10.034 e	414.6	10.561	18.31	2.458
7.000 e	477.2	11.883	12.29	2.377	9.077 e	372.8	10.029	23.86	2.754
6.177 e	438.3	11.561	14.98	2.562	9.061 l	371.7	10.018	24.03	2.755
5.735 l	413.2	11.347	17.16	2.713	8.035 l	316.2	9.138	36.39	3.403
5.565 e	402.6	11.254	18.23	2.788	7.049 l	250.7	7.495	70.61	4.424
4.855 e	346.2	10.746	25.82	3.326	6.707 l	231.8	6.618	93.54	4.453
4.610 e	318.4	10.488	31.28	3.724	6.323 l	223.5	5.522	120.5	4.245
4.584 e	314.9	10.456	32.08	3.783	6.063 l	224.5	4.832	136.6	3.689

Fig. 2 Speed of sound in saturated liquid ● and in compressed liquid ○ ethane as a function of pressure

wave guide and they concluded that this kind of effect could be explained on the assumption that a pure plane wave is not propagated. The inside diameter of our spacer was about 1.9 cm, and from the former discussion it is believed that the data measured at 10 MHz is free from this kind of dispersion but that it probably affected this work at 1 MHz near the triple point and also the work of Vangeel at 2 MHz. It is not possible to conclude whether the measurements of Poole and Aziz were affected in the same way because they used a resonance technique.

Sound speeds for saturated liquid ethane, calculated[1] from volumetric[2] and calorimetric data,[14] are compared with the present sound speed measurements in Fig. 1. Although in the critical region the difference becomes large, at temperatures below 270 K the maximum difference is approximately 1.6%. The overall agreement between measured and calculated values is not unreasonable in view of the great demands placed on the precision and accuracy of the $P\rho T$ data and its representation and of the rather complicated series of calulations necessary to obtain sound speeds from $P\rho T$ and specific heat data.

The measured sound speeds for the compressed fluid are tabulated along isotherms in Table 2 and plotted as a function of pressure in Fig. 2. No measurements for the sound speeds in the compressed liquid are available for comparison. Measurements by Terres et al[15] along a compressed gas isotherm at 323.15 K are lower than this work by about 2 to 4% in the pressure range 8 to 10 MPa but higher at pressures around 6 MPa. We can offer no explanation for this difference.

Sound speeds calculated[1] for compressed fluid ethane from volumetric data[2] and calorimetric data[14] were compared with the present sound speed measurements (see reference 1, Table 19). The agreement in the compressed liquid (at 300 K and below) is in general within 1% except near the triple point where the differences increase to 2%. The quality of the $P\rho T$ correlation of Goodwin et al is manifested again by the general agreement within 1% with the data for the single phase fluid.

The measured sound speeds have been combined with newly available volumetric data[2] to calculate adiabatic compressibilities $K_s = -(1/V)(\partial V/\partial P)_s$ and specific heat ratios $\gamma = C_p/C_v$. The results are given in Tables 1 and 2 for the saturated and compressed fluids, respectively. Far from the critical point, the uncertainty is K_s is estimated at about ± 0.3% due to the combined uncertainty in the measured sound speed and the maximum uncertainty in the density estimated by Goodwin[1] at ± 0.2%. The uncertainty in γ is expected to be somewhat larger because of the larger uncertainty in the derivative $(\partial P/\partial\rho)_T$ obtained from the $P\rho T$ data. It is difficult to estimate the uncertainty in γ but examination of the differences between the measured and calculated speed of sound suggest the uncertainty is less than 2% at higher temperatures and lower densities far from the critical point. For the low temperature high density liquid region where $(\partial P/\partial\rho)_T$ becomes very large and where accurate determination of this derivative becomes very difficult the uncertainty is estimated to be less than 4%. Near the critical point the uncertainty in γ and K_s, is estimated to be several percent, as is suggested from the differences between the measured and calculated speeds of sound, and is the result of the inherent difficulties associated with measurements near critical points.

We would like to thank D.E. Diller for his useful comments and helpful discussions during the course of this research.

References

1 Goodwin, R.D., Roder, H.M., Straty, G.C. NBS (US) Tech Note 684, forthcoming
2 Straty, G.C., Tsumura, R. *J Res NBS (US)* 80A (1976) 35
3 Haynes, W.M., Hiza, M.J. *J Chem Thermo* (forthcoming)
4 Younglove, B.A. *J Acoust Soc Am* 38 (1965) 433
5 Straty, G.C., Younglove, B.A. *J Chem Thermo* 5 (1973) 305
6 Straty, G.C., Younglove, B.A. *J Chem Phys* 58 (1973) 2191
7 Straty, G.C. *Cryogenics* 14 (1974) 367
8 The number of digits in these coefficients are given in order to reproduce the table and are not all necessarily significant
9 Poole, G.R., Aziz, R.A. *Can J Phys* 50 (1972) 721
10 Vangeel, E. Katholieke Universiteit, Leuven, Belgium, unpublished data
11 Straty, G.C., Tsumura, R. *J Chem Phys* 64 (1976) 859
12 Gammon, B.E., Douslin, D.R. *J Chem Phys* 64 (1976) 203
13 Lastovka, J.B., Carome, E.F. *J Acoust Soc Am* 35 (1963) 1279
14 Roder, H.M. *J Res NBS (US)* 80A (1976) 739
15 Terres, V.E., Jahn, W., Reissmann, H. *Brennstoff-Chemie* 38 (1957) 129

A Correlation of the Existing Viscosity and Thermal Conductivity Data of Gaseous and Liquid Ethane

H. J. M. Hanley

Cryogenics Division, Institute for Basic Standards, National Bureau of Standards, Boulder, Colorado 80302

and

K. E. Gubbins and S. Murad

School of Chemical Engineering, Olin Hall, Cornell University, Ithaca, New York 14853

Data for the viscosity and thermal conductivity coefficients of ethane have been evaluated and represented by an empirical function. Tables of values have been prepared for the range 200–500 K, for pressure to 75 MPa ($\approx$ 750 atm). The tables include an estimate of the anomalous contribution to the thermal conductivity in the neighborhood of the critical point. The estimated uncertainties of the tabular values are $\pm 5\%$ and $\pm 8\%$ for the viscosity and thermal conductivity coefficient, respectively.

Key words: Critical point enhancement; data evaluation; ethane; thermal conductivity coefficient; viscosity coefficient.

Contents

Nomenclature

T	temperature
p	pressure
K_T	compressibility
ρ	mass density
η	viscosity coefficient
η_0	dilute gas viscosity
η_1	viscosity first density correlation
$\Delta\eta$	excess viscosity
$\Delta\eta'$	dense gas and liquid viscosity
$\Delta\eta_c$	critical region excess viscosity
j_i ($i = 1, 7$), E	viscosity equation parameters

1167

B–1

J. Phys. Chem. Ref. Data, Vol. 6, No. 4, 1977

$GV(i)$ $(i=1, 9)$ dilute gas viscosity equation parameters

λ thermal conductivity coefficient

λ_0 dilute gas thermal conductivity

λ_1 thermal conductivity first density correction

$\Delta\lambda$ excess thermal conductivity

$\Delta\lambda'$ dense gas and liquid thermal conductivity

$\Delta\lambda_c$ critical region excess thermal conductivity

k_i $(i=1, 7)$, D thermal conductivity equation parameters

$GT(i)$ $(i=1, 9)$ dilute gas thermal conductivity equation parameters

M molecular weight

N Avogadro constant

k Boltzmann constant

Φ intermolecular pair potential

$m, \gamma', \sigma, r_m, d, \epsilon$ potential parameters

A, B, C, F first density correction equation parameters

θ viscosity and thermal conductivity equation variable

$*$ reduced variable superscript

c critical point variable subscript

$x_0, \beta, E_1, E_2, \delta, \gamma$ scaling parameters for the compressibility in the critical region

R length parameter in the critical point equation

μ chemical potential

A' viscosity critical region parameter

1. Introduction

In reference [1][1] we set up a procedure to evaluate and represent the viscosity coefficient (η) and the thermal conductivity coefficient (λ) of simple fluids which has been applied to argon (with krypton and xenon), oxygen and nitrogen [1], and to methane [2, 3]. The object of this work is to include ethane; specifically to present tables of values of the transport coefficients covering a broad range of experimental conditions.

Several correlations of the ethane transport coefficients have been published [4]. Most, however, are restricted to one coefficient and most cover a limited experimental range. One of the difficulties is that the data base cannot be considered satisfactory by comparison with those of other simple fluids, such as the fluids studied in references [1–3]. For example, there are some gaps in the data coverage and the majority of the data available was published more than ten years ago. Data cannot, of course, be judged solely by their publication date, but it is generally accepted that much of the older data for many simple fluids are suspect.

(In the last ten years or so, the conventional experimental procedures (e.g., the capillary flow and oscillating disc methods for the viscosity, and the hot wire and parallel plate methods for the thermal conductivity) have been re-examined and new techniques and modifications have been proposed [5].)

In summary, we do not think it possible to present authoritative tables, with a significant assessment of accuracy, until more, and more accurate, data are available. However there is considerable technical interest in ethane at this time and it was felt worthwhile to present tables of both the viscosity and the thermal conductivity coefficients over a wide experimental range. Guidelines for work which would lead to improved tables are suggested.

In reference [1], criteria for evaluating data in the literature were discussed, and an equation for the viscosity and thermal conductivity coefficient was proposed. This paper will follow closely the format of reference [1], so the criteria and the correlating equations will be used here with only minimal comments.

2. Correlating Equations

The correlation for ethane is based on the behavior of the transport coefficients with respect to temperature (T) and density (ρ) according to the equations

$$\eta(\rho, T) = \eta_0(T) + \eta_1(T)\rho + \Delta\eta'(\rho, T) + \Delta\eta_c(\rho, T),$$

(1)

$$\lambda(\rho, T) = \lambda_0(T) + \lambda_1(T)\rho + \Delta\lambda'(\rho, T) + \Delta\lambda_c(\rho, T),$$

(2)

for the viscosity and thermal conductivity, respectively. In these equations, $\eta_0(T)$ and $\lambda_0(T)$ are the dilute gas values; $\eta_1(T)$ and $\lambda_1(T)$ represent first density corrections for the moderately dense gas; while $\Delta\eta'(\rho, T)$ and $\Delta\lambda'(\rho, T)$ are remainders. The term $\eta_1(T)$ is given by the empirical expression

$$\eta_1(T) = A + B\,[C - \ln(T/F)]^2, \qquad (3)$$

and similarly for $\lambda_1(T)$. The coefficients A, B, C and F can be found from a fit of data, but we set $F = \epsilon/k$ where ϵ is the energy parameter of the methane pair potential function and k is Boltzmann's constant. See section 3.

The terms $\Delta\eta'(\rho, T)$ and $\Delta\lambda'(\rho, T)$ are expressed empirically by the relations

$$\Delta\eta'(\rho, T) = E \exp[j_1 + j_4/T] \{\exp[\rho^{0.1}(j_2 + j_3/T^{3/2}) + \theta\rho^{0.5}(j_5 + j_6/T + j_7/T^2)] - 1.0\},$$

(4)

and

$$\Delta\lambda'(\rho, T) = D \exp\left[k_1 + k_4/T\right]\{\exp$$
$$\left[\rho^{0.1}(k_2 + k_3/T^{3/2}) + \theta\rho^{0.5}(k_5 + k_6/T + k_7/T^2)\right] - 1.0\}. \tag{5}$$

The parameter θ is included to account specifically for the high density behavior of the transport coefficients and is a function of the density with respect to the critical density, ρ_c:

$$\theta = (\rho - \rho_c)/\rho_c. \tag{6}$$

The coefficients, E, D, $j_1 \ldots j_7$, $k_1 \ldots k_7$, are to be obtained from experimental data.

Finally, equations (1) and (2) include the terms $\Delta\eta_c(\rho, T)$ and $\Delta\lambda_c(\rho, T)$, respectively, to account for the known enhancement of the coefficients in the vicinity of the critical point, see section 3.3.

As the form of the equations suggest, the transport coefficients are correlated and evaluated by examining their behavior with respect to density: thus for the viscosity, (a) we first evaluate the dilute gas and (b), with the critical region excluded, the experimental quantity $(\eta_{exp}(\rho, T) - \eta_0(T))$ is identified with the terms $\eta_1(T)\rho + \Delta\eta'(\rho, T)$. Similarly for the thermal conductivity. The critical point behavior is treated separately.

2.1. The Equation of State

Since the correlation of the transport coefficients requires temperature-density coordinates, but the majority of data are reported in temperature-pressure coordinates, an accurate equation of state is essential. The equation of state for ethane used here was derived by Goodwin and discussed in reference [6].

3. Data

Our search of the literature produced the following papers reporting experimental measurements for the transport coefficients of ethane: viscosity, references [7–21], thermal conductivity, references [10], [13], [22–30].

Criteria for selecting data for correlation are discussed in section 2 of reference [1] and the ethane measurements were evaluated according to these criteria as far as possible. For example, it was pointed out that a plot of the excess function $\Delta\eta$ or $\Delta\lambda$ (defined as $\eta_{exp}(\rho, T) - \eta_0(T)$ and $\lambda_{exp}(\rho, T) - \lambda_0(T)$, respectively) versus density leads to a good first guess as to the precision and internal consistency of a given data set; it is a convenient format to compare different data sets; the plot also allows one to judge if the qualitative behavior of the coefficients for ethane is consistent with that of other simple fluids.

We constructed figures 1 and 2 for the excess functions of ethane. Dilute gas data were represented by the empirical function discussed in section 3.1. Based on the corresponding behavior of simple fluids other than
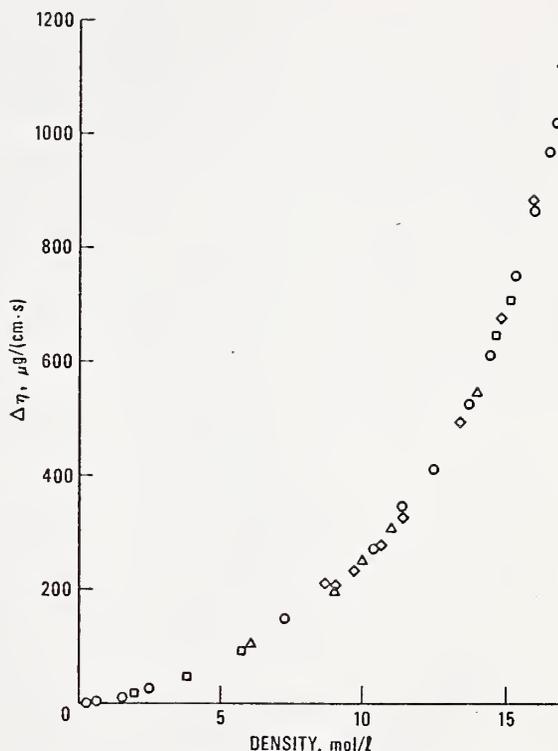

FIGURE 1. Plot of the excess viscosity coefficient versus density. O [7], ◇ [19], △ [3], □ [20].

ethane (Ar, N_2, O_2, CO_2, F_2, H_2, CH_4, etc.) one would expect that both $\Delta\eta$ and $\Delta\lambda$ for ethane would be essentially temperature independent at a given density. (See figure 1 of reference [1], however.) The plot for the excess viscosity coefficient for several temperatures, figure 1, is in fact a reasonably smooth curve, but the plot for the excess thermal conductivity coefficient shows considerable scatter.

The behavior of the excess thermal conductivity coefficient suggests that much of this data is of questionable quality.

In summary, the data base for this correlation is references [7–13], [15], [19] and [20] for the viscosity, and references [13], [22–27], and [30] for the thermal conductivity. Equal weight was given to the measurements reported in these sources.

3.1. The Dilute Gas

It is convenient to consider the dilute gas, the dense gas and liquid, and the critical region separately, as suggested by equations (1) and (2).

Viscosity Coefficient

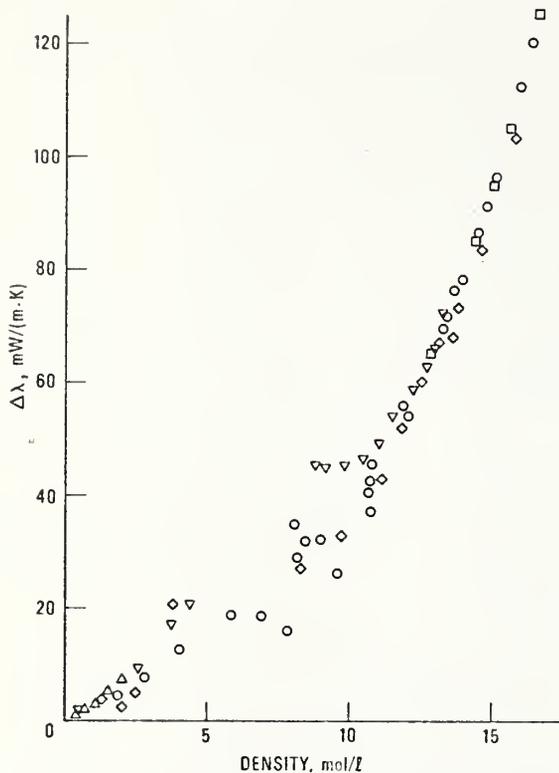Data from references [7–15] were fitted to the empirical function found suitable in our previous work [1, 2]:

B–3

FIGURE 2. Plot of the excess thermal conductivity coefficient versus density. ▽ [25–27], O [22[, △ [23], ◇ [30[, □, saturated liquid values, see text, section 3.2.

$$\eta_0 = GV(1)T^{-1} + GV(2)T^{-2/3} + GV(3)T^{-1/3} + GV(4)$$
$$+ GV(5)T^{1/3} + GV(6)T^{2/3} + GV(7)T$$
$$+ GV(8)T^{4/3} + GV(9)T^{5/3}. \qquad (7)$$

Values of the coefficients, $GV(1) \ldots GV(9)$, are listed in table 1 and a percent deviation plot is shown in figure 3. In this figure, and in subsequent figures, percent deviation is defined as

$$\frac{\eta(\text{expt}) - \eta(\text{cale})}{\eta(\text{expt})} \times 100. \qquad (8)$$

Of the data fitted, those from reference [15] are judged to be the most accurate with an estimate of inaccuracy (uncertainty) of $\pm 0.5\%$ (see the discussion in reference [1]). However, only two values at room temperature are reported. An objective assessment of the uncertainty in the data from the other authors is difficult since details of the experiments are often not available; some of the data have been extrapolated to lower pressures; the data of reference [11] can be expected to be slightly in error based on our analysis of the apparatus used [31]. It turns out, however, as can be seen in figure 3, that the data of all authors are within $\pm 2\%$. Overall, we estimate that values of the viscosity coefficient generated from equation (3) are accurate to $\pm 4\%$.
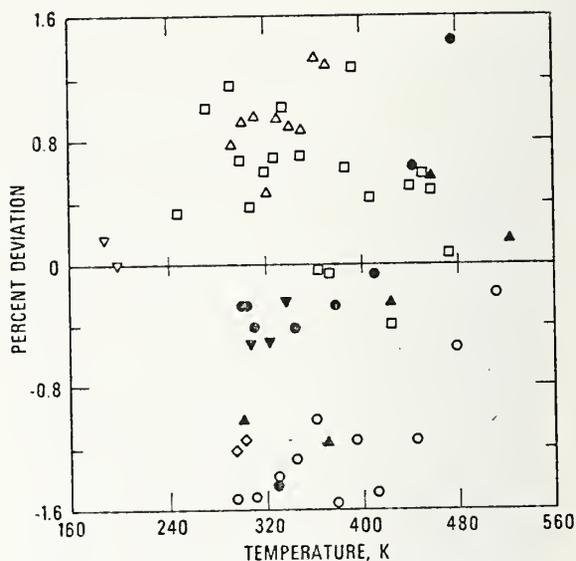

FIGURE 3. Deviation plot between dilute gas viscosity data and values calculated from equation (7): O [7], ⊕ [8], ▽ [10[, □ [9], ◇ [15], ▼ [13[, △ [12], ▲ [11].

Thermal Conductivity Coefficient

Dilute gas thermal conductivity data from references [13], [22–27], [30] were fitted to equation (9):

$$\lambda_0 = GT(1)T^{-1} + GT(2)T^{-2/3} + GT(3)T^{-1/3} + GT(4)$$
$$+ GT(5)T^{1/3} + GT(6)T^{2/3} + GT(7)T$$
$$+ GT(8)T^{4/3} + GT(9)T^{5/3}, \qquad (9)$$

which is of the same form as the dilute gas viscosity equation (7). Values of the coefficients, $GT(1) \ldots GT(9)$ are listed in table 1. A deviation curve is shown as figure 4. The thermal conductivity data cannot be considered to be very accurate (cf., figure 2); there is scatter between data sets and the internal consistency is often poor for a given data set. An estimate of inaccuracy of the values obtained from equation (9) is $\pm 6\%$.

Theoretical Calculation of the Dilute Gas Transport Coefficients

In our previous work [32], it has been shown that kinetic theory and statistical mechanics can be useful aids to assess the consistency and accuracy of data. For several gases, carbon dioxide for example [32], it was possible to show that the independently measured properties, the viscosity and thermal conductivity coefficients, the thermal diffusion factor, and the equilibrium pressure and dielectric virial coefficients, were mutually consistent. The potential function required to carry out the calculations was the m-6-8 discussed extensively

J. Phys. Chem. Ref. Data, Vol. 6, No. 4, 1977

B–4

TABLE 1. DILUTE GAS PARAMETERS FOR EQUATIONS (7) AND (9). UNITS: TEMPERATURE IN K, VISCOSITY IN MICRO-G/(CM*S) AND THERMAL CONDUCTIVITY IN MILLI-W/(M*K)

GV(1)=-.1987890689E+08
GV(2)= .1265234425E+08
GV(3)=-.2682486613E+07
GV(4)= .1518198258E+06
GV(5)= .2421166581E+04
GV(6)= .5847272516E+04
GV(7)=-.1547974517E+04
GV(8)= .1379214849E+03
GV(9)=-.4308581804E+01

GT(1)=-.1098251238E+08
GT(2)= .9388820895E+07
GT(3)=-.2962175792E+07
GT(4)= .3125105169E+06
GT(5)= .4546887452E+05
GT(6)=-.1730924346E+05
GT(7)= .2128092919E+04
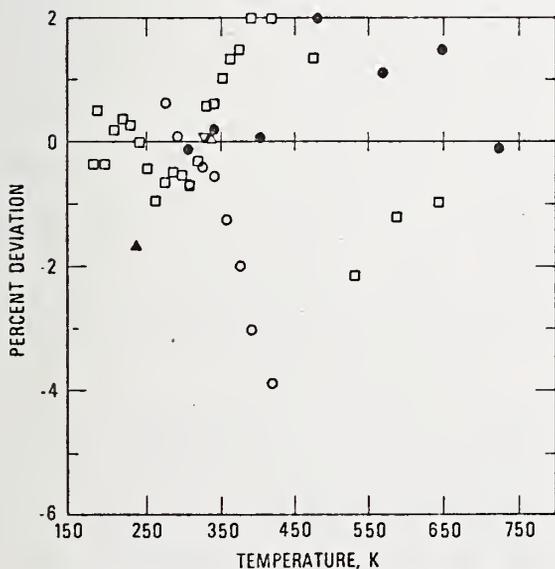GT(8)=-.1237826311E+03
GT(9)= .2869768987E+01

FIGURE 4. Deviation plot between dilute gas thermal conductivity data and values calculated from equation (9): O [30], ▽ [23], ▲ [24], △ [13], □ [25,27], ● [22].

in references [1, 2], [32] and elsewhere[2]. Following our previous work therefore, we have obtained m-6-8 para-

meters for ethane from the viscosity data which are listed in table 2.

TABLE 2. m-6-8 potential function [1] parameters and critical point parameters for ethane

Critical point constants		
$T_c = 305.4$ K		
$\rho_c = 0.2015$ g/cm³ (6.70 mol/l)		
$P_c = 4.8755$ MPa (48.117 atm)		
$M = 30.07$		
Parameters for equation (15)		
$E_1 = 2.1$		
$E_2 = 0.287$		
$x_0 = 0.166$		
$\beta = 0.355$		
$\gamma = 1.190$		
$\delta = 4.352$		
m-6-8 parameters		
$\epsilon/k = 240.0$ K		
$\sigma = 4.38 \times 10^{-10}$ m		
$r_m = 4.88 \times 10^{-10}$ m		
$\gamma' = 3.0$		
$m = 11$		

3.2. The Dense Gas and Liquid

Having values for $\eta_0(T)$, and with $\Delta\eta^c(\rho, T)$ set equal to zero, dense gas and liquid data were fitted by the method of least squares [1] to the terms $\eta_1(T)\rho + \Delta\eta'$ (ρ, T) of equation (1).

The data selected were those of references [7], [8], [19] and [20]. Equal weight was given to the data points. The accuracy of the data was judged to be ±5%. Values of the coefficients A, B, C, F, and $J_1 \ldots J_7$ are given in table 3.

Similarly for the thermal conductivity coefficient: the data selected was extracted from references [22], [23], [25–27] and [30]. As noted for figure 2, much of the data must be regarded as suspect. It is difficult to justify anything but to give equal weight to all data points.

One of the drawbacks of the thermal conductivity data base is that no values for the saturated liquid are available, but we have found by experience that equation (5) for $\Delta\lambda'$ requires data at, or close to, saturation if the equation is to represent properly the dense liquid. To ensure, therefore, that equation (5) is well-behaved at low temperatures and high densities, we considered dummy saturated liquid points obtained from the excess function graph, figure 2.

Sample deviation curves are given in figures 5–8 which indicate that the data have been fitted to within their estimated accuracy.

3.3. The Critical Region

Thermal Conductivity

As remarked, the quantity $\Delta\lambda_c(\rho, T)$ of equation (2) represents the anomalous behavior of the thermal

---

[2] The m-6-8 potential is given by the expression

$$\frac{\Phi(r^*)}{\epsilon} = \frac{1}{m-6}[6 + 2\gamma'](d/r^*)^m - \frac{1}{m-6}[m - \gamma'(m-8)] (d/r^*)^6 - \gamma'(d/r^*)^8.$$

where $d = r_m/\sigma$ and $r^* = r/\sigma$. The distance parameters σ and r_m, and the energy parameter, ϵ, are defined by the relationships $\Phi(r_m) = -\epsilon$ and $\Phi(\sigma) = 0$ while γ' is a parameter representing inverse eighth attraction in the potential.

TABLE 3. PARAMETERS FOR EQUATIONS (3)-(5).
          UNITS: TEMPERATURE IN K, VISCOSITY
          IN MICRO-G/(CM*S) AND THERMAL CON-
          DUCTIVITY IN MILLI-W/(M*K).

VISCOSITY

EQUATION 3   A=-3.911393979
                B=4.202777039
                C=1.12
                F=305.4

EQUATION 4   E=1.0
                J1=-.1005624181E+02
                J2= .3708447683E+00
                J3= .1730063144E+02
                J4= .1214721698E+05
                J5=-.3715982490E+04
                J6= .1934946036E+03
                J7= .8669596196E+02

THERMAL CONDUCTIVITY

EQUATION 3   A=.20556824905
                B=.91610917354
                C=1.12
                F=305.4

EQUATION 5   D=1.0
                K1=-.94345320091E+01
                K2= .19662879028E+01
                K3= .13089936918E+02
                K4= .14811587268E+06
                K5=-.17755038676E+05
                K6= .13738492230E+04
                K7=-.91049943375E+03
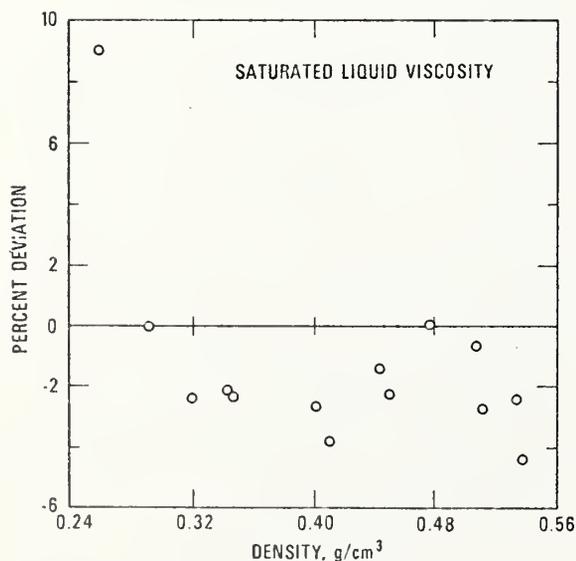
FIGURE 5. Deviation plot for the viscosity coefficient at saturated liquid boundary. Data from reference [19] compared to equation (1).
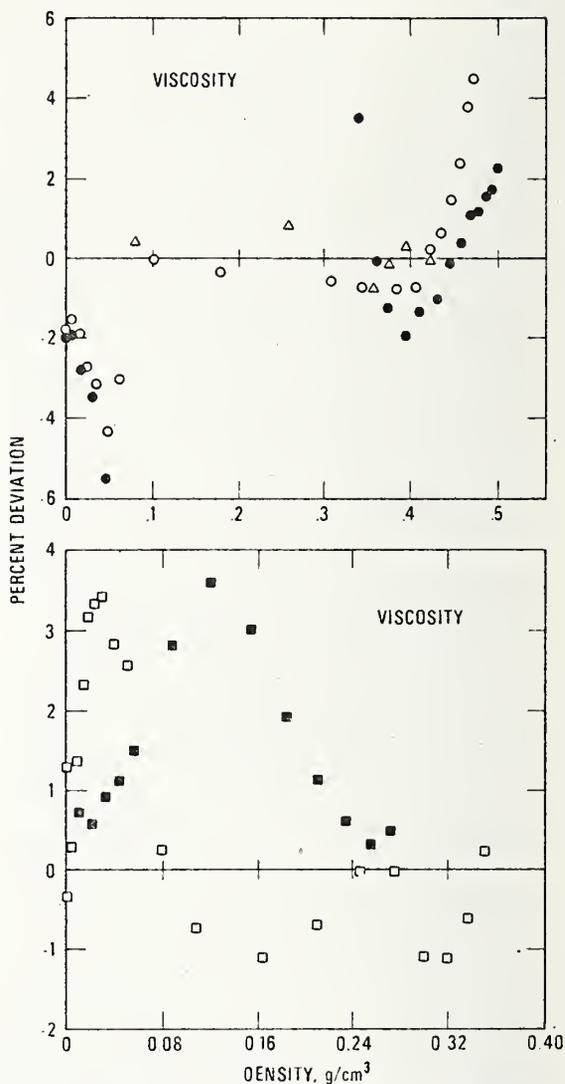

FIGURE 6. Deviation plots for the viscosity coefficient for several isotherms: top, ◉ [7] at 294 K, △ [8] at 326 K; O [7] at 327 K; bottom, ▨ [8] at 478 K, □ [7] at 511 K.

conductivity coefficient in the neighborhood of the critical point. There is no doubt that $\Delta\lambda_c$ can contribute significantly to the value of the thermal conductivity coefficient and has to be included in a correlation [1]. Conductivity data, however, in the critical region for ethane are nonexistent, hence $\Delta\lambda_c$ is obtained by calculation. The procedure is discussed in section 3.2 of reference [1] and in reference [33].

According to reference [33],

$$\Delta\lambda_c(\rho, T) = \left(\frac{M}{\rho NkT}\right)^{1/2} \frac{kT^2}{6\pi\eta R} \left(\frac{\partial P}{\partial T}\right)^2_\rho (K_T)^{1/2}$$

$$\exp\left(-18.66\ \tilde{\Delta}T^2\right) \exp\left(-4.25\ \tilde{\Delta}\rho^4\right), \qquad (10)$$

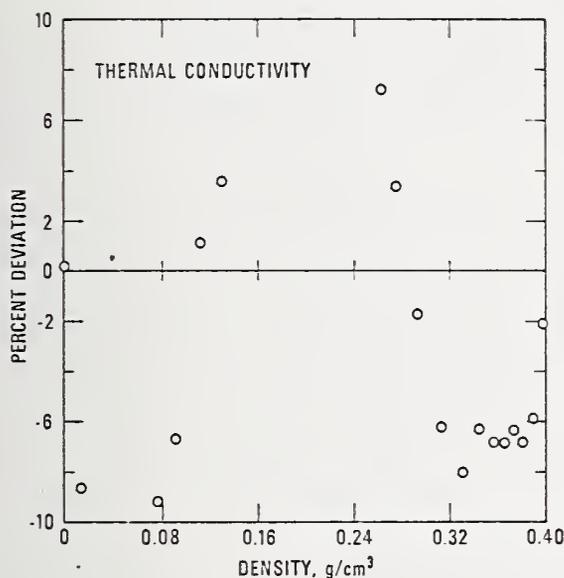J. Phys. Chem. Ref. Data, Vol. 6, No. 4, 1977

B-6

FIGURE 7. Deviation plots for the thermal conductivity coefficient at 315 K. Data from reference [26] compared to equation (2).
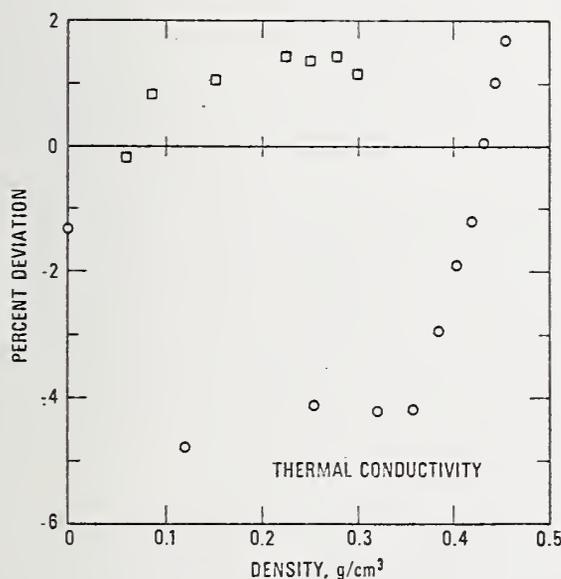

FIGURE 8. Deviation plot for the thermal conductivity coefficient at 649 K, □, and 406 K, O. Data from reference [22].

where

$$\tilde{\Delta}T = |T - T_c|/T_c;\ \tilde{\Delta}\rho = |\rho - \rho_c|/\rho_c, \qquad (11)$$

with T_c and ρ_c the critical temperature and density, respectively. In equation (10), k is Boltzmann's constant, N is Avogadro's constant, $K_T = \rho^{-1} (\partial\rho/\partial P)_T$ (the compressibility), R is a length parameter and M is the molecular weight. R is given by:

$$R = r_m^{5/2} \left(\frac{N\rho}{T^*}\right)^{1/2} \left(\frac{2\pi}{3}\right) \left[\frac{m - \gamma'(m-8)}{m-6} + \frac{\gamma'}{3}\right]^{1/2}, \qquad (12)$$

where $T^* = T/(\epsilon/k)$. m, γ', r_m and ϵ/k are the m-6-8 parameters of table 2.

One can see that the calculation of $\Delta\lambda_c$ at a given density and temperature requires the viscosity, the derivative $(\partial P/\partial T)_\rho$, and K_T. The viscosity is obtained from our correlation, and $(\partial P/\partial T)_\rho$ and K_T can be obtained from the equation of state [6]. However, it turns out that while the determination of $(\partial P/\partial T)_\rho$ presents no real difficulty, the determination of K_T does: it is now well-known that the classical, analytical, equations of state cannot describe the large compressibilities in the critical region. The equation of Goodwin used here, however, is nonanalytic and could, in principle, be used for K_T. Nevertheless, we prefer to be consistent with our previous work and introduce the scaled equation of state:

$$\rho^2 K_T = \frac{\rho_c}{P_c} |\tilde{\Delta}\rho|^{1-\delta} \left[h(x) - \frac{x}{\beta} h'(x)\right]^{-1}, \qquad (13)$$

where $h'(x) \equiv dh(x)/dx$. The derivation of equation (13) is based on the observation that the asymptotic behavior of various thermodynamic properties can be described in terms of power laws when the critical point is approached along specific paths in the $\tilde{\Delta}T - \tilde{\Delta}\rho$ plane. For example, the density along the gas and liquid branch of the coexistence curve varies asymptotically as $|\tilde{\Delta}\rho| \propto |\tilde{\Delta}T|^\beta$; the chemical potential $\mu(\rho, T)$ along the critical isotherm varies as $\mu(\rho, T_c) - \mu(\rho_c, T_c) \propto |\tilde{\Delta}\rho|^\delta$; the compressibility K_T and specific heat c_p at constant pressure vary along the critical isochore as $|\tilde{\Delta}T|^{-\gamma}$. The quantity x is given by the ratio:

$$x = \tilde{\Delta}T/|\tilde{\Delta}\rho|^{1/\beta}, \qquad (14)$$

and $h(x)$ is a function:

$$h(x) = E_1 \left(\frac{x + x_0}{x_0}\right) \left[1 + E_2 \left(\frac{x + x_0}{x_0}\right)^{2\beta}\right]^{(\gamma-1)/2\beta}. \qquad (15)$$

This equation contains the critical parameters ρ_c and T_c (through the definition of x), two critical exponents β and $\gamma[=\beta(\delta-1)]$, and three constants x_0, E_1 and E_2. Values of the constants and exponents are listed in table 2.

As an example, the total thermal conductivity coefficient $\lambda(\rho, T)$ has been calculated at three temperatures: 400 K, 310 K and 305.7 K. The appropriate excess function $\Delta\lambda[=\lambda(\rho, T) - \lambda_0(T)]$ has been plotted versus density in figure 9. It is seen that the influence of the critical point increases significantly the value of $\Delta\lambda$.
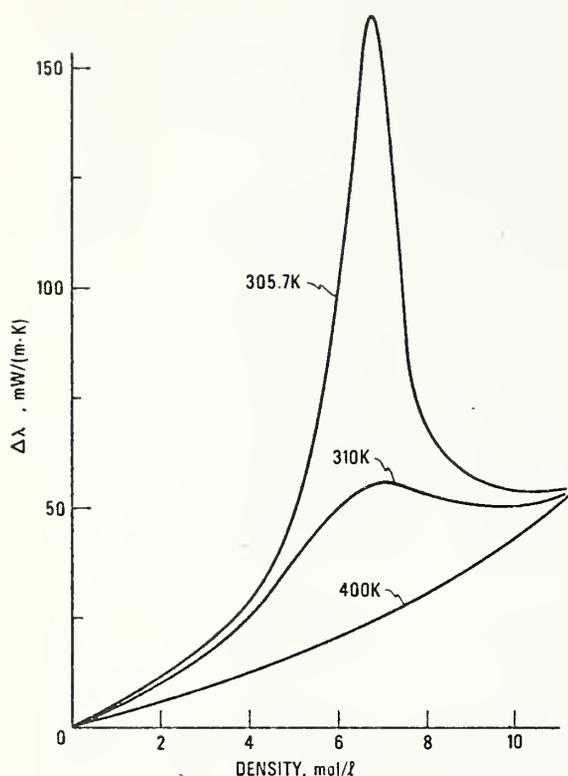
B-7

J. Phys. Chem. Ref. Data, Vol. 6, No. 4, 1977

FIGURE 9.   Plot of the calculated excess thermal conductivity coefficient, using equation (10), at 305.7 K, 310 K, and 400 K.

Viscosity Coefficient

Although it has been suspected for a long time that the viscosity coefficient of a pure fluid displays anomalous behavior in the critical region, the magnitude and quantitative features of the anomaly are still under investigation but it is generally conceded that any anomalous behavior of the viscosity is much weaker than the corresponding behavior of the thermal conductivity. Recently, however, Strumpf, Collings and Pings investigated experimentally the viscosity of ethane in the vicinity of the critical point [21]. They report an anomalous increase in the viscosity of about 16% if $\widetilde{\Delta} T \leq 0.0025$ and $\widetilde{\Delta} \rho \leq 0.25$. Further, the results agree with theoretical predictions [34] that $\Delta \eta_c / \eta(\text{back}) = A \ln \widetilde{\Delta} T$, where $\eta(\text{back})$ is the viscosity in the absence of anomaly, and A is a constant which has a numerical value of approximately 0.034. There seems little doubt that Strumpf, Collings, and Pings have verified quantitatively the existence of a critical point anomaly in the viscosity of ethane. Unfortunately, from our viewpoint, the absolute values of the coefficients are uncertain. It turns out that the coefficients away the critical point differ systematically by 5–10% from those of Carmichael and Sage [8], and of the other authors considered here. The latter results are higher

at a given temperature and density. Possible reasons for the discrepancies are discussed in reference [21].

Accordingly, in view of the discrepancies, and since the data of reference [21] cover a limited experimental region, the data were excluded from the correlation.

4. Tables of Values

The viscosity and thermal conductivity coefficients of ethane have been calculated for 200–300 K for pressures up to 50 MPa ($\approx$500 atm) and from 300–500 K for pressures to 75 MPa. Tabular values are presented as tables 4 and 5. We ensured that an entry in the table would not require an extrapolation beyond the range of data, with the exception that the low temperature-high pressure thermal conductivity coefficients required our generated saturated liquid values from the excess function. Gaps in the tables at low temperatures indicate that these *P-T* points correspond to densities exceeding 17 mol/l: the upper density limit for the data. For convenience saturated liquid values have been listed separately as table 6. (The tables contain more significant figures than the accuracy of the data warrant. The extra figures are given to facilitate reproduction and interpolation of the tables.)

4.1. Uncertainty of the Tables

We have been able to fit the data to within their estimated accuracy. The tabular values are judged to have an uncertainty of ±5% for the viscosity coefficient and ±8% for the thermal conductivity coefficient. These estimates of uncertainty refer to an estimate of accuracy on a 2σ basis. Here σ is based on the following: the scatter of the experimental data, deviations between the data and our correlation, an assessment of the data according to the criteria of reference [1] and, finally, our experience of evaluating similar data for other simple fluids. Close to the critical point, the estimated uncertainties are increased to ±10% for the viscosity coefficient, and ±20% for the thermal conductivity coefficient.

5. Conclusion

The viscosity and thermal conductivity coefficient data for ethane over a wide temperature and pressure range have been represented by an empirical function. Tables of values have been prepared. Our assessment and evaluation of the results has been handicapped by lack of reliable data. A significant improvement requires (a) data for the dilute gas over a wide temperature range, e.g., about 200–1500 K, particularly for the viscosity coefficient, (b) viscosity data for the saturated liquid from the triple point (90.35 K) to 200 K, and (c) thermal conductivity data for the saturated liquid over the whole temperature range. It would also be helpful if the more recent techniques, e.g., those using the torsional oscillating crystal for the viscosity [1], and the transient hot wire method [2], could be applied to ethane.

TABLE 4. Viscosity coefficient of ethane for various temperatures (K) and pressures (MPa). The units are μg/(cm·s)

T, K	.1	.5	1.0	1.5	2.0	2.5	3.0	3.5	4.0	5.0
200.	65.6									
205.	67.2									
210.	68.6									
215.	70.0	1173.6	1179.9	1186.1	1192.3	1198.5	1204.6	1210.7	1216.7	1228.7
220.	71.4	1109.0	1115.4	1121.7	1128.0	1134.2	1140.3	1146.4	1152.5	1164.5
225.	72.7	74.5	1054.4	1060.8	1067.2	1073.5	1079.7	1085.9	1092.0	1104.1
230.	74.1	75.9	996.5	1003.0	1009.5	1015.9	1022.3	1028.5	1034.8	1047.1
235.	75.5	77.2	941.2	947.9	954.6	961.1	967.6	974.1	980.4	992.9
240.	76.8	78.5	888.1	895.1	902.0	908.8	915.4	922.0	928.6	941.4
245.	78.2	79.9	82.4	844.2	851.4	858.4	865.4	872.2	878.9	892.1
250.	79.7	81.2	83.7	794.8	802.4	809.8	817.0	824.2	831.2	844.9
255.	81.1	82.6	85.0	746.6	754.6	762.5	770.1	777.7	785.0	799.3
260.	82.5	84.1	86.4	89.4	707.6	716.1	724.3	732.3	740.1	755.1
265.	84.0	85.5	87.7	90.6	660.9	670.1	679.1	687.7	696.1	712.1
270.	85.5	86.9	89.1	91.8	95.5	624.0	633.9	643.4	652.6	669.9
275.	87.0	88.4	90.5	93.1	96.5	576.7	588.1	598.9	609.1	628.1
280.	88.5	89.9	91.9	94.4	97.6	102.0	540.3	553.1	564.8	586.3
285.	90.0	91.4	93.3	95.7	98.7	102.7	108.7	504.3	518.7	543.8
290.	91.5	92.8	94.8	97.1	99.9	103.6	108.7	117.5	468.4	499.6
295.	93.0	94.3	96.2	98.5	101.2	104.6	109.1	115.9	407.4	451.7
300.	94.5	95.8	97.7	99.8	102.4	105.6	109.7	115.4	124.7	395.9

T, K	6.0	7.0	8.0	9.0	10.0	15.0	20.0	30.0	40.0	50.0
220.	1176.4	1188.1	1199.7	1211.1	1222.5					
225.	1116.1	1127.9	1139.5	1151.0	1162.3	1217.0				
230.	1059.2	1071.0	1082.8	1094.3	1105.7	1160.4	1212.3			
235.	1005.2	1017.3	1029.1	1040.8	1052.2	1107.2	1158.9			
240.	953.9	966.2	978.2	990.0	1001.6	1056.9	1108.7	1204.3		
245.	905.0	917.5	929.8	941.8	953.6	1009.4	1061.3	1156.5		
250.	858.1	871.0	883.6	895.9	907.9	964.4	1016.5	1111.5		
255.	813.1	826.4	839.4	852.0	864.2	921.6	974.1	1068.9	1154.8	
260.	769.6	783.5	796.9	809.8	822.5	880.9	933.8	1028.7	1114.0	
265.	727.4	741.9	755.9	769.3	782.3	842.1	895.6	990.6	1075.5	1153.6
270.	686.2	701.6	716.2	730.2	743.7	805.1	859.2	954.5	1039.0	1116.4
275.	645.7	662.1	677.6	692.4	706.5	769.6	824.6	920.3	1004.4	1081.1
280.	605.6	623.4	640.0	655.6	670.3	735.6	791.5	887.7	971.6	1047.7
285.	565.6	585.1	603.0	619.6	635.2	702.9	759.9	856.7	940.4	1016.0
290.	524.9	546.8	566.4	584.3	600.9	671.4	729.6	827.2	910.7	985.9
295.	492.8	508.1	530.0	549.5	567.4	641.2	700.7	799.1	882.5	957.2
300.	438.0	468.5	493.4	515.0	534.4	612.0	673.3	772.3	855.7	929.9

TABLE 4. Viscosity coefficient of ethane for various temperatures (K) and pressures (MPa). The units are μg/(cm·s)—Continued

T, K					P, MPa					
	.1	.5	1.0	1.5	2.0	2.5	3.0	3.5	4.0	5.0
300.	94.5	95.8	97.7	99.8	102.4	105.6	109.7	115.4	124.7	395.9
310.	97.5	98.8	100.6	102.6	105.8	107.9	111.4	115.8	121.9	149.5
320.	100.5	101.7	103.4	105.4	107.6	110.2	113.3	117.1	121.8	136.5
330.	103.5	104.7	106.3	108.1	110.2	112.6	115.4	118.7	122.6	133.5
340.	106.4	107.6	109.1	110.9	112.9	115.1	117.7	120.6	124.0	132.9
350.	109.3	110.4	111.9	113.6	115.5	117.6	119.9	122.6	125.7	133.2
360.	112.2	113.2	114.7	116.3	118.1	120.1	122.3	124.7	127.5	134.2
370.	115.0	116.0	117.4	119.0	120.7	122.5	124.6	126.9	129.5	135.5
380.	117.8	118.8	120.1	121.6	123.2	125.0	127.0	129.1	131.5	137.0
390.	120.5	121.5	122.8	124.2	125.8	127.5	129.3	131.4	133.6	138.6
400.	123.2	124.2	125.4	126.8	128.3	129.9	131.7	133.6	135.7	140.4
410.	125.9	126.8	128.0	129.4	130.8	132.4	134.1	135.9	137.8	142.2
420.	128.5	129.4	130.6	131.9	133.3	134.8	136.4	138.1	140.0	144.1
430.	131.1	132.0	133.2	134.4	135.7	137.2	138.7	140.4	142.2	146.1
440.	133.7	134.6	135.7	136.9	138.2	139.6	141.1	142.6	144.3	148.0
450.	136.2	137.1	138.2	139.3	140.6	141.9	143.4	144.9	146.5	150.0
460.	138.7	139.5	140.6	141.7	143.0	144.3	145.6	147.1	148.6	152.0
470.	141.2	142.0	143.0	144.1	145.3	146.5	147.9	149.3	150.8	154.0
480.	143.6	144.3	145.3	146.4	147.6	148.8	150.1	151.4	152.9	156.0
490.	145.9	146.6	147.6	148.7	149.8	151.0	152.2	153.5	154.9	157.9
500.	148.1	148.9	149.8	150.8	151.9	153.1	154.3	155.6	156.9	159.8

T, K					P, MPa					
	6.0	7.0	8.0	9.0	10.0	15.0	20.0	30.0	50.0	75.0
300.	438.8	468.5	493.4	515.0	534.4	0.0	0.0	0.0	0.0	0.0
310.	324.6	382.8	417.9	445.9	469.4	556.5	0.0	0.0	0.0	0.0
320.	176.8	273.7	335.7	375.1	405.1	504.6	0.0	0.0	0.0	0.0
330.	152.5	192.5	251.7	303.2	341.6	456.2	528.6	0.0	0.0	0.0
340.	146.0	167.5	201.8	243.4	293.5	411.2	487.8	0.0	0.0	0.0
350.	143.6	158.4	180.0	208.6	240.4	370.2	450.5	561.3	0.0	0.0
360.	142.0	154.3	169.8	190.0	214.1	333.9	416.6	529.1	0.0	0.0
370.	142.9	152.4	164.5	179.8	198.2	303.2	336.0	499.7	0.0	0.0
380.	143.6	151.7	161.7	174.0	188.6	278.5	359.0	472.9	0.0	0.0
390.	144.6	151.8	160.4	170.6	182.6	259.5	335.5	448.5	0.0	0.0
400.	145.9	152.3	159.8	168.6	178.8	245.1	315.4	426.3	577.4	0.0
410.	147.3	153.1	159.9	167.6	176.5	234.2	298.5	406.3	555.7	0.0
420.	148.8	154.2	160.4	167.3	175.1	226.0	284.6	388.3	535.7	0.0
430.	150.5	155.5	161.1	167.4	174.4	219.7	273.1	372.2	517.2	0.0
440.	152.2	156.9	162.1	167.8	174.2	215.0	263.8	357.8	500.1	0.0
450.	154.0	158.3	163.2	168.5	174.4	211.4	256.1	345.1	484.3	0.0
460.	155.7	159.9	164.4	169.4	174.8	208.6	249.9	333.9	469.7	596.7
470.	157.6	161.5	165.7	170.4	175.5	206.6	244.7	323.9	456.2	581.2
480.	159.4	163.1	167.1	171.5	176.2	205.1	240.5	315.2	443.7	566.6
490.	161.1	164.7	168.5	172.7	177.1	204.1	237.0	307.6	432.1	552.9
500.	162.9	166.3	169.9	173.9	178.1	203.3	234.1	300.8	421.4	540.0

TABLE 5.   Thermal conductivity of ethane for various temperatures (K) and pressures (MPa). The units are mW/(m·K)

T, K	.1	.5	1.0	1.5	2.0	2.5	3.0	3.5	4.0	5.0
					P, MPa					
200.	12.78									
205.	13.17									
210.	13.56									
215.	13.97	145.23	145.77	146.31	146.85	147.38	147.91	148.43	148.95	149.98
220.	14.40	138.54	139.08	139.62	140.15	140.69	141.20.	141.72	142.23	143.24
225.	14.83	17.10	133.17	133.70	134.24	134.76	135.29	135.80	136.32	137.33
230.	15.28	17.49	127.86	128.41	128.95	129.48	130.01	130.53	131.05	132.06
235.	15.74	17.89	123.03	123.59	124.15	124.69	125.23	125.76	126.29	127.32
240.	16.21	18.31	118.57	119.15	119.73	120.29	120.85	121.40	121.94	122.99
245.	16.69	18.73	20.65	114.98	115.59	116.18	116.76	117.33	117.89	118.99
250.	17.18	19.17	21.03	111.00	111.65	112.28	112.89	113.50	114.09	115.23
255.	17.68	19.61	21.42	107.14	107.83	108.51	109.17	109.82	110.44	111.66
260.	18.20	20.07	21.82	23.58	104.07	104.81	105.53	106.23	106.91	108.21
265.	18.72	20.54	22.24	23.91	100.27	101.10	101.91	102.68	103.42	104.83
270.	19.25	21.02	22.67	24.27	26.13	97.31	98.22	99.09	99.92	101.48
275.	19.79	21.51	23.11	24.65	26.38	93.34	94.40	95.40	96.34	98.09
280.	20.34	22.00	23.56	25.04	26.67	28.78	90.37	91.55	92.64	94.64
285.	20.90	22.52	24.02	25.46	27.00	28.89	31.86	87.50	88.80	91.10
290.	21.48	23.04	24.50	25.88	27.35	29.08	31.52	36.48	84.82	87.48
295.	22.05	23.57	24.99	26.32	27.72	29.33	31.44	34.85	80.85	83.87
300.	22.64	24.11	25.49	26.78	28.11	29.62	31.50	34.21	39.25	80.40

T, K	6.0	7.0	8.0	9.0	10.0	15.0	20.0	30.0	40.0	50.0
					P, MPa					
220.	144.24	145.22	146.19	147.15	148.09	0.00	0.00	0.00	0.00	0.00
225.	138.32	139.29	140.25	141.19	142.12	146.58	0.00	0.00	0.00	0.00
230.	133.06	134.03	134.99	135.93	136.85	141.27	145.38	0.00	0.00	0.00
235.	128.33	129.31	130.28	131.22	132.15	136.55	140.63	0.00	0.00	0.00
240.	124.02	125.03	126.01	126.97	127.90	132.33	136.40	143.77	0.00	0.00
245.	120.05	121.08	122.09	123.07	124.02	128.50	132.59	139.92	0.00	0.00
250.	116.34	117.41	118.45	119.46	120.44	125.00	129.12	136.46	0.00	0.00
255.	112.82	113.95	115.03	116.07	117.09	121.76	125.95	133.32	139.80	0.00
260.	109.45	110.63	111.77	112.86	113.92	118.74	123.01	130.45	136.93	0.00
265.	106.17	107.43	108.64	109.79	110.90	115.90	120.27	127.80	134.31	140.14
270.	102.93	104.29	105.58	106.81	107.98	113.20	117.69	125.34	131.89	137.73
275.	99.70	101.18	102.58	103.89	105.13	110.61	115.24	123.04	129.65	135.51
280.	96.43	98.07	99.59	101.01	102.34	108.11	112.91	120.88	127.56	133.45
285.	93.12	94.94	96.60	98.14	99.58	105.68	110.67	118.83	125.63	131.54
290.	89.76	91.79	93.61	95.28	96.83	103.31	108.50	116.88	123.76	129.74
295.	86.42	88.65	90.64	92.45	94.11	100.99	106.41	115.01	122.00	128.05
300.	83.18	85.59	87.73	89.67	91.44	98.72	104.37	113.22	120.33	126.45

B-11

J. Phys. Chem. Ref. Data, Vol. 6, No. 4, 1977

TABLE 5. Thermal conductivity of ethane for various temperatures (K) and pressures (MPa). The units are mW/(m·K)—Continued

					P, MPa					
T, K	.1	.5	1.0	1.5	2.0	2.5	3.0	3.5	4.0	5.0
300.	22.64	24.11	25.49	26.78	28.11	29.62	31.5G	34.21	39.25	80.4J
310.	23.85	25.23	26.53	27.73	28.96	30.29	31.86	33.86	36.68	51.35
320.	25.09	26.39	27.61	28.74	29.87	31.07	32.43	34.04	36.88	42.73
330.	26.37	27.60	28.75	29.80	30.85	31.94	33.14	34.49	36.11	40.61
340.	27.69	28.84	29.93	30.92	31.89	32.89	33.96	35.14	36.47	39.89
350.	29.05	30.13	31.16	32.09	32.99	33.92	34.88	35.92	37.06	39.81
360.	30.44	31.46	32.43	33.36	34.15	35.01	35.88	36.81	37.81	40.10
370.	31.86	32.83	33.75	34.57	35.37	36.16	36.97	37.80	38.69	40.66
380.	33.32	34.24	35.10	35.88	36.63	37.37	38.12	38.88	39.68	41.41
390.	34.82	35.68	36.50	37.24	37.94	38.64	39.33	40.04	40.76	42.31
400.	36.34	37.16	37.94	38.64	39.30	39.95	40.60	41.26	41.93	43.33
410.	37.89	38.67	39.41	40.07	40.70	41.31	41.92	42.54	43.16	44.44
420.	39.47	40.21	40.91	41.54	42.14	42.72	43.29	43.87	44.45	45.64
430.	41.07	41.78	42.45	43.04	43.61	44.16	44.70	45.25	45.79	46.90
440.	42.69	43.37	44.01	44.58	45.12	45.64	46.15	46.67	47.18	48.22
450.	44.34	44.98	45.59	46.14	46.65	47.15	47.64	48.12	48.61	49.58
460.	46.00	46.62	47.20	47.72	48.21	48.69	49.15	49.61	50.07	50.99
470.	47.68	48.27	48.83	49.33	49.79	50.25	50.69	51.13	51.56	52.44
480.	49.37	49.94	50.47	50.95	51.40	51.83	52.26	52.67	53.09	53.92
490.	51.08	51.62	52.14	52.59	53.02	53.44	53.84	54.24	54.64	55.43
500.	52.80	53.32	53.81	54.25	54.67	55.06	55.45	55.83	56.21	56.96

					P, MPa					
T, K	6.0	7.0	8.0	9.0	10.0	15.0	20.0	30.0	50.0	75.0
300.	83.19	85.59	87.73	89.67	91.44	0.00	0.00	0.00	0.00	0.00
310.	77.01	79.91	82.34	84.47	86.41	94.34	0.00	0.00	0.00	0.00
320.	58.30	72.47	76.94	79.69	81.89	90.27	0.00	0.00	0.00	0.00
330.	48.10	59.12	68.28	73.76	77.13	86.61	93.3G	0.00	0.00	0.00
340.	44.79	51.62	59.19	65.77	70.90	83.18	90.16	0.00	0.00	0.00
350.	43.42	48.12	53.67	59.24	64.31	79.62	87.24	98.20	0.00	0.00
360.	42.95	46.45	50.58	55.02	59.39	75.78	84.40	95.76	0.00	0.00
370.	42.99	45.75	48.94	52.46	56.09	71.90	81.55	93.49	0.00	0.00
380.	43.38	45.64	48.21	51.04	54.04	68.44	78.71	91.36	0.00	0.00
390.	44.02	45.93	48.06	50.39	52.89	65.70	76.05	89.34	0.00	0.00
400.	44.84	46.50	48.32	50.29	52.40	63.72	73.71	87.44	104.67	0.00
410.	45.81	47.28	48.86	50.56	52.38	62.40	71.81	85.69	103.23	0.00
420.	46.89	48.21	49.62	51.12	52.71	61.61	70.36	84.13	101.91	0.00
430.	48.05	49.26	50.53	51.88	53.30	61.26	69.35	82.86	100.71	0.00
440.	49.29	50.40	51.57	52.79	54.07	61.25	68.73	81.70	99.64	0.00
450.	50.56	51.62	52.70	53.82	54.99	61.51	68.42	80.84	98.69	0.00
460.	51.93	52.90	53.90	54.94	56.01	61.98	68.36	80.21	97.86	113.60
470.	53.33	54.23	55.17	56.13	57.13	62.62	68.56	79.80	97.16	112.87
480.	54.76	55.61	56.49	57.39	58.32	63.40	68.92	79.57	96.59	112.22
490.	56.22	57.03	57.86	58.71	59.58	64.30	69.44	79.53	96.14	111.67
500.	57.72	58.48	59.26	60.06	60.88	65.29	70.09	79.64	95.81	111.20

TABLE6. VISCOSITY AND THERMAL CONDUCTIVITY
COEFFICIENTS OF SATURATED LIQUID ETHANE.

TEMPERATURE	DENSITY	VISCOSITY	THERMAL CONDUCTIVITY
KELVIN	MOLES/L	MICRO-G/(CM*S)	MILLI-W/(M°K)
200.0	17.456	1399.9	172.0
205.0	17.235	1313.1	161.6
210.0	17.009	1241.4	152.8
215.0	16.778	1174.3	145.3
220.0	16.541	1111.2	138.7
225.0	16.296	1051.5	132.9
230.0	16.044	995.1	127.7
235.0	15.784	941.4	123.0
240.0	15.514	890.1	118.7
245.0	15.233	841.0	114.7
250.0	14.939	793.8	110.9
255.0	14.631	748.1	107.3
260.0	14.306	703.8	103.7
265.0	13.961	660.6	100.2
270.0	13.592	618.2	96.8
275.0	13.193	576.3	93.3
280.0	12.755	534.4	89.8
285.0	12.265	492.1	86.4
290.0	11.702	448.3	83.2
295.0	11.021	401.5	80.5
300.0	10.105	347.3	78.8
305.0	8.073	254.7	55.1

6. Acknowledgments

References

[1] Hanley, H. J. M., McCarty, R. D., and Haynes, W. M., J. Phys. Chem. Ref. Data 4, 979 (1974).

[2] Hanley, H. J. M., Haynes, W. M., and McCarty, R. D., J. Phys. Chem. Ref. Data 6, 597 (1977).

[3] Hanley, H. J. M., McCarty, R. D., and Haynes, W. M., Cryogenics 15, 413 (1975).

[4] For example: Makita, T., Tanaka, Y., and Nagashima, A., Rev. Phys. Soc. (Japan) 44, 98 (1974); Galloway, T. R., and Sage, B. H., J. Chem. Eng. Data 12, 59 (1967); Rossini, F. D., Pitzer, K. S., and Taylor, W. J., Nat. Bur. Stand. (U.S.) Cir. C-461 (1947); Vargaftik, N. B., Filippov, L. P., Tarzimanov, A.A., and Yurchak, R. P., "Thermal Conductivity of Gases and Liquids," Moscow (1970); Golubev, I. F., "The Viscosity of Gases and Gas Mixtures," Israel Program for Scientific Translations, Jerusalem (1970) (available from the U.S. Department of Commerce); Guereca, R. A., et al., "Thermophysical Properties of Selected Gases Below 300 K," Bureau of Mines Cir. 8317 (1967); "Thermophysical properties of matter," Vols. 3 and 11. IFI/Plenum, New York, 1975. Eds. Y. S. Touloukian, S. C. Saxena and P. Hestermans.

[5] See the references in [1].

[6] Goodwin, R. D., NBSIR 74-398 (June 1974).

[7] Eakin, B. E., Starling, K. E., Dolan, J. P., and Ellington, R. T., J. Chem. Eng. Data 7, 33 (1962).

[8] Carmichael, L. T., and Sage, B. H., J. Chem. Eng. Data 8, 94 (1963).

[9] De Rocco, A. G., and Halford, J. O., J. Chem. Phys. 28, 1152 (1958).

[10] Vogel, H., Ann Physik. 43, 1235 (1914).

[11] Trautz, M., and Sorg, K. G., Ann Physik 10, 81 (1931).

[12] Adzumi, H., Bull. Chem. Soc. (Japan) 12, 199 (1937).

[13] Lambert, J. D., Cotton, K. J., et al., Proc. Roy. Soc. (London) 231A, 280 (1955).

[14] Craven, P. M., and Lambert, J. D., Proc. Roy. Soc. (London) 205A, 439 (1951).

[15] Kestin, J., Ro. S. T., and Wakeham, W. A., Trans. Faraday Soc. 67, 2308 (1971).

[16] Ishida, Y., Phys. Rev. 21, 550 (1923).

[17] Titani, T., Bull. Chem. Soc. (Japan) 5, 98 (1930).

[18] Gerf, S. F., and Galkov, G. I., Zhur. Tekh. Fiz. 10, 725 (1940); 11, 801 (1941); 11, 613 (1941).

[19] Swift, G. W., Lorenz, J. and Kurata, F., AIChE J. 6, 415 (1960).

[20] Baron, J. D., Roof, J. G., and Wells, F. W., J. Chem. Eng. Data 4, 283 (1959).

[21] Strumpf, H. J., Collings, A. F. and Pings, C. J., J. Chem. Phys. 60, 3109 (1974).

[22] Le Neindre, B., Ph.D. Thesis, Univ. of Paris (1969).

[23] Keys, F. G., Trans. Am. Soc. Mech. Engs. 75, 809 (1954).

[24] Eucken, A., Physik Z. 14, 342 (1913).

[25] Lenoir, J. M., and Comings, E. W., Chem. Eng. Progr. 47, 223 (1951).

[26] Lenoir, J. M., Junk, W. A., and Comings, E. W., Chem. Eng. Progr. 49, 539 (1953).

[27] Gilmore, T. F., and Comings, E. W., AIChE J. 12, 1172 (1966).

[28] Zeigler, Dissertation, Halle Univ., 1904, International Critical Tables, 5, 212, McGraw-Hill, New York (1929).

[29] Moser, Ph.D. Thesis, Berlin Univ., International Critical Tables, 5, 212, McGraw-Hill, New York (1929).

[30] Carmichael, L. T., Berry, V., and Sage, B. H., J. Chem. Eng. Data 8, 281 (1963).

[31] Guevara, F. A., McInteer, B. B., Ottesen, D., and Hanley, H. J. M., Los Alamos Publ. No. LA-4643-MS (1971).

[32] For example, Ely, J. F., and Hanley, H. J. M., Molec. Phys. 30, 565 (1975).

[33] Hanley, H. J. M., Sengers, J. V., and Ely, J. F., 14th Int. Conf. on Thermal Conductivity (Storrs, Conn., June 1975) Klemens, P. G., and Chu, T. K., Eds. (Plenum Press N.Y., 1976) p. 383.

[34] Sengers, J. V., in "Transport Phenomena—1973," (AIP, New York, 1973), Kestin, J., and Ross, J., Eds., p. 229.

Measurements of the orthobaric liquid densities of methane, ethane, propane, isobutane, and normal butane [a]

W. M. HAYNES and M. J. HIZA

Cryogenics Division, National Bureau of Standards,
Institute for Basic Standards, Boulder, Colorado 80302, U.S.A.

The orthobaric liquid densities of the major components of natural gas have been determined with a magnetic suspension densimeter. This paper reports results for methane (105 to 160 K), ethane (100 to 270 K), propane (100 to 288 K), isobutane (115 to 300 K), and normal butane (135 to 300 K). The imprecision of the measured densities is approximately 0.015 per cent; the estimated overall uncertainty is 0.1 per cent at low temperatures and decreases to 0.06 per cent at 300 K. A simple expression has been used to represent the densities as a function of temperature. Comprehensive comparisons with the experimental results of other investigators are presented.

1. Introduction

Liquefied natural gas (LNG) is expected to become an increasingly important commodity on the world energy market. The basis for sale of LNG is its total heating value, which requires a knowledge of both density and composition. A project was initiated at this laboratory to provide orthobaric (saturated) liquid densities for the major components of LNG, and for mixtures of these components. The densities will be used to develop a mathematical model or correlation that predicts the density of LNG type mixtures with an inaccuracy of 0.1 per cent, given a knowledge of the composition and temperature of the liquid. In the development of an accurate mathematical model (correlation), it is important to have both an accurate and an internally consistent set of density data.

Before this project was started there were significant temperature ranges for which saturated (orthobaric) liquid density data did not exist for some of the major components of LNG. For nitrogen and methane there were discrepancies as large as 0.5 per cent between different sets of data. Not only was it important to fill in

gaps, but also to provide new independent measurements of sufficient accuracy to help resolve inconsistencies.

In this paper orthobaric liquid densities for methane, ethane, propane, isobutane, and normal butane are reported. Results for nitrogen were presented in an earlier paper.[1] Major emphasis has been placed on the low temperature region of 105 to 140 K; however, measurements have been carried out to 160 K for methane, to 270 K for ethane, to 288.7 K for propane, and to 300 K for isobutane and normal butane. The densities have been represented as a function of temperature with an expression that is used to facilitate comparisons with other measurements.

The present measurements were carried out with a magnetic suspension densimeter.[1] In this method a magnetic buoy is freely suspended in the liquid of interest by the force generated from the axial magnetic fields of air-core solenoids. The motion of the buoy is controlled by the automatic regulation of a servo-circuit. The magnetic force necessary to maintain the buoy at a given position is inversely proportional to the buoyant force on the buoy. Thus, using Archimedes' principle, along with measurements of the mass and volume of the buoy, the density of the liquid is obtained.

2. Experimental

The experimental apparatus and its operation have been described in detail elsewhere.[1] At low temperatures the experimental procedures for the measurements on the hydrocarbons other than methane differed significantly from those for nitrogen and methane. The density of a given fluid is determined from measurements of the magnetic force necessary to support a barium ferrite buoy in a vacuum and in the fluid at the same position and temperature. For nitrogen and methane the vacuum measurements were performed immediately before or after the liquid measurements. At low temperatures it has been found impossible to evacuate the sample cell within a reasonable time after it has been filled with one of the heavier hydrocarbons. Most of the liquid can be removed by pressurizing with helium gas; however, a liquid film is left on the surfaces, including those of the buoy, inside the cell. The buoy cannot be brought into support until the film is removed. Thus, for the heavy hydrocarbons at low temperatures, the vacuum points must be obtained before the liquid measurements.

So that more than one point could be obtained in a given day for a heavy hydrocarbon at low temperatures, vacuum points were obtained at two temperatures separated by 5 K before liquid was condensed into the cell. Then the liquid measurements were performed at each of these temperatures. Performance tests had demonstrated that the barium ferrite buoy does not exhibit any detectable hysteresis at low temperatures within the precision of the current measurements for a temperature range of, at least, 20 K. After the vacuum and liquid measurements were performed for one of the heavy hydrocarbons at low temperatures the cell was warmed to a temperature above the normal boiling temperature of the test fluid for evacuation.

Methane was used as a control fluid during the heavy-hydrocarbon measurements at low temperatures. Each day a new methane point was taken to insure that the

warm-up and cool-down of the apparatus did not affect the apparent position of the buoy from liquid-to-vacuum measurements. The position of the buoy was determined with a high-powered microscope that had been adjusted initially so that the apparent position of the buoy did not depend on the index of refraction of the fluid inside the cell. It was found that the temperature cycling of the cell had no detectable effect on the apparent buoy position.

Some of the results presented in this paper were taken with a one-coil system instead of the three-coil arrangement described in the apparatus paper.[1] The evolution to the use of only one coil is discussed in reference 2.

All of the gases were of research grade quality. The minimum purities as specified by the suppliers were 99.9 moles per cent for isobutane and normal butane and 99.99 moles per cent for methane, ethane, and propane. The gases were analyzed chromatographically with a thermal-conductivity detector and found to be within the specified purities except for isobutane. It was found that the isobutane contained approximately 0.15 per cent of normal butane. This relatively large amount of normal-butane impurity has a negligible effect (< 0.01 per cent) on the density results.

The methane gas was passed through a room-temperature molecular-sieve trap to remove moisture and any heavy contaminants not detected by analysis. The other hydrocarbon gases were normally not passed through a molecular-sieve trap.

3. Results

The experimental orthobaric liquid densities of methane, ethane, propane, isobutane, and normal butane are presented as a function of temperature (IPTS-68) in tables 1 to 5. The relatively large number of points for methane at any given temperature resulted from the use of methane as a control fluid throughout the project. Although the mean experimental densities of methane have been given in an earlier paper[1] they are presented again here, along with other information (calculated densities, etc.), so that the orthobaric liquid densities of all the low molecular-weight alkanes

TABLE 1. Orthobaric liquid densities of methane, where T is the temperature (IPTS-68), ρ_{expt} is the mean experimental density for n observations at a given temperature, ρ_{calc} is the density calculated from equation (1) and Δ_{max} is the largest value of $(\rho_{expt} - \rho_{calc})/\rho_{calc}$

T/K	ρ_{expt}/mol dm^{-3}	n	ρ_{calc}/mol dm^{-3}	$10^2\Delta_{max}$
105.000	26.9458	12	26.9456	0.030
110.000	26.4985	11	26.5005	0.035
115.000	26.0443	12	26.0429	0.028
120.000	25.5721	17	25.5712	0.036
125.000	25.0845	18	25.0839	0.037
130.000	24.5775	16	24.5790	0.036
135.000	24.0540	23	24.0540	0.031
140.000	23.5067	5	23.5060	0.024
145.000	22.9312	5	22.9311	0.024
150.000	22.3218	2	22.3243	0.014
160.000	20.9876	2	20.9857	0.037

13

TABLE 2. Orthobaric liquid densities of ethane, where T is the temperature (IPTS-68), ρ_{expt} is the experimental density, ρ_{calc} is the density calculated from equation (1), and Δ is the value of $(\rho_{expt} - \rho_{calc})/\rho_{calc}$

$\dfrac{T}{K}$	$\dfrac{\rho_{expt}}{mol\ dm^{-3}}$	$\dfrac{\rho_{calc}}{mol\ dm^{-3}}$	$10^2\Delta$	$\dfrac{T}{K}$	$\dfrac{\rho_{expt}}{mol\ dm^{-3}}$	$\dfrac{\rho_{calc}}{mol\ dm^{-3}}$	$10^2\Delta$
100.000	21.3408	21.3388	0.009	170.000	18.6867	18.6869	−0.001
105.000	21.1585	21.1568	0.008	180.000	18.2793	18.2787	0.003
110.000	20.9746	20.9742	0.002	190.000	17.8612	17.8586	0.015
115.000	20.7927	20.7907	0.010	200.000	17.4289	17.4240	0.028
120.000	20.6022	20.6063	−0.020	210.000	16.9713	16.9720	−0.004
125.000	20.4186	20.4208	−0.011	220.000	16.4988	16.4989	−0.001
130.000	20.2317	20.2343	−0.013	230.000	15.9973	15.9994	−0.013
135.000	20.0461	20.0466	−0.002	240.000	15.4642	15.4670	−0.018
140.000	19.8566	19.8575	−0.005	250.000	14.8899	14.8919	−0.013
150.000	19.4751	19.4748	0.002	260.000	14.2610	14.2598	0.008
160.000	19.0857	19.0850	0.004	270.000	13.5493	13.5477	0.012

TABLE 3. Orthobaric liquid densities of propane, where T is the temperature (IPTS-68), ρ_{expt} is the experimental density, ρ_{calc} is the density calculated from equation (1), and Δ is the value of $(\rho_{expt} - \rho_{calc})/\rho_{calc}$

$\dfrac{T}{K}$	$\dfrac{\rho_{expt}}{mol\ dm^{-3}}$	$\dfrac{\rho_{calc}}{mol\ dm^{-3}}$	$10^2\Delta$	$\dfrac{T}{K}$	$\dfrac{\rho_{expt}}{mol\ dm^{-3}}$	$\dfrac{\rho_{calc}}{mol\ dm^{-3}}$	$10^2\Delta$
100.075	16.3065	16.3048	0.011	140.075	15.3751	15.3755	−0.002
105.075	16.1872	16.1885	−0.008	145.075	15.2588	15.2590	−0.002
110.075	16.0718	16.0723	−0.003	150.075	15.1400	15.1424	−0.016
115.075	15.9557	15.9562	−0.003	200.000	13.9560	13.9524	0.026
120.075	15.8411	15.8401	0.006	240.000	12.9271	12.9285	−0.010
125.075	15.7250	15.7241	0.006	270.000	12.0733	12.0742	−0.008
130.075	15.6085	15.6080	0.003	280.000	11.7622	11.7631	−0.008
135.075	15.4910	15.4918	−0.005	288.706	11.4790	11.4775	0.013

TABLE 4. Orthobaric liquid densities of isobutane, where T is the temperature (IPTS-68), ρ_{expt} is the experimental density, ρ_{calc} is the density calculated from equation (1), and Δ is the value of $(\rho_{expt} - \rho_{calc})/\rho_{calc}$

$\dfrac{T}{K}$	$\dfrac{\rho_{expt}}{mol\ dm^{-3}}$	$\dfrac{\rho_{calc}}{mol\ dm^{-3}}$	$10^2\Delta$	$\dfrac{T}{K}$	$\dfrac{\rho_{expt}}{mol\ dm^{-3}}$	$\dfrac{\rho_{calc}}{mol\ dm^{-3}}$	$10^2\Delta$
115.075	12.7305	12.7313	−0.006	145.075	12.2353	12.2372	−0.015
120.075	12.6489	12.6491	−0.001	150.075	12.1534	12.1544	−0.008
125.075	12.5687	12.5669	0.015	228.000	10.8273	10.8263	0.009
130.075	12.4850	12.4846	0.003	288.706	9.6676	9.6687	−0.012
135.075	12.4015	12.4022	−0.005	290.000	9.6411	9.6417	−0.007
140.075	12.3215	12.3197	0.014	300.000	9.4300	9.4287	0.014

TABLE 5. Orthobaric liquid densities of normal butane, where T is the temperature (IPTS-68), ρ_{expt} is the experimental density, ρ_{calc} is the density calculated from equation (1), and Δ is the value of $(\rho_{expt} - \rho_{calc})/\rho_{calc}$

$\dfrac{T}{K}$	$\dfrac{\rho_{expt}}{\text{mol dm}^{-3}}$	$\dfrac{\rho_{calc}}{\text{mol dm}^{-3}}$	$10^2\Delta$	$\dfrac{T}{K}$	$\dfrac{\rho_{expt}}{\text{mol dm}^{-3}}$	$\dfrac{\rho_{calc}}{\text{mol dm}^{-3}}$	$10^2\Delta$
135.075	12.6517	12.6524	−0.005	165.075	12.1634	12.1659	−0.020
140.075	12.5706	12.5714	−0.006	170.075	12.0839	12.0846	−0.005
145.075	12.4920	12.4904	0.013	230.000	11.0911	11.0905	0.005
150.075	12.4089	12.4093	−0.003	288.706	10.0325	10.0324	0.001
155.075	12.3299	12.3283	0.014	290.000	10.0067	10.0073	−0.007
160.075	12.2484	12.2471	0.010	300.000	9.8103	9.8099	0.004

investigated in the present work are included in a single paper. All of the experimental points for methane will be presented in a future report.[3] Each methane point was taken from a new filling of the cell. For the other hydrocarbons no more than two points were taken from a single filling.

The experimental densities ρ have been fitted as a function of temperature T to the expression:

$$(\rho - \rho_c)/\text{mol dm}^{-3} = a(1 - T/T_c)^{0.35} + \sum_{i=1}^{3} b_i(1 - T/T_c)^{(1 + (i-1)/3)}, \qquad (1)$$

which incorporates a scaling-law modification[4] to a generalized Guggenheim equation.[5] The coefficients a, b_i determined by least squares, and selected values of the critical temperature T_c and density ρ_c for each fluid are given in table 6.[6-11] Only three coefficients were needed to fit the results for methane, which covered a relatively small temperature range compared with that for the other fluids.

The residual standard deviations of the fit to equation (1) for each fluid are given in table 6. These values substantiate the estimate of the imprecision of the density measurements, which is approximately 0.015 per cent. The estimated inaccuracy in

TABLE 6. Parameters of equation (1),

$$(\rho - \rho_c)/\text{mol dm}^{-3} = a(1 - T/T_c)^{0.35} + \sum_{i=1}^{3} b_i(1 - T/T_c)^{(1 + (i-1)/3)}$$

where T_c and ρ_c are the critical temperature and density. The coefficients a, b_1, b_2, b_3 were obtained from a least-squares program in which the experimental mass densities to five digits were converted to molar densities within the program. The standard deviations σ and molar masses M are also given

	Methane	Ethane	Propane	Isobutane	Normal butane
a	18.65812	12.55205	8.684459	7.657535	7.286063
b_1	6.712030	13.43284	18.04086	8.145251	11.96308
b_2	−0.9472020	−19.00461	−29.46261	−13.10582	−19.87592
b_3		11.07716	16.43559	8.145894	11.60211
T_c/K	190.555[6]	305.33[8]	369.82[9]	408.13[10]	425.16[11]
$\rho_c/\text{mol dm}^{-3}$	10.16[7]	6.86[8]	5.00[9]	3.80[10]	3.92[11]
$10^2\sigma/<\rho>$	0.016	0.012	0.011	0.013	0.012
$M/\text{g mol}^{-1}$	16.04303	30.07012	44.09721	58.1243	58.1243

the densities is 0.1 per cent at low temperatures and decreases to 0.06 per cent at 300 K. The total uncertainty in the reported temperatures is estimated to be less than 30 mK at 100 K and less than 40 mK at 300 K. These uncertainty limits in the temperature correspond to a maximum uncertainty of 0.02 per cent in the density for the results reported in this paper. A detailed error analysis of the magnetic suspension densimeter used in the present work has been given elsewhere.[1]

Equation (1), along with the parameters given in table 6, has been used for comparisons of the present results with independent experimental data.[8, 12–25] Deviation plots for ethane, propane, isobutane, and normal butane are presented in figures 1
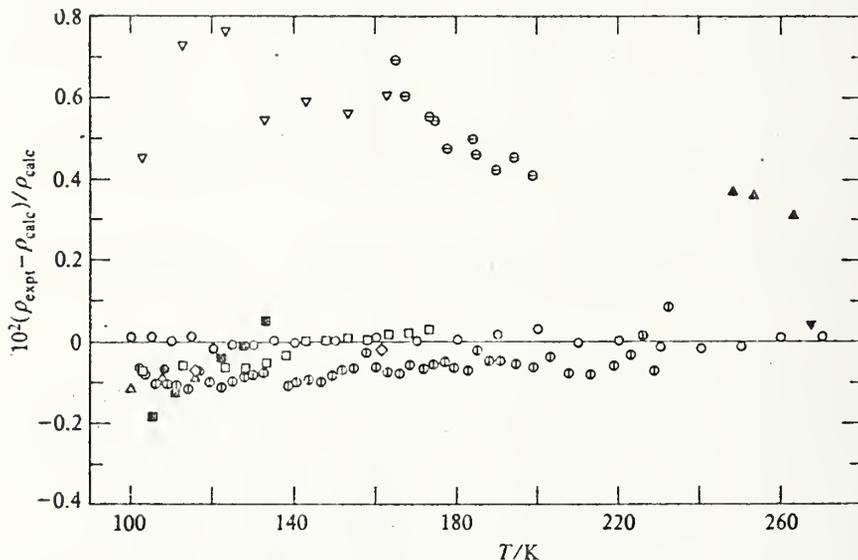
FIGURE 1. Deviation plot of experimental orthobaric liquid densities of ethane compared with values calculated from equation (1) using parameters from table 6. ○, present results; ◉, Shana'a and Canfield;[12] ◇, Chui and Canfield;[13] ◐, Orrit and Olives;[14] △ Rodosevich and Miller;[15] □, McClune;[16] ◙, Klosek and McKinley;[17] ▲, Douslin and Harrison;[18] ⊖, Maass and Wright;[19] ▽, Jensen and Kurata;[20] ▼, Kahre.[21]

through 4. The deviation plot for methane was presented in an earlier paper;[1] thus, it is not included here.

In comparing the results of other investigators with equation (1) some general trends are observed. Below 140 K the densities of Shana'a and Canfield,[12] Chui and Canfield,[13] Orrit and Olives,[14] Rodosevich and Miller,[15] McClune,[16] and Klosek and McKinley[17] are generally lower than the present results by 0.05 to 0.1 per cent. Exceptions to this trend are: for isobutane the densities of Rodosevich and Miller[15] between 114 and 120 K are larger (maximum of 0.1 per cent) than the present results and exhibit a significantly different temperature dependence; and for ethane the change in density with temperature reported by Klosek and McKinley[17] is appreciably larger than that observed in the present work.
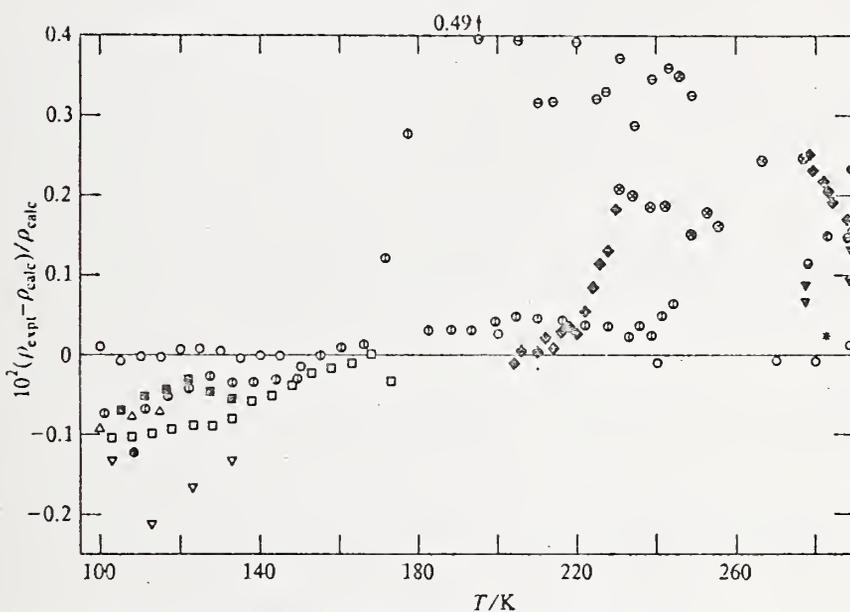
FIGURE 2. Deviation plot of experimental orthobaric liquid densities of propane compared with values calculated from equation (1) using parameters from table 6. ○, present results; *, Sliwinski;[8] ◉, Shana'a and Canfield;[12] ⊕, Orrit and Olives;[14] △, Rodosevich and Miller;[15] □, McClune;[16] ▨, Klosek and McKinley;[17] ⊖, Maass and Wright;[19] ▽, Jensen and Kurata;[20] ▼, Kahre;[21] ⊖, Tomlinson;[22] ◆, Seeman and Urban;[23] ⊗, NGAA;[24]; ◑, Van der Vet.[25]
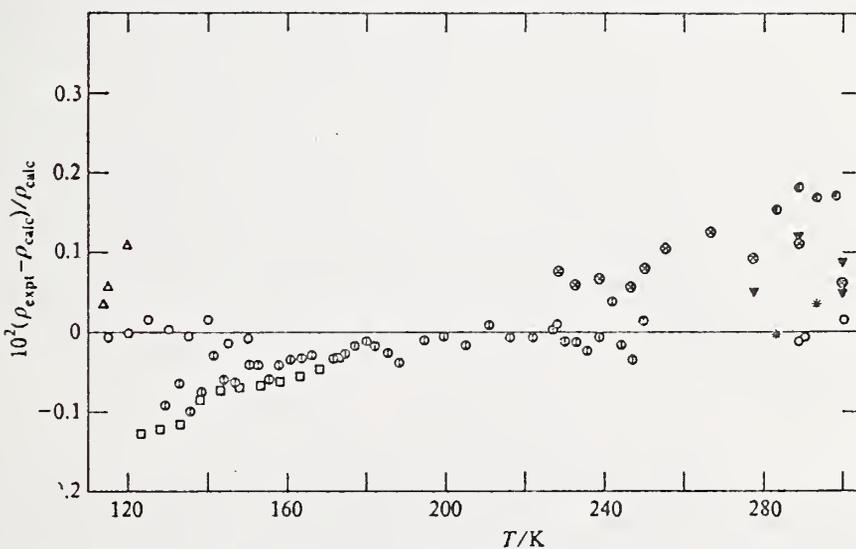
FIGURE 3. Deviation plot of experimental orthobaric liquid densities of isobutane compared with values calculated from equation (1) using parameters from table 6. ○, present results; *, Sliwinski;[8] ⊕, Orrit and Olives;[14] △, Rodosevich and Miller;[15] □, McClune;[16] ▼, Kahre;[21] ⊗, NGAA;[24] ◑, Van der Vet.[25]
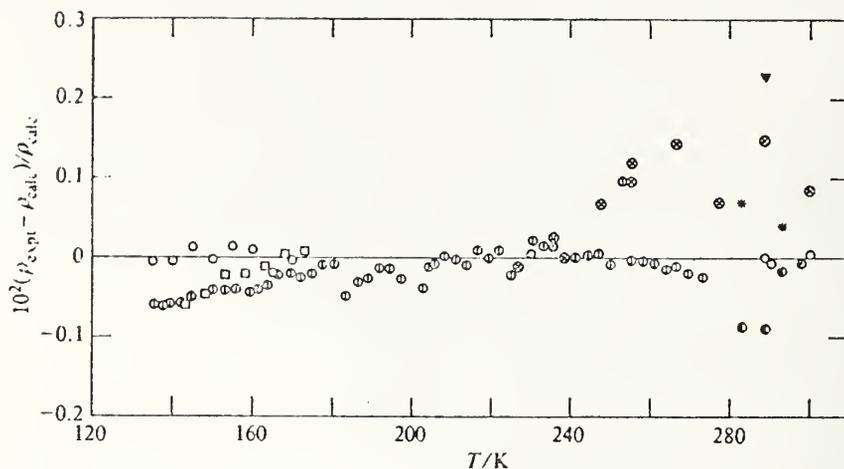
FIGURE 4. Deviation plot of experimental orthobaric liquid densities of normal butane compared with values calculated from equation (1) using parameters from table 6. ○, present results; *, Sliwinski;[8] ⊕, Orrit and Olives;[14] □, McClune;[16] ▼, Kahre;[21] ⊗, NGAA;[24] ◖, Van der Vet.[25]

Above 140 K the data of Chui and Canfield,[13] Orrit and Olives,[14] and McClune[16] differ from the present results by less than 0.05 per cent. At higher temperatures (above 280 K) the data of Sliwinski[8] for propane, isobutane, and normal butane generally differ from the present results by less than 0.05 per cent. The orthobaric liquid densities reported by Douslin and Harrison[18] for ethane at temperatures between 248 and 263 K were systematically larger than the present results by 0.3 to 0.35 per cent. Some of the older less precise (but frequently used) data have been included on the deviation plots for the sake of completeness.

Although Klosek and McKinley[17] give densities for isobutane and normal butane at temperatures between 105 and 133 K, these densities are not experimental, and therefore, are not plotted on figures 3 and 4. A few comments on the reliability of the omitted values are appropriate. Their densities were obtained from the Francis equation.[26] For normal butane at temperatures below its triple-point temperature, their results were systematically higher by less than 0.2 per cent than the densities obtained through extrapolation of the present results.[27] However, their isobutane densities at temperatures between 116 and 133 K were 1.5 per cent higher than those of the present work.

4. Summary

This research has provided accurate and self-consistent measurements of the orthobaric liquid densities of methane, ethane, propane, isobutane, and normal butane at temperatures down to 100 K. Most of the measurements recently reported by other workers differ from the present results by less than 0.1 per cent. In subsequent papers, density measurements on liquefied mixtures of the major components of liquefied natural gas will be reported.

The authors would like to acknowledge R. D. McCarty and M. J. Brown for assistance with the correlation and reduction of the data.

REFERENCES

1. Haynes, W. M.; Hiza, M. J.; Frederick, N. V. *Rev. Sci. Instrum.* 1976, 47, 1237.
2. Haynes, W. M. *Rev. Sci. Instrum.* In press.
3. Methane data are available from authors upon request and will be published in a Nat. Bur. Stand. (U.S.) report.
4. McCarty, R. D. *Nat. Bur. Stand. (U.S.), Internal Rept.* 1974, 74–357.
5. Hou, Y. C.; Martin, J. J. *A.I.Ch..E.. J.* 1959, 5, 125.
6. Goodwin, R. D. *Nat. Bur. Stand. (U.S.), Tech. Note* 653, 1974.
7. Olson, J. D. *J. Chem. Phys.* 1975, 63, 474.
8. Sliwinski, P. *Z. Phys. Chem. (Frankfurt)* 1969, 63, 263.
9. Das, T. R.; Eubank, P. T. *Advances in Cryogenic Engineering* Vol. 18. Timmerhaus, K. D.: editor. Plenum Press: New York. 1973, p, 208.
10. Das, T. R.; Reed, Jr., C. O.; Eubank, P. T. *J. Chem. Eng. Data* 1973, 18, 253.
11. Das, T. R.; Reed, Jr., C. O.; Eubank, P. T. *J. Chem. Eng. Data* 1973, 18, 244.
12. Shana'a, M. Y.; Canfield, F. B. *Trans. Faraday Soc.* 1968, 64, 2281.
13. Chui, C. H.; Canfield, F. B. *Trans. Faraday Soc.* 1971, 67, 2933.
14. Orrit, J.; Olives, J. distributed at 4th International Conference on Liquefied Natural Gas, Algeria, 1974.
15. Rodosevich, J. B.; Miller, R. C. *A.I.Ch..E. J.* 1973, 19, 729.
16. McClune, C. R. *Cryogenics* 1976, 16, 289.
17. Klosek, J.; McKinley, C. *Proc. 1st Int. Conf. on LNG*, Paper 22, Chicago, 1968.
18. Douslin, D. R.; Harrison, R. H. *J. Chem. Thermodynamics* 1973, 5, 491.
19. Maass, O.; Wright, C. H. *J. Am. Chem. Soc.* 1921, 43, 1098.
20. Jensen, R. H.; Kurata, F. *J. Petrol. Technol.* 1969, 21, 683.
21. Kahre, L. C. *J. Chem. Eng. Data* 1973, 18, 267.
22. Tomlinson, J. R. *Natural Gas Processors Assoc. Tech. Publ.* TP-1, Tulsa, Oklahoma, 1971.
23. Seeman, F.-W.; Urban, M. *Erdöl und Kohle Erdgas Petrochem.* 1963, 16, 117.
24. *Tech. Comm., Natl. Gas. Assoc. Am. Ind. Eng. Chem.* 1942, 34, 1240.
25. Van der Vet, A. P. *Congress Mondial du Petrol., Paris,* Vol. II, 1937, p. 515.
26. Francis, A. W. *Ind. Eng. Chem.* 1957, 49, 1779.
27. Haynes, W. M.; Hiza, M. J. *Advances in Cryogenic Engineering* Vol. 21. Timmerhaus, K. D.; Weitzel, D. H.; editors. Plenum Press: New York. 1976, p. 516.

Orthobaric liquid densities and excess volumes for binary mixtures of low molar-mass alkanes and nitrogen between 105 and 140 K [a]

M. J. HIZA, W. M. HAYNES, and W. R. PARRISH

Cryogenics Division, Institute for Basic Standards,
National Bureau of Standards, Boulder, Colorado 80302, U.S.A.

A magnetic suspension densimeter has been used to determine orthobaric liquid densities of gravimetrically prepared binary mixtures of the major components of liquefied natural gas (LNG) *i.e.* nitrogen, methane, ethane, propane, *i*-butane, and *n*-butane, generally between 105 and 140 K. All binary combinations were included in this study, with the exception of nitrogen + *i*-butane and nitrogen + *n*-butane. Uncertainties in the reported liquid-mixture densities are discussed in detail. Comparisons are made between excess volumes computed from the present results and comparable values from the literature. It was found that the volumetric properties of binary liquid mixtures of the heavy hydrocarbons (those mixtures not containing nitrogen or methane) are closely approximated by ideal mixing. Some observations are included on the use of excess volumes of the heavy hydrocarbon systems to determine effective molar volumes of *n*-butane in liquid mixtures below its triple-point temperature. For mixtures containing nitrogen or methane, approximate total vapor pressures are given.

1. Introduction

Custody transfer of liquefied natural gas (LNG) on the world energy market has imposed one of the most stringent requirements for accuracy in the prediction of orthobaric (saturated) liquid mixture densities. Since heating value is directly related to the density and composition of the liquid, it is desirable to be able to predict LNG densities within a small known uncertainty, preferably within ± 0.1 per cent, for any condition encountered in commerce.

The most promising theoretical methods for predicting the properties of fluid mixtures require that the pure-component characteristic parameters be combined to give the mixture characteristic parameters of the included binary pairs. It is well known that small adjustments to these parameters can significantly affect the difference

between predicted and actual mixture properties. Though reasonable estimates of deviations from the combining rules can be made in special cases,[1] the best values for a given application and model must still be derived from accurate and consistent experimental results at several temperatures for the binary mixtures and pure components of interest.

For the development of a model to predict LNG densities reliably, for example, one needs sufficiently accurate densities of uniformly high precision for the pure components and the possible binary combinations, as well as for selected multi-component mixtures, to test and optimize the prediction method. To provide this data base, a comprehensive study was initiated in our laboratory to obtain orthobaric liquid densities of the desired accuracy for the major components of LNG and for their mixtures.

Previously, orthobaric liquid densities were reported for nitrogen[2] and the low molecular-weight alkanes—methane,[2, 3] ethane, propane, i-butane, and n-butane[3] —as determined with a magnetic suspension densimeter.

The present study was conducted with the same apparatus to obtain orthobaric liquid densities for gravimetrically prepared binary mixtures of these components, generally between 105 and 140 K. All of the possible binary systems were studied, with the exception of nitrogen + i-butane and nitrogen + n-butane. Based on the phase equilibria for nitrogen + ethane[4] and nitrogen + propane[5] it was estimated that the limits of miscibility for the nitrogen + butane systems would preclude the possibility of obtaining experimental densities for these systems in the temperature range of interest. Where possible, total vapor pressures were also determined, but these are considered approximate since the main focus was to assure the reliability of the density measurements.

Excess volumes, computed for each of the binary mixtures studied, show that mixtures of the heavy hydrocarbons exhibit nearly ideal mixing. Effective liquid-phase molar volumes for n-butane below its triple-point temperature were obtained from the ethane + n-butane liquid-mixture densities by assuming that the small excess volume remains constant in the temperature range studied.

Only a few sets of orthobaric liquid-mixture densities in the literature[6] provide data applicable to the LNG problem discussed above. These data are generally limited in either the temperatures or compositions covered, or have admitted in-accuracies significantly larger than the desired ±0.1 per cent. Comparisons are made between excess volumes from the present study and comparable values taken from the literature. Prior to the present study, there were no liquid densities in the tempera-ture range of interest for nitrogen + ethane, nitrogen + propane, ethane + i-butane, propane + i-butane, propane + n-butane, or i-butane + n-butane.

2. Experimental

The magnetic suspension densimeter used in this study was discussed in detail else-where.[2, 7] All of the results reported here were obtained with the one solenoid arrangement.[7] With this arrangement a barium ferrite magnetic buoy of known mass and volume is freely suspended, in vacuum and in the liquid, by the force

generated from the axial magnetic field of a single air-core solenoid. The position of the buoy is controlled by automatic regulation of the solenoid current with a radio-frequency servo-circuit. Since the magnetic force necessary to support the buoy at a given position is dependent on the buoyant force, measurement of the solenoid current needed to support the buoy in the liquid relative to vacuum at the same position and temperature yields the liquid density directly.

The relation used to compute the density of the liquid with the one solenoid system is

$$\rho_1 = (m_b/V_b)\{1 - (I_1/I_v)\}, \tag{1}$$

where ρ_1 is the mass density of the liquid, m_b is the mass of the buoy, V_b is the volume of the buoy, and I_1 and I_v are the solenoid currents required to support the buoy at the same position in the liquid and vacuum, respectively.

The procedures used in this study were basically the same as those used in measuring liquid densities of the pure fluids.[2,3,7] Vacuum measurements were made immediately before or after those for nitrogen + methane liquid-mixture points, and each measurement was made with a separate fill. Since the temperature of the equilibrium cell had to be increased nearly to room temperature for effective removal of the heavy hydrocarbons, it was necessary to make vacuum measurements before introducing mixtures containing the heavy hydrocarbons. Measurements for these mixtures generally were made in pairs at 5 K increments with a single fill. With few exceptions a liquid-methane density measurement was made each day as a control on the measurement parameters. Liquid methane was used as the vapor-bulb fluid to provide the criteria for adjusting the control heat to the top and bottom of the cell to minimize temperature gradients. The heater currents were adjusted so that the methane vapor pressure was consistent with the temperature (IPTS-68) determined with a platinum resistance thermometer mounted near the bottom of the cell. Vapor bulb and equilibrium cell pressures were measured simultaneously with quartz Bourdon-tube pressure gages (0 to 0.69 MPa) calibrated against an air dead-weight gage. The estimated maximum uncertainty in calibration of these gages is about ±70 Pa.

Since the uncertainty in the measured density of a binary liquid mixture is inherently larger than for the pure fluids due to the added uncertainty in composition, precautions were taken to assure that the uncertainty in composition was minimized and that the composition in the equilibrium cell was homogeneous.

Basically, there are three options available to fix the composition of a liquid mixture to be studied experimentally. These are (1) liquid-phase sampling and analysis relative to calibration mixtures, (2) introducing known quantities of each pure component and mixing within the experimental chamber, and (3) introducing the desired mixture, prepared under carefully controlled conditions, into the equilibrium chamber in the mixed state. Each method, or the various combinations, requires an exact accounting of the amount of each component at some point in the process. The third method was considered to be the most desirable and potentially the most accurate for this study.

The mixtures were prepared gravimetrically in thoroughly cleaned and dried metal

cylinders, each with a free volume of about 3 dm³ and a tare mass of about 4 kg. In a few cases, cylinders with about 7 dm³ free volume and a tare mass of about 12 kg were used. All gases were research grade, and were analyzed chromatographically before use. In addition, nitrogen and methane were passed through room-temperature molecular-sieve adsorption columns to remove moisture and any heavy contaminants not detected by analysis. The amount of each component added to a cylinder was determined by difference weighings using a Class S weight set and a precision equal-arm balance with a capacity of 25 kg. An identical cylinder filled with nitrogen gas at atmospheric pressure was used as ballast on the opposite pan. The standard deviation of 10 repetitive weighings with the balance was determined by the manufacturer to be 0.51 mg. The standard deviation of 11 repetitive weighings as used in the preparation of mixtures in the laboratory was determined to be 0.67 mg. Since the uncertainty in the Class S weights is ten times lower than the standard deviation in the weighings, the uncertainty in the amount of substance of each component in the mixture prepared is dependent only on the random error in the weighing-

TABLE 1. Uncertainty δx in mole fraction of each component in the prepared mixtures based on the total amount of substance n prepared

Component	δx	
	$n = 1$ mol	$n = 5$ mol
N_2	±0.00014	±0.00003
CH_4	±0.00025	±0.00005
C_2H_6	±0.00013	±0.00003
C_3H_8	±0.00009	±0.00002
C_4H_{10}	±0.00007	±0.00001

The estimated error in mole fraction of each component is given in table 1 for both 1 and 5 mol of mixture prepared. Since two weighings are required to determine the amount of substance of each component added, the estimated errors are based on 6 times the standard deviation determined in our laboratory.

The composition, molar mass, and the total amount of substance prepared are given in table 2 for each of the binary mixtures included in this study. A comparison of the uncertainties in component composition given in table 1 with the total amount of substance of mixture prepared, given in table 2, is a direct indication of the uncertainty in composition of each mixture. Three of the mixtures given in table 2 (mixtures with $x \approx 0.5$ of methane + ethane, methane + propane, and ethane + propane) were obtained from the U.S. Bureau of Mines in Amarillo, Texas. The estimated uncertainties in component composition of these gravimetrically prepared mixtures are roughly the same as those given in table 1.[8]

A schematic diagram of the apparatus as used to measure liquid mixture densities is given in figure 1. This arrangement incorporates the same capabilities as the closed loop vapor-recirculation apparatus used in liquid-vapor equilibrium measurements[9, 10] except for vapor sampling. A window in the equilibrium cell allows visual observation of the liquid sample from about 2 cm above the bottom of the cell cavity

TABLE 2. Prepared binary mixtures: M denotes molar mass and n the total amount of substance prepared

Mixture	M/g mol^{-1}	n/mol
$0.04752N_2 + 0.95248CH_4$	16.6119	6.30
$0.30349N_2 + 0.69651CH_4$	19.6759	4.37
$0.49242N_2 + 0.50758CH_4$	21.9375	6.00
$0.05933N_2 + 0.94067C_2H_8$	29.9481	5.42
$0.02014N_2 + 0.97986C_3H_8$	43.7733	1.30
$0.03794N_2 + 0.96206C_3H_8$	43.4870	3.73
$0.06740N_2 + 0.93260C_3H_8$	43.0132	1.23
$0.35457CH_4 + 0.64543C_2H_6$	25.0965	5.04
$0.49325CH_4 + 0.50675C_2H_6$ [a]	23.1513	25.56
$0.68006CH_4 + 0.31994C_2H_6$	20.5309	4.87
$0.29538CH_4 + 0.70462C_3H_8$	35.8106	1.27
$0.49637CH_4 + 0.50363C_3H_8$ [a]	30.1720	2.19
$0.74920CH_4 + 0.25080C_3H_8$	23.0790	3.54
$0.85796CH_4 + 0.14204C_3H_8$	20.0279	4.79
$0.48687CH_4 + 0.51313i\text{-}C_4H_{10}$	37.6362	1.63
$0.58828CH_4 + 0.41172n\text{-}C_4H_{10}$	33.3687	1.92
$0.91674CH_4 + 0.08326n\text{-}C_4H_{10}$	19.5467	3.85
$0.50105C_2H_6 + 0.49895C_3H_8$ [a]	37.0689	2.23
$0.67287C_2H_6 + 0.32713C_3H_8$	34.6588	3.04
$0.68939C_2H_6 + 0.31061i\text{-}C_4H_{10}$	38.7840	1.21
$0.72436C_2H_8 + 0.27564i\text{-}C_4H_{10}$	37.8030	1.78
$0.65343C_2H_6 + 0.34657n\text{-}C_4H_{10}$	39.7929	0.83
$0.67117C_2H_6 + 0.32883n\text{-}C_4H_{10}$	39.2952	0.96
$0.49030C_3H_8 + 0.50970i\text{-}C_4H_{10}$	51.2468	0.74
$0.50326C_3H_8 + 0.49674i\text{-}C_4H_{10}$	51.0650	0.75
$0.58692C_3H_8 + 0.41308n\text{-}C_4H_{10}$	49.8915	0.53
$0.60650C_3H_8 + 0.39350n\text{-}C_4H_{10}$	49.6169	0.54
$0.60949C_3H_8 + 0.39051n\text{-}C_4H_{10}$	49.5749	0.58
$0.47039i\text{-}C_4H_{10} + 0.52961n\text{-}C_4H_{10}$	58.1243	1.03

[a] Obtained from the U.S. Bureau of Mines, Helium Operations, Amarillo, Texas.

up to the base of the vapor bulb. The vapor bulb, attached directly to the closure plug, is a slip fit in the top section of the cell. The vapor leaves the top of cell through a capillary tube passing through the vapor bulb. The density equilibrium system was designed so that the vapor volume, excluding the free volume (65 cm³) in the recirculation pump, is extremely small relative to the liquid volume. The vapor volume includes approximately 0.42 cm³ in the cell, 0.43 cm³ in the access tubing within the cryostat, and 3.3 cm³ in the pressure gage and tubing outside the cryostat. The volume occupied by the liquid is approximately 20.5 cm³. The vapor volumes were calculated from known dimensions, the liquid volume was determined by filling the cell with water, and the pump volume was determined by gas expansion. Without the pump volume, the effect of the vapor volumes on composition and density of the liquid is quite small and becomes important only at the higher mixture vapor pressures (0.2 to 0.3 MPa).

60
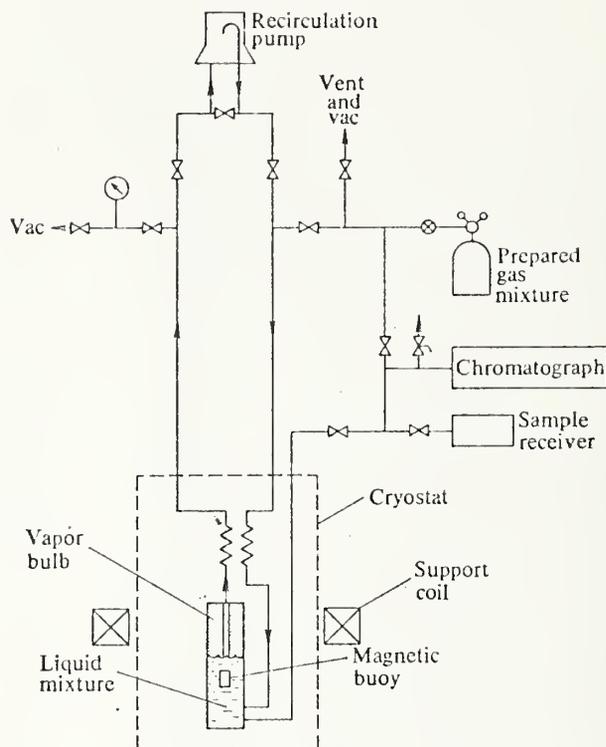
FIGURE 1. Schematic diagram of experimental apparatus.

The prepared gas mixtures were condensed directly and continuously into the equilibrium cell through the capillary vapor inlet tube at the bottom of the cell until the last vapor bubble disappeared below the vapor bulb. This filling method was used to provide continuous mixing of the liquid during the fill, analogous to vapor recirculation. For mixtures containing only the heavy hydrocarbons, the vapor pressures were extremely low, and the amount of vapor space left in the cell was unimportant. Nevertheless, the cell was filled with liquid as discussed above. There were no visible bubbles when filling with these mixtures.

For methane + heavy hydrocarbon mixtures, comparison of the measured densities before and after vapor recirculation provided a simple test of homogeneity of the liquid mixture. For these mixtures, the vapor phase is essentially pure methane at the temperatures included in this study. Ethane, the most volatile of the heavy components, has a vapor pressure of only 0.00383 MPa at 140 K.[11] Initially, the recirculation pump was filled with pure methane gas at a pressure equivalent to the vapor pressure of the mixture for the second experimental temperature, and isolated from the system. The solenoid currents for a pure liquid methane point and two vacuum points, separated by 5 K, were taken first. The prepared binary gas mixture to be studied was then condensed into the equilibrium cell in the manner discussed above. Solenoid currents for the two liquid-mixture points were measured at tempera-

tures corresponding to those of the vacuum points, the lower-temperature point generally being taken last. Subsequently, the system was opened to the pump, and vapor was recirculated through the liquid at one to three bubbles per second (probably less than 1 cm^3 min^{-1}) for several minutes. A low recirculation rate was used to avoid entrainment. The pump was then turned off, and the solenoid current for the liquid mixture point was remeasured. No change in density could be detected outside the precision of the measurement for any of the reported binary-mixture points thus tested.

For mixtures containing heavy hydrocarbons only, the most direct means to determine that the liquid sample was homogeneous and of the same composition as the prepared mixture was by liquid sampling and analysis. Ethane + propane was selected for this test. Liquid samples were withdrawn under constant helium-gas pressure (about 0.3 MPa) after the density measurements were completed. During sample withdrawal, the solenoid current was monitored to detect any variations in density as a different part of the liquid sample surrounded the magnetic buoy. Due to the extremely low vapor pressures, the compositions of these liquid mixtures are not subject to change by preferential vaporization during sampling. Each liquid sample was analyzed chromatographically using the prepared gas mixture for calibration. For these liquid mixtures, no change in solenoid current could be detected during sample withdrawal, and the composition of the liquid was found to be consistent with that of the prepared mixture within the precision of the gas analysis, *i.e.* within a few hundredths of 1 mole per cent.

Liquid samples of methane + ethane and methane + propane were also withdrawn and analyzed subsequent to the density measurements and recirculation of the vapor. However, it was extremely difficult to obtain samples of consistent composition due to preferential vaporization. At the higher temperatures ($\geqslant 135$ K) samples with compositions consistent with the prepared mixtures could be obtained by using the recirculation-pump volume as pressure ballast during withdrawal. At lower temperatures it was necessary to pressurize the cell with helium gas to obtain samples with compositions equivalent to those of the prepared mixtures. In general, however, analyses of liquid samples of the methane + hydrocarbon mixtures were mainly useful to determine that there were no gross discrepancies (greater than a few tenths of 1 mole per cent) in composition and that the liquid mixtures were not inadvertently contaminated. No attempt was made to recirculate the vapor or to sample and analyze the liquid mixtures containing nitrogen.

3. Results and discussion

EXPERIMENTAL RESULTS

The experimental orthobaric liquid-mixture amount-of-substance densities are given in table 3 as a function of temperature. The excess volumes V^E, also given in table 3, were computed from the expression:

$$V^E = V_m - \sum_i x_i \{V_i + \beta_i V_i (p_i - p_m)\}, \tag{2}$$

where V_m is the molar volume, p is the saturation pressure, x is mole fraction, and β

TABLE 3. Orthobaric liquid amount-of-substance densities ρ of binary mixtures of low molar-mass alkanes and nitrogen. T, temperature (IPTS-68); ρ_{calc}, ρ calculated from equation (4); p, pressure; V^E, excess volume

Mixture	$\dfrac{T}{K}$	$\dfrac{\rho}{\text{mol dm}^{-3}}$	$10^2\dfrac{\rho_{\text{expt}}-\rho_{\text{calc}}}{\rho_{\text{calc}}}$	$\dfrac{p}{\text{MPa}}$	$\dfrac{V^E}{\text{cm}^3\,\text{mol}^{-1}}$
$0.04752N_2 + 0.95248CH_4$	105.00	26.8476	−0.006	0.138	−0.144
	110.00	26.4052	0.010	0.199	−0.258
	115.00	25.9374	−0.002	0.263	−0.442
	120.00	25.4522	−0.006	0.350	−0.889
	125.00	24.9496	0.005	0.460	
	130.00	24.4210	0.007	0.583	
	135.00	23.8600	−0.017	0.730	
	140.00	23.2809	0.009	0.920	
$0.30349N_2 + 0.69651CH_4$	100.00	26.8735	−0.010	0.345	−0.584
	105.00	26.3393	0.023	0.456	−0.885
	110.00	25.7686	−0.005	0.618	−1.353
	115.00	25.1790	−0.017	0.801	−2.253
	120.00	24.5737	0.010	1.011	−4.510
$0.49242N_2 + 0.50758CH_4$	95.00	27.0801	0.006	0.330	−0.541
	100.00	26.4588	0.003	0.465	−0.777
	105.00	25.8106	−0.012	0.637	−1.154
	110.00	25.1387	−0.016	0.844	−1.803
	115.00	24.4431	0.006	1.097	−3.056
	120.00	23.7096	0.017	1.398	−6.110
	125.00	22.9315	0.010	1.731	
	130.00	22.1005	−0.015	2.110	
$0.05933N_2 + 0.94067C_2H_6$	105.00	21.4718		0.385	−0.423
	110.00	21.2912		0.463	−0.590
	115.00	21.0845		0.547	−0.804
	120.00	20.8998		0.638	−1.385
$0.02014N_2 + 0.97986C_3H_8$	110.00	16.2131		0.357	−0.208
	115.00	16.0931		0.471	−0.289
$0.03794N_2 + 0.96206C_3H_8$	105.00	16.4638		0.495	−0.310
	110.00	16.3410		0.671	−0.392
$0.06740N_2 + 0.93260C_3H_8$	100.00	16.8055		0.631	−0.427
	105.00	16.7084		0.880	−0.628
$0.35457CH_4 + 0.64543C_2H_6$	105.00	23.1032	0.002	0.0256	−0.382
	110.00	22.8777	0.009	0.0392	−0.442
	115.00	22.6478	0.007	0.0580	−0.505
	120.00	22.4035	−0.050	0.0826	−0.554
	125.00	22.1872	0.030	0.115	−0.673
	130.00	21.9441	0.002	0.155	−0.798
$0.49325CH_4 + 0.50675C_2H_6$	105.00	23.9619	0.031	0.0325	−0.525
	110.00	23.6937	−0.004	0.0503	−0.569
	115.00	23.4328	0.003	0.0749	−0.639
	120.00	23.1559	−0.047	0.108	−0.697
	125.00	22.8933	−0.024	0.150	−0.801
	130.00	22.6290	0.007	0.205	−0.927
	135.00	22.3581	0.024	0.272	−1.068
	140.00	22.0765	0.009	0.355	−1.223

TABLE 3—*continued*

Mixture	$\dfrac{T}{K}$	$\dfrac{\rho}{\text{mol dm}^{-3}}$	$10^2\,\dfrac{\rho_{\text{expt}} - \rho_{\text{calc}}}{\rho_{\text{calc}}}$	$\dfrac{p}{\text{MPa}}$	$\dfrac{V^{E}}{\text{cm}^3\,\text{mol}^{-1}}$
$0.68006CH_4 + 0.31994C_2H_6$	105.00	25.1027	0.002	0.0416	−0.524
	110.00	24.7802	−0.004	0.0645	−0.562
	115.00	24.4612	0.003	0.0963	−0.621
	120.00	24.1402	−0.001	0.138	−0.698
	125.00	23.8212	0.002	0.193	−0.802
	130.00	23.5007	−0.001	0.262	−0.933
$0.29538CH_4 + 0.70462C_3H_8$	105.00	18.5132		0.0270	−0.469
	110.00	18.3624		0.0409	−0.524
$0.49637CH_4 + 0.50363C_3H_8$	105.00	20.4909	0.005	0.0384	−0.727
	110.00	20.3046	−0.002	0.0591	−0.814
	115.00	20.1180	−0.006	0.0874	−0.915
	120.00	19.9311	−0.007	0.125	−1.033
	125.00	19.7471	0.014	0.173	−1.179
	130.00	19.5546	−0.004	0.232	−1.329
$0.74920CH_4 + 0.25080C_3H_8$	105.00	23.4768	0.005	0.0478	−0.700
	110.00	23.2064	−0.009	0.0738	−0.783
	115.00	22.9364	−0.004	0.110	−0.887
	120.00	22.6665	0.017	0.158	−1.014
	125.00	22.3818	−0.010	0.222	−1.141
	130.00	22.1019	0.002	0.303	−1.310
$0.85796CH_4 + 0.14204C_3H_8$	105.00	24.9622	−0.007	0.0516	−0.553
	110.00	24.6331	0.009	0.0801	−0.617
	115.00	24.2941	0.006	0.120	−0.684
	120.00	23.9491	0.002	0.173	−0.764
	125.00	23.5941	−0.021	0.242	−0.855
	130.00	23.2461	0.012	0.330	−0.992
$0.48687CH_4 + 0.51313i\text{-}C_4H_{10}$	110.00	17.3575		0.0629	−0.803
	115.00	17.2076		0.0938	−0.884
	120.00	17.0639		0.1361	−1.002
	125.00	16.9156		0.1852	−1.125
$0.58828CH_4 + 0.41172n\text{-}C_4H_{10}$	120.00	18.6495		0.1636	−1.312
	125.00	18.4772		0.2281	−1.466
	125.00	18.4853		0.2281	−1.489
	130.00	18.3058		0.3183	−1.646
$0.91674CH_4 + 0.08326n\text{-}C_4H_{10}$	105.00	25.1536	0.009		−0.599
	110.00	24.7960	−0.021		−0.638
	115.00	24.4512	0.010		−0.719
	120.00	24.0910	−0.011		−0.797
	125.00	23.7370	0.006		−0.916
	130.00	23.3789	0.018		−1.063
	135.00	23.0110	0.003		−1.234
	140.00	22.6391	−0.015		−1.451
$0.50105C_2H_6 + 0.49895C_3H_8$	105.00	18.3618	0.021		−0.040
	110.00	18.2169	0.001		−0.036
	115.00	18.0726	−0.012		−0.034
	120.00	17.9282	−0.020		−0.033
	125.00	17.7880	0.000		−0.047

TABLE 3—*continued*

Mixture	$\dfrac{T}{\text{K}}$	$\dfrac{\rho}{\text{mol dm}^{-3}}$	$10^2\,\dfrac{\rho_{\text{expt}} - \rho_{\text{calc}}}{\rho_{\text{calc}}}$	$\dfrac{p}{\text{MPa}}$	$\dfrac{V^{\text{E}}}{\text{cm}^3\,\text{mol}^{-1}}$
$0.50105C_2H_6 + 0.49895C_3H_8$	130.00	17.6412	-0.011		-0.041
	135.00	17.4988	0.009		-0.051
	140.00	17.3526	0.013		-0.051
$0.67287C_2H_6 + 0.32713C_3H_8$	125.00	18.6192			-0.044
	130.00	18.4646			-0.053
	135.00	18.3059			-0.052
	140.00	18.1509			-0.065
$0.68939C_2H_6 + 0.31061i\text{-}C_4H_{10}$	115.00	17.3716			$+0.012$
	120.00	17.2344			$+0.015$
$0.72436C_2H_6 + 0.27564i\text{-}C_4H_{10}$	105.00	17.9779			$+0.013$
	110.00	17.8401			$+0.008$
	125.00	17.4235			-0.010
	130.00	17.2825			-0.013
$0.65343C_2H_8 + 0.34657n\text{-}C_4H_{10}$	115.00	17.2184			-0.055
	120.00	17.0824			-0.045
$0.67117C_2H_6 + 0.32883n\text{-}C_4H_{10}$	110.00	17.5047	0.003		-0.045
	115.00	17.3706	-0.000		-0.050
	125.00	17.1031	0.009		-0.060
	130.00	16.9626	-0.020		-0.042
	135.00	16.8285	-0.006		-0.045
	140.00	16.6947	0.014		-0.054
$0.49030C_3H_8 + 0.50970i\text{-}C_4H_{10}$	105.00	14.3080	-0.002		$+0.086$
	110.00	14.2136	-0.007		$+0.078$
	115.00	14.1219	0.011		$+0.056$
	120.00	14.0257	0.001		$+0.057$
	125.00	13.9300	-0.002		$+0.054$
	130.00	13.8342	-0.002		$+0.052$
$0.50326C_3H_8 + 0.49674i\text{-}C_4H_{10}$	125.00	13.9718			$+0.047$
	130.00	13.8737			$+0.054$
$0.58692C_3H_8 + 0.41308n\text{-}C_4H_{10}$	110.00	14.6839			-0.034
	135.00	14.1748			$+0.021$
	140.00	14.0786			$+0.006$
$0.60650C_3H_8 + 0.39350n\text{-}C_4H_{10}$	140.00	14.1343			$+0.010$
	145.00	14.0333			$+0.015$
	150.00	13.9346			$+0.009$
$0.60949C_3H_8 + 0.39051n\text{-}C_4H_{10}$	115.00	14.6487			-0.017
	120.00	14.5521			-0.036
$0.47039i\text{-}C_4H_{10} + 0.52961n\text{-}C_4H_{10}$	125.00	12.6943			$+0.016$
	130.00	12.6133			$+0.013$
	135.00	12.5271			$+0.048$
	140.00	12.4447			$+0.053$

is the isothermal compressibility. Subscripts m and i refer to the mixture and to the pure components, respectively. The pure-component molar volumes were calculated from the fit of the experimental results.[2,3] Only those for nitrogen, methane, and ethane were adjusted to the mixture pressure where appropriate. Isothermal compressibilities for nitrogen and methane were taken from Rowlinson[12] and those for ethane were taken from Miller[13] assuming linear temperature dependence. Excess volumes for a few representative methane + ethane points were also computed using isothermal compressibilities derived from the recent methane data of Goodwin.[14] The excess volumes using Goodwin's values of β were less than 0.1 per cent different from the excess volumes computed using those of Rowlinson. Rowlinson's values were used here only because excess volumes for methane and nitrogen systems reported in the literature are based on his values. Thus, a direct comparison of excess volumes can be made without assessing the contribution of different compressibility values. The ethane compressibility values of Miller were chosen for the same reason. Vapor pressures for nitrogen, methane, and ethane were taken from Strobridge,[15] Goodwin,[14] and Goodwin, Roder, and Straty,[11] respectively.

Effective molar volumes for n-butane below its triple-point temperature (134.8 K) were obtained from equation (2) by assuming that the small negative excess volume of ethane + n-butane was constant and equal to the average value of the excess volumes above the triple-point temperature of n-butane. These subcooled liquid molar volumes were fitted as a linear function of temperature to obtain the equation:

$$V(n\text{-}C_4) = 65.63936 + 0.0992160(T/K). \qquad (3)$$

The molar volumes calculated from this expression at 135 and 140 K agree with the experimental values[3] within 0.01 per cent. At 105 K, the molar volume of n-butane calculated from the equation given in reference 3 fitted to the experimental liquid densities is 0.056 per cent larger than the value given by equation (3). Equation (3) was used to compute the excess volumes given in table 3 for all of the n-butane mixtures below 135 K. For i-butane, the liquid-phase equation given in reference 3 was used to obtain subcooled liquid molar volumes below the triple-point temperature (113.6 K).

In examining the excess volumes for propane + n-butane and i-butane + n-butane using n-butane molar volumes from equation (3), an interesting anomaly was noted. The excess volumes for these systems, as shown in figure 2, appear to have a discontinuity at about the triple-point temperature of n-butane. Molar volumes of n-butane determined from these systems in the same manner as those determined from ethane + n-butane are in good agreement with each other. However, the molar volumes calculated from a linear fit of the values from propane + n-butane and i-butane + n-butane are 0.14 and 0.09 per cent lower than those from equation (3) at 110 and 130 K, respectively, and the extrapolated volumes are about 0.075 per cent lower than the experimental liquid molar volumes at 135 and 140 K.

Though the differences noted are not very large, the imprecision of the density measurements for these heavy hydrocarbons and their mixtures is small enough (see

the ethane + n-butane and propane + i-butane mixtures in table 3) to suggest that this behavior is real and would be worth investigating in more detail. This behavior might also be important in the development of precise methods to predict densities of mixtures containing n-butane.

The pressures listed in table 3 are considered only approximate mixture vapor pressures, and not all of these were directly measured in the present experiment. Pressures are given only for mixtures where sufficient measurements were made to allow either interpolation in temperature or composition for a given system or comparison with existing phase equilibria. For nitrogen + methane, several random pressure measurements were made which were consistent with those interpolated from previous phase-equilibrium measurements in our laboratory.[16, 17] As a result, all of the pressures listed for nitrogen + methane were obtained from graphical
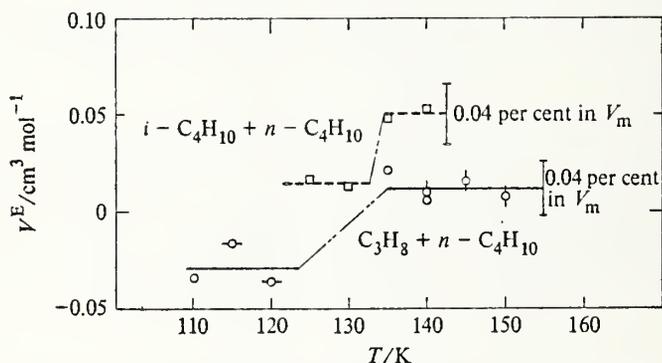
FIGURE 2. Excess volumes of propane + n-butane and i-butane + n-butane from the present study. O, $0.58692C_3H_8 + 0.41308n\text{-}C_4H_{10}$; ◇, $0.60650C_3H_8 + 0.39350n\text{-}C_4H_{10}$; ⊖, 0.60949 $C_3H_8 + 0.39051n\text{-}C_4H_{10}$; □, $0.47039i\text{-}C_4H_{10} + 0.52961n\text{-}C_4H_{10}$.

interpolations of the phase-equilibrium measurements. Pressures for nitrogen + ethane and nitrogen + propane were difficult to measure with any consistency since they are very strong functions of composition. Most of these pressures were estimated by comparison of the present measurements with the phase-equilibrium data of Lu and his colleagues.[4, 5] For methane + ethane, the pressure corresponding to the second point from one filling of the equilibrium cell was generally consistent with phase-equilibrium data,[18, 20] while the first point was usually high by a few per cent. Pressures for these mixtures were smoothed to the pressures of the second point by comparison with the data of Miller and Staveley[18] and of Miller, Kidnay, and Hiza.[19] For methane + propane, discrepancies in the pressures between points taken with the same fill were not as apparent, and the values given in table 3 were not smoothed. Comparisons between the ratios of measured to Raoult's law pressures from the present study with those from the measurements of Stoeckli and Staveley,[21] Cutler and Morrison,[22] and Calado, Garcia, and Staveley[23] are shown in figure 3. Pressures given for methane + i-butane and methane + n-butane, though no phase
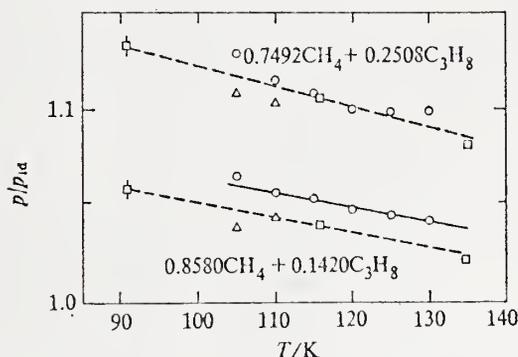
FIGURE 3. Comparison of ratios of actual to ideal total vapor pressures for methane + propane at two compositions. O, present study; ⧄, Stoeckli and Staveley;[21] △, Cutler and Morrison;[22] □, Calado, Garcia, and Staveley.[23]

equilibrium measurements are available for comparison, would probably exhibit departures similar to those shown in figure 3.

ANALYSIS OF ERRORS IN LIQUID-MIXTURE DENSITIES

Where density measurements were made at five or more temperatures, amount-of-substance densities ρ at constant composition were fitted as a function of temperature to the expression previously used in representing orthobaric amount-of-substance densities of the pure components:[2,3]

$$\rho - \rho_c = a\{1 - (T/T_c)\}^{0.35} + \sum_{i=1}^{3} b_i\{1 - (T/T_c)\}^{\{1 + (i-1)/3\}}. \qquad (4)$$

The least-squares coefficients a and b_i, and the values of the critical temperature T_c and critical amount-of-substance density ρ_c for each mixture thus treated are given in table 4. The fourth coefficient b_3 was not statistically significant in the fit of any of these results. Since experimental critical parameters are rarely available for mixtures at the desired composition, those used here were obtained from the correlation of Chueh and Prausnitz.[24] The standard deviations from the fit of the experimental densities to equation (4) are also given in table 4 as a percentage of ρ. The largest standard deviation obtained was 0.029 per cent in ρ for $(0.35457\text{CH}_4 + 0.64543\text{C}_2\text{H}_6)$.

The overall uncertainty in the measured densities of the binary mixtures is slightly larger than for the pure fluids due to the added uncertainty in composition and is dependent on the type of mixture. Estimated uncertainties in the density measurements for three representative mixtures—nitrogen + methane, methane + ethane, and ethane + n-butane—are given in table 5. The estimated errors due to mixture preparation were determined from the uncertainty in mole fraction of each component in the mixture for total amount of substance of mixture prepared (tables 1 and 2). The errors due to vapor-volume correction were estimated by assuming a volume uncertainty equivalent to that portion of the vapor volume in the equilibrium cell at the experimental temperature. The sources of the other systematic errors are

TABLE 4. Parameters of equation (4) where T_c and ρ_c are the critical temperature and critical amount-of-substance density of the mixture. The coefficients a, b_1, and b_2 were obtained from a least-squares program in which the experimental mass densities to five digits were converted to amount-of-substance densities within the program; σ is the standard deviation

Mixture	$\dfrac{a}{\text{mol dm}^{-3}}$	$\dfrac{b_1}{\text{mol dm}^{-3}}$	$\dfrac{b_2}{\text{mol dm}^{-3}}$	$\dfrac{T_c}{\text{K}}$	$\dfrac{\rho_c}{\text{mol dm}^{-3}}$	$\dfrac{10^2 \times}{\sigma \langle \rho^{-1} \rangle}$
$0.04752N_2 + 0.95248CH_4$	16.41033	18.47257	-11.57943	188.04	10.258	0.011
$0.30349N_2 + 0.69651CH_4$	14.92272	20.19078	-10.85599	173.20	10.747	0.023
$0.49242N_2 + 0.50758CH_4$	14.54530	20.60585	-10.07112	161.48	11.018	0.014
$0.35457CH_4 + 0.64543C_2H_0$	13.02060	6.275239		276.40	8.196	0.029
$0.49325CH_4 + 0.50675C_2H_6$	12.99333	7.219530		262.24	8.762	0.028
$0.68006CH_4 + 0.31994C_2H_6$	18.86369	-16.08578	19.91557	239.93	9.482	0.003
$0.49637CH_4 + 0.50363C_3H_8$	9.168092	7.647523		320.33	7.372	0.009
$0.74920CH_4 + 0.25080C_3H_8$	6.367272	24.40468	-11.53932	271.15	9.163	0.013
$0.85796CH_4 + 0.14204C_3H_8$	8.371599	23.49229	-10.69945	241.28	9.836	0.016
$0.91674CH_4 + 0.08326n\text{-}C_4H_{10}$	8.975024	12.09284		238.92	11.044	0.015
$0.50105C_2H_6 + 0.49895C_3H_8$	9.598348	5.440200		344.42	6.125	0.015
$0.67117C_2H_6 + 0.32883n\text{-}C_4H_{10}$	8.334169	5.886011		359.88	6.082	0.013
$0.49030C_3H_8 + 0.50970i\text{-}C_4H_{10}$	7.647038	4.065571		392.63	4.472	0.007

TABLE 5. Estimated uncertainties in density measurements

Source of error	$10^2\|\delta\rho\|/\rho$					
	$0.49242N_2$ $+0.50758CH_4$		$0.49325CH_4$ $+0.50675C_2H_6$		$0.67117C_2H_6$ $+0.32883n\text{-}C_4H_{10}$	
Systematic errors						
	110 K	130 K	110 K	130 K	110 K	130 K
Mass of float	0.002	0.002	0.002	0.002	0.002	0.002
Volume of float at 300 K	0.020	0.020	0.020	0.020	0.020	0.020
Thermal expansion coefficient of barium ferrite	0.022	0.020	0.022	0.020	0.022	0.020
Position of float	0.012	0.013	0.012	0.012	0.009	0.009
Position of main coil, determined from relative measurements	0.020	0.020	0.020	0.020	0.020	0.020
Temperature uncertainty of 0.030 K	0.016	0.023	0.007	0.007	0.005	0.005
Mixture preparation	0.001	0.002	0.001	0.001	0.002	0.002
Vapor volume correction	0.006	0.020	0.001	0.005	0.000	0.000
Total systematic error [a]	0.042	0.048	0.039	0.038	0.037	0.036
Three times standard deviation [a]	0.042	0.048	0.081	0.084	0.039	0.039
Total uncertainty [a]	0.08	0.10	0.12	0.12	0.08	0.08

[a] The total uncertainty was determined from the square root of the sum of the squares of the systematic errors added to three times the standard deviation from the fit to equation (4).

the same as those discussed earlier[2] for pure-fluid measurements. The total uncertainty was taken as the square root of the sum of the squares of the systematic errors plus three times the standard deviation for random error. The standard deviations are those obtained from the fit of the results to equation (4) taken as a percentage of the mixture amount-of-substance density at the specified temperature. For the estimate of random errors for pure-fluid measurements given in reference 2, the standard deviation of a single density measurement was computed relative to the density and temperature of methane at 105 K for which repetitive measurements had been obtained. This method of assessing random error could not be used here. Since the standard deviation for methane obtained from equation (4)[2] was in good agreement with that computed from repetitive measurements, standard deviations for the binary mixtures obtained with equation (4) are considered a reasonable basis for estimating the random error.

It is probable that the overall uncertainties in the densities for some of the mixtures investigated in this study are larger than those shown in table 5. Uncertainties in the results for nitrogen + ethane and nitrogen + propane could exceed the maximum total uncertainty shown in table 5 by a few hundredths of a per cent. Because of the dew-point limitations on the pressure of the gas mixtures prepared and the high liquid-mixture vapor pressures, it was difficult to maintain adequate driving force during the fill to provide continuous condensation and mixing. Of these two systems, results for nitrogen + propane are considered the least reliable. Also, during the course of this study, difficulties were encountered in attempting to obtain consistent results for methane + i-butane where $x(CH_4) > 0.9$. This difficulty could have been due to a problem in the filling procedure or to a dew-point related problem in the prepared gas mixture. Though this problem was not encountered in measurements of the $(0.91674CH_4 + 0.08326n\text{-}C_4H_{10})$ densities, it is quite possible that the overall uncertainties in these results are also larger by a few hundredths of a per cent than the maximum given in table 5.

Fitting the results for mixtures to equation (4) does not allow a test of their consistency as a function of composition. Where densities are available for a given binary system at several temperatures and at three or more compositions, preferably at mole fractions of approximately 0.3, 0.5, and 0.7, excess volumes can be examined for consistency using a temperature-dependent Redlich-Kister expansion. In this study, compositions for methane + ethane and methane + propane were selected to allow this treatment. As shown in table 2, each of these systems also includes one mixture obtained from a laboratory with many years of experience in preparing gravimetric standards. Excess volumes for these systems were fitted to a Redlich-Kister expansion of the form:

$$V^E/cm^3\,mol^{-1} = x_1 x_2 [\{a_0 + a_1(T/K) + a_2(T/K)^2\}$$
$$+ \{b_0 + b_1(T/K) + b_2(T/K)^2\}(2x_1 - 1) + \{c_0 + c_1(T/K) + c_2(T/K)^2\}(2x_1 - 1), \quad (5)$$

where x_1 is the mole fraction of methane. The least-squares coefficients a_i, b_i, and c_i, and the standard deviation, in per cent of the average mixture molar volume, for each system are given in table 6. The c_i coefficients were not statistically significant

TABLE 6. Parameters of equation (5) for methane + ethane and for methane + propane; x_1 is the methane mole fraction and σ the standard deviation

	methane + ethane	methane + propane
a_0	−14.22184	−11.96725
a_1	0.2649993	0.236748
a_2	−0.001419196	−0.001429237
b_0	−18.87392	16.59465
b_1	0.3108472	−0.3212125
b_2	−0.001349755	0.001398221
c_0		−52.93613
c_1		0.9887147
c_2		−0.004667488
$10^2\sigma\langle V^{-1}\rangle$	0.030	0.040

for methane + ethane. The excess volumes calculated from equation (5) are compared in figure 4 with the experimental values at 110 K from the present study.

The standard deviation for methane + ethane obtained with equation (5) is in very good agreement with that obtained with equation (4) for the methane + ethane mixture in table 5. However, the standard deviation for methane + propane obtained with equation (5) is more than a factor of two higher than that obtained with equation (4) for any of the individual mixtures in the set. The higher value from equation (5) is considered to be more indicative of the random error in the results for methane + propane.

The standard deviation given in table 6 for methane + propane was the highest value obtained in the analysis. With a total systematic error of about ±0.04 per cent added to three times this standard deviation (±0.12 per cent), the overall uncertainty for methane + propane would be approximately ±0.16 per cent. With the possible exceptions noted above (*i.e.* nitrogen + ethane, nitrogen + propane, and methane + *n*-butane), this is believed to be a suitable estimate of the maximum overall uncertainty in the densities of binary liquid mixtures obtained in this study.
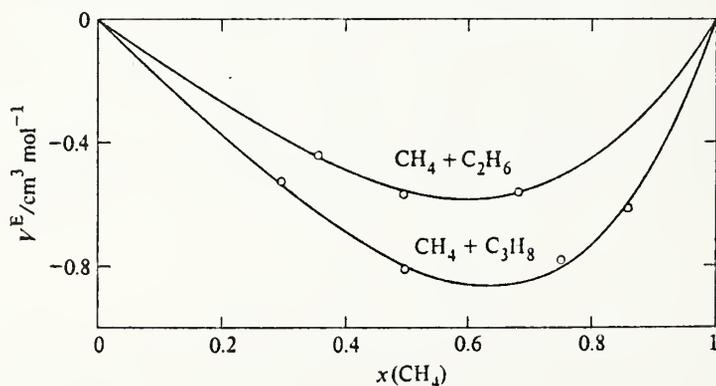
FIGURE 4. Excess volumes for methane + ethane and methane + propane from the present study at 110 K. ○, experimental; ——, calculated from fit to equation (5).

COMPARISONS OF EXCESS VOLUMES

Equation (5) has also been used to compare the present results for methane + ethane and methane + propane with those of other investigators at 108.15 K, a temperature approximately common to all of their measurements. The excess volumes were taken directly from the literature where reported, or otherwise were calculated from the pure-fluid molar volumes in their data set. Though some of the results were 0.1 to 0.3 K below 108.15 K, the differences in temperature do not affect the comparisons of excess volumes appreciably. From equation (5), a change in temperature of 0.1 K results in a change in excess volume of 0.001 cm^3 mol^{-1} for methane + ethane and about 0.002 cm^3 mol^{-1} for methane + propane.
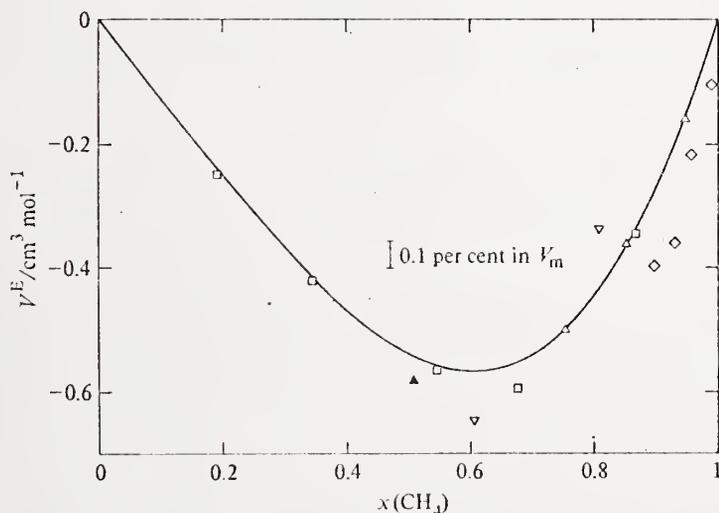
FIGURE 5. Comparison of excess volumes for methane + ethane at 108.15 K. ——, Calculated from fit of present results to equation (5); □, Shana'a and Canfield;[25] △, Rodosevich and Miller;[26] ▲, Pan, Mady, and Miller;[27] ▽, Klosek and McKinley;[28] ◇, Jensen and Kurata.[29]

In figure 5, excess volumes for methane + ethane calculated from equation (5) at 108.15 K are compared with those from the experimental data of Shana'a and Canfield,[25] Rodosevich and Miller,[26] Pan, Mady, and Miller,[27] Klosek and McKinley,[28] and Jensen and Kurata.[29] The data from references 26 and 27 are at about 108 K and those from reference 28 are at about 107.9 K. The excess volumes from Shana'a and Canfield and from Miller and his colleagues are in excellent agreement with the curve calculated from the present results. With the exception of one point each from Shana'a and Canfield and from Miller and his colleagues, the differences are equivalent to much less than 0.1 per cent in the mixture molar volume. In contrast, the excess volumes from Klosek and McKinley and from Jensen and Kurata are much less consistent with the present results. The differences from the calculated curve are equivalent to 0.15 to 0.3 per cent in the mixture molar volume.

In figure 6, excess volumes for methane + propane calculated from equation (5)
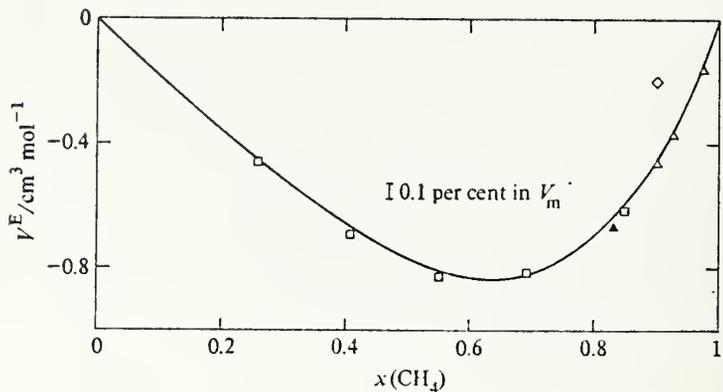
FIGURE 6. Comparison of excess volumes for methane + propane at 108.15 K. ——, Calculated from fit of present results to equation (5); □, Shana'a and Canfield;[25] △, Rodosevich and Miller;[26] ▲, Pan, Mady, and Miller;[27] ◇, Jensen and Kurata.[29]

at 108.15 K are compared with those from the experimental data of Shana'a and Canfield,[25] Rodosevich and Miller,[26] Pan, Mady, and Miller,[27] and Jensen and Kurata.[29] For this system the excess volumes from Shana'a and Canfield and from Miller and his colleagues are also in excellent agreement with the curve from the present results with a maximum difference of about 0.06 per cent in the mixture molar volume. The excess volume from Jensen and Kurata again is not consistent with the present results. The difference is about 0.5 per cent in the average mixture molar volume, in the opposite direction from that found for methane + ethane.

Though there are only a few methane + n-butane points reported in the literature, a comparison can be made at 108.15 K in the methane-rich region between the excess volume interpolated from the present results for the $(0.91674CH_4 + 0.08326n\text{-}C_4H_{10})$ mixture and excess volumes from the experimental data reported by Shana'a and Canfield[25] and by Miller.[13] This comparison is given in figure 7. The excess volume from Shana'a and Canfield was computed using their pure methane data and the
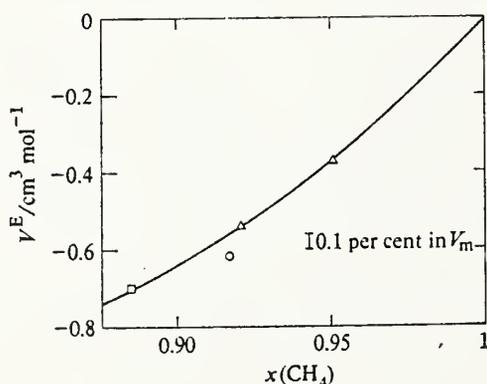
FIGURE 7. Comparison of excess volumes of methane + n-butane at 108.15 K. ○, Interpolated from the present study; □, Shana'a and Canfield;[25] △, Rodosevich and Miller.[26]

molar volume of n-butane obtained from equation (3). The excess volumes of Miller are those reported in his paper. The n-butane molar volumes used by Miller are within 0.02 per cent of the values given by equation (3). The difference between the excess volume interpolated from the present results and the curve drawn through the excess volumes of Shana'a and Canfield and of Miller is about 0.14 per cent of the mixture molar volume. Since the data from Shana'a and Canfield and from Miller appear to be in as good agreement for methane + n-butane as for methane + ethane and methane + propane, it is possible that at least part of the 0.14 per cent difference is due to an unaccounted error in our results for the mixture, as suggested earlier in this paper. Unfortunately, data are not available for comparison with the present results for $(0.58828CH_4 + 0.41172n\text{-}C_4H_{10})$, the accuracy of which we have no reason to question. Measurements for this mixture could not be made at the lower temperatures since the n-butane content is the solid solubility limit at about 116 K.[30]
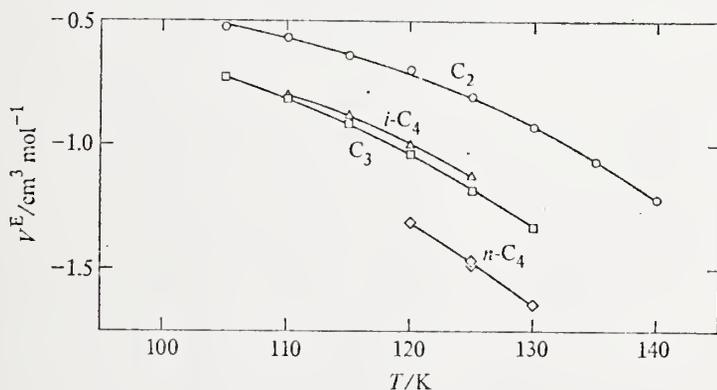
FIGURE 8. Comparison of excess volumes from the present study for methane + heavy hydrocarbon mixtures having $x \approx 0.5$, ○, $0.49325CH_4 + 0.50675C_2H_6$; □, $0.49637CH_4 + 0.50363C_3H_8$; △, $0.48687CH_4 + 0.51313i\text{-}C_4H_{10}$; ◇, $0.58828CH_4 + 0.41172n\text{-}C_4H_{10}$.

The only data for methane + i-butane in this temperature range are those of Rodosevich and Miller[26] for two mixtures with mole fractions 0.9152 and 0.9462 of CH_4. The excess volumes they report for these mixtures at 108 K are about half-way between their results for methane + propane and for methane + n-butane at the same methane mole fraction. The excess volumes for the mixture of methane + i-butane with $x \approx 0.5$ from the present study are equivalent to those obtained for methane + propane at 110 K and the same composition. Excess volumes from the present study are shown in figure 8 for mixtures with $x \approx 0.5$ of methane + ethane, + propane, and + i-butane. Excess volumes are also included for $(0.58828CH_4 + 0.41172n\text{-}C_4H_{10})$ for comparison. It is clear that more extensive measurements of high precision are needed to describe accurately the composition dependence of the excess volumes for both methane + butane systems.

The small excess volumes given in table 3 for binary mixtures containing the higher molar-mass alkanes—ethane, propane, i-butane, and n-butane—show that at

cryogenic temperatures the molar volumes for binary mixtures of these components are closely approximated by the assumption of ideal mixing. The only other investigators who report data for binary mixtures of these alkanes at cryogenic temperatures are Shana'a and Canfield.[25] They report densities for several mixtures of ethane + propane and for one mixture of ethane + n-butane.

For ethane + propane, the excess volume reported by Shana'a and Canfield at 108.15 K for the mixture $(0.5852 C_2H_6 + 0.4148 C_3H_8)$ is compared in figure 9 with those determined from the present results at two similar compositions. If the excess volumes for ethane + propane exhibit an asymmetry similar to those for methane + ethane (figure 5), the excess volumes for the two ethane + propane mixtures from the present study should be nearly the same, with the excess volume at the higher mole fraction of C_2H_6 slightly larger. Shana'a and Canfield report a maximum
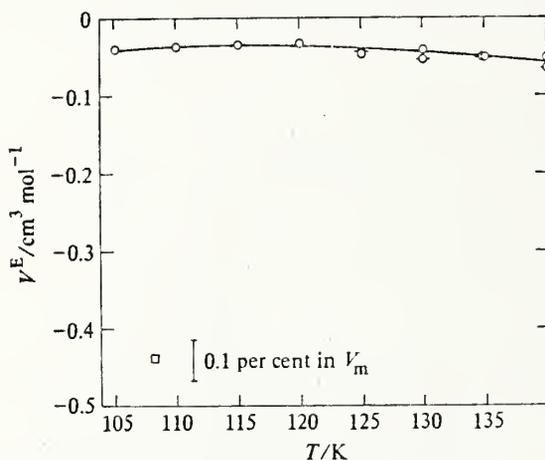
FIGURE 9. Comparison of excess volumes for ethane + propane. $\bigcirc$, $\ominus$, Present study at $x(C_2H_6) = 0.50105$ and 0.67287, respectively; $\square$, Shana'a and Canfield[25] at $x(C_2H_6) = 0.5852$.

excess volume for this system of $-0.485\ \mathrm{cm^3\ mol^{-1}}$ for a mixture containing $(0.7036 C_2H_6 + 0.2964 C_3H_8)$. The difference in excess volumes from the two sets of measurements is surprisingly large, equivalent to approximately 0.8 per cent in the mixture molar volume. Since the pure-fluid molar volumes for ethane and propane from Shana'a and Canfield are only higher than those determined with the present apparatus[3] by approximately 0.06 and 0.12 per cent, respectively, it is logical to suspect composition error or incomplete mixing as the source of this disagreement.

To assess the effect of composition uncertainty on the excess volume, it was assumed that the mixture mass density from the present study was exact and that the actual mole fraction of propane was 0.01 larger than the composition of the prepared mixture with $x = 0.5$. This results in an error of $-0.062\ \mathrm{cm^3\ mol^{-1}}$ in the excess volume. If the excess volume reported by Shana'a and Canfield were assumed to be correct, it would be necessary for the actual mole fraction of ethane in the liquid in the present study to be larger by 0.064 than that of the prepared mixture.

As discussed in the experimental section of this paper, chromatographic comparisons of the compositions of liquid samples for ethane + propane were in agreement with the composition of the prepared mixture within a few hundredths of 1 mole per cent. The fact that no change in density of the mixture could be detected during sample withdrawal is considered evidence that the liquid mixture was homogeneous. The fact that the two mixtures studied were prepared independently in two separate laboratories is also confirmation that there was no significant error in the mixture preparation.

Recent enthalpy of mixing measurements in binary mixtures of methane, ethane, and propane reported by Miller and Staveley[18] should also be referred to in regard to the ethane + propane results discussed above. These investigators report that the enthalpy of mixing at 112 K is about 129 J mol^{-1} for methane + propane with $x = 0.5$, about 69 J mol^{-1} for methane + ethane with $x = 0.5$, and probably less than 5 J mol^{-1} for ethane + propane throughout the composition range. A comparison of ratios of the enthalpies of mixing with ratios of the excess volumes for these systems also tends to support the more ideal excess volumes obtained in the present investigation.

Shana'a and Canfield include a discussion on the invalidity of the principle of congruence based on a comparison of their excess volumes for ethane + propane and methane + ethane with those for methane + propane as a function of the equivalent carbon number. When the excess volumes from the present study are used, methane + ethane shows the same departure as expected, but ethane + propane is in excellent agreement with methane + propane. For a detailed discussion of the method, the reader is referred to Shana'a and Canfield's paper.

In figure 10, the excess volume computed from the molar volume of the $(0.8833C_2H_6 + 0.1167n\text{-}C_4H_{10})$ mixture reported by Shana'a and Canfield is compared with the excess volumes of this system computed from our results. The excess volume of Shana'a and Canfield was computed using their density for pure ethane and the molar
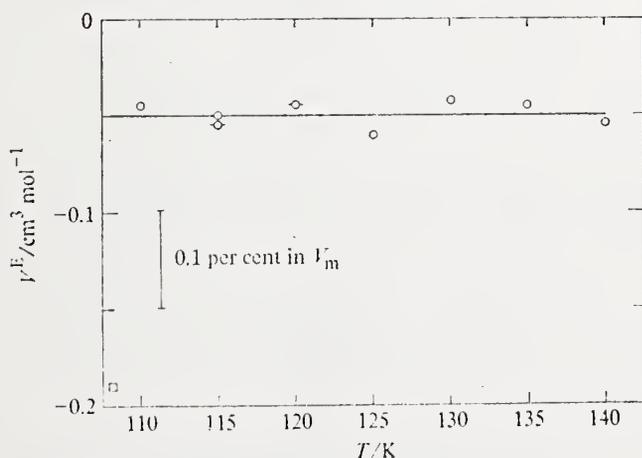
FIGURE 10. Comparison of excess volumes for ethane + n-butane. $\bigcirc$, $\diamondsuit$, Present study at $x(C_2H_6) = 0.67117$ and 0.65343, respectively; $\square$, Shana'a and Canfield[25] at $x(C_2H_6) = 0.8833$.

61

volume of n-butane from equation (3). For this system the difference in excess volumes is equivalent to about 0.25 per cent in the mixture molar volume. Since the molar volumes for n-butane in the subcooled liquid region given by equation (3) were obtained from the results for this system the lack of temperature dependence is an artificial constraint. For this system, if the actual mole fraction of n-butane in the liquid mixture at 110 K was 0.01 larger than the composition of the mixtures prepared for this study, an error of -0.119 cm^3 mol^{-1} in the excess volume would result.
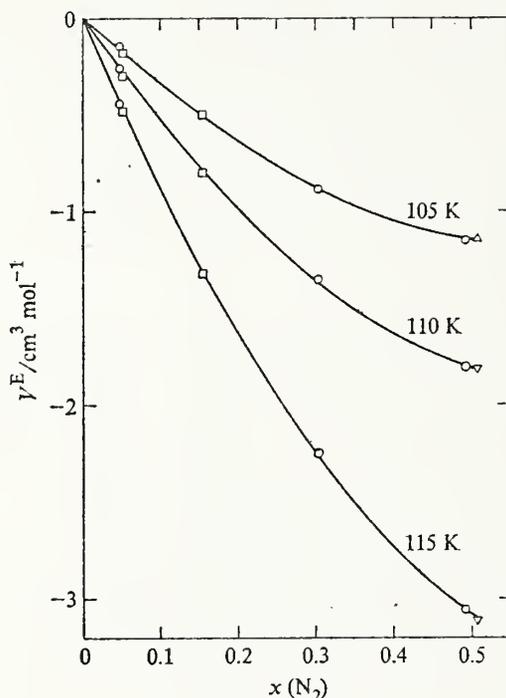
FIGURE 11. Comparison of excess volumes for nitrogen + methane. $\bigcirc$, Present study; $\square$, Rodosevich and Miller;[26] $\triangle$, Liu and Miller;[31] $\triangledown$, Massengill and Miller.[32]

Of the data available for liquid mixtures of nitrogen + methane,[6] the excess volumes reported by Rodosevich and Miller,[26] Liu and Miller,[31] and Massengill and Miller[32] were selected for comparison with excess volumes from the present results. These comparisons are shown in figure 11. The excess volumes of Massengill and Miller are from the data of Liu and Miller adjusted with additional nitrogen measurements. All of the excess volumes of Miller and his colleagues appear to be in agreement with excess volumes from the present results within 0.1 per cent of the mixture molar volumes. The height of the symbols is equivalent to about 0.1 per cent of the mixture molar volumes.

The fact that the nitrogen + methane excess volumes are in good agreement does not mean that the mixture molar volumes are in agreement. It is worth noting that the data reported by Liu and Miller and by Massengill and Miller were obtained with

a calibration based on the molar volumes of saturated liquid argon reported by Terry *et al.*[33] while all of the other data of Miller and his colleagues[13, 26, 27] referred to here were obtained with a calibration based on molar volumes of saturated liquid methane taken from Goodwin and Prydz.[34] From the discussion given earlier,[2] the nitrogen + methane molar volumes of Rodosevich and Miller should be higher but consistent with the present results within about 0.1 per cent, while those of Liu and Miller and of Massengill and Miller should be higher than the present results by about 0.4 per cent.

4. Summary

The measurements of the present study provide a set of orthobaric liquid densities for binary mixtures of the major components of LNG which are generally consistent with those for the pure components within the precision of the measurements. The maximum random error in the densities of the binary mixtures is believed to be about ± 0.12 per cent, roughly twice that for the pure fluid densities. The known systematic errors in the densities for both the pure fluids and the binary mixtures were estimated to be from 0.03 to 0.05 per cent. As noted, the uncertainties in the densities for methane + n-butane with $x(CH_4) > 0.9$, and for nitrogen + ethane and nitrogen + propane, could exceed these estimates.

The largest excess volume found was -6.11 cm^3 mol^{-1} for nitrogen + methane with $x = 0.5$ at 120 K. This is equivalent to 13 per cent of the ideal mixture molar volume. In contrast, the present results show that molar volumes of mixtures of the alkanes, excluding methane, are closely approximated by ideal mixing in the temperature range studied. The most significant disagreement between the present results and published data is the 0.8 per cent difference in density for ethane + propane from that of Shana'a and Canfield.

Based on the excess volumes of the alkane mixtures, excluding methane, from the present study, it was shown also that effective molar volumes of subcooled n-butane in a binary liquid mixture may differ by a small but significant amount dependent on the other components present. It is suggested that this behavior would be worth investigating in more detail for n-butane and other fluids such as n-pentane. There is also a definite need for additional measurements on the binary mixtures containing both n-butane and i-butane with methane.

In subsequent papers, the results of measurements of orthobaric liquid densities of multicomponent mixtures and the ability of theoretical models to predict the measured densities will be reported.

REFERENCES

1. Robinson, R. L., Jr.; Hiza, M. J. In *Advances in Cryogenic Engineering*, Vol. 20. Timmerhaus, K. D.: editor. Plenum Press: New York. 1975. p. 218.
2. Haynes, W. M.; Hiza, M. J.; Frederick, N. V. *Rev. Sci. Instrum.* 1976, 47, 1237.
3. Haynes, W. M.; Hiza, M. J. *J. Chem. Thermodynamics* 1977, 9, 179.

4. Yu, P.; Elshayal, I. M.; Lu, B. C.-Y. *Can. J. Chem. Eng.* 1969, 47, 495.
5. Poon, D. P. L.; Lu, B. C.-Y. In *Advances in Cryogenic Engineering*, Vol. 19. Timmerhaus, K. D.: editor. Plenum Press: New York. 1974, p. 292.
6. Hiza, M. J.; Kidnay, A. J.; Miller, R. C. *Equilibrium Properties of Fluid Mixtures, A Bibliography of Data on Fluids of Cryogenic Interest*. NSRDS Bibliographic Series. IFI Plenum: New York. 1975.
7. Haynes, W. M. *Rev. Sci. Instrum.* 1977, 48, 39.
8. Tully, P. C.; Emerson, D. Personal communications. November 1974, August 1976.
9. Duncan, A. G., Hiza, M. J. In *Advances in Cryogenic Engineering* Vol. 15. Timmerhaus, K. D.: editor. Plenum Press: New York. 1970. p. 42.
10. Hiza, M. J.; Duncan, A. G. *Rev. Sci. Instrum.* 1969, 40, 513.
11. Goodwin, R. D.; Roder, H. M.; Straty, G. C. *Nat. Bur. Stand. U.S., Tech. Note* 684, 1976.
12. Rowlinson, J. S. *Liquids and Liquid Mixtures*. 2nd Ed. Butterworths: London. 1969.
13. Miller, R. C. *Chem. Eng.* 1974, 81, 134.
14. Goodwin, R. D. *Nat. Bur. Stand. U.S., Tech. Note* 653, 1974.
15. Strobridge, T. R. *Nat. Bur. Stand. U.S., Tech. Note* 129, 1962.
16. Parrish, W. R.; Hiza, M. J. In *Advances in Cryogenic Engineering* Vol. 19. Timmerhaus, K. D.: editor. Plenum Press: New York. 1974, p. 300.
17. Kidnay, A. J.; Miller, R. C.; Parrish, W. R.; Hiza, M. J. *Cryogenics* 1975, 15, 531.
18. Miller, R. C.; Staveley, L. A. K. In *Advances in Cryogenic Engineering*, Vol. 21. Timmerhaus, K. D. and Weitzel, D. H.: editors. Plenum Press: New York. 1976, p. 493.
19. Miller, R. C.; Kidnay, A. J.; Hiza, M. J. *J. Chem. Thermodynamics* 1977, 9, 167.
20. Wichterle, I.; Kobayashi, R. *J. Chem. Eng. Data* 1972, 17, 9.
21. Stoeckli, H. F.; Staveley, L. A. K. *Helv. Chim. Acta* 1970, 53, 1961.
22. Cutler, A. J. B.; Morrison, J. A. *Trans. Faraday Soc.* 1965, 61, 429.
23. Calado, J. C. G.; Garcia, G.; Staveley, L. A. K. *J. Chem. Soc., Faraday Trans. I*, 1974, 70, 1445.
24. Chueh, P. L.; Prausnitz, J. M. *AIChE J.* 1967, 13, 1107.
25. Shana'a, M. Y.; Canfield, F. B. *Trans. Faraday Soc.* 1968, 64, 2281.
26. Rodosevich, J. B.; Miller, R. C. *AIChE J.* 1973, 19, 729.
27. Pan, W. P.; Mady, M. H.; Miller, R. C. *AIChE J.* 1975, 21, 283.
28. Klosek, J.; McKinley, C. In *Proceedings of the First International Conference on LNG*. White, J. W. and Neumann, A. E. S.: editors. Institute of Gas Technology, Chicago, Illinois. 1968. Paper No. 22.
29. Jensen, R. H.; Kurata, F. *J. Petrol. Technol.* 1969, 21, 683.
30. Kuebler, G. P.; McKinley, C. In *Advances in Cryogenic Engineering* Vol. 21. Timmerhaus, K. D.; Weitzel, D. H.: editors. Plenum Press: New York. 1976, p. 509.
31. Liu, Y.-P.; Miller, R. C. *J. Chem. Thermodynamics* 1972, 4, 85.
32. Massengill, D. R.; Miller, R. C. *J. Chem. Thermodynamics* 1973, 5, 207.
33. Terry, M. J.; Lynch, J. F.; Bunclark, M.; Mansell, K. R.; Staveley, L. A. K. *J. Chem. Thermodynamics* 1969, 1, 413.
34. Goodwin, R. D.; Prydz, R. *J. Res. Nat. Bur. Stand. U.S.* 1972, 76A, 81.

Gas Processing

System is accurate, precise for LNG sampling

Heating value can be well defined in LNG transfer

W. R. Parrish, J. M. Arvidson and **J. F. LaBrecque,**
National Bureau of Standards, Boulder, Colo.

LNG SAMPLES may be obtained and analyzed from flowing streams with a precision of ±0.20% in the computed heating value. This value is derived from laboratory and field tests and is based on three standard deviations, including ±0.06% random error for gas analysis. The accuracy of the measurement depends only on the accuracy of the gas analysis; all tests show that a properly designed and operated sampling system produces no detectable systematic offsets in the computed heating values.

Since LNG is bought and sold on a heating value basis, accurate and precise LNG composition measurement is a necessity. At current prices, a composition uncertainty corresponding to a one percent error in the computed heating value means an inequity of nearly $65,000 for one 125,000 m³ shipment.

Sampling LNG presents special problems because the component normal boiling points are so different—methane, the major component, has a boiling point of −161° C; while n-butane, the minor component, has a boiling point of −0.4° C.

Accurate LNG composition measurement requires a system containing

- A sampling probe which transfers a representative sample into the sampling system

- A sample conditioner which completely vaporizes the sample

- A gas analyzer which accurately and precisely analyzes the sample.

Finally, all operating variables must be carefully selected to insure that all system components perform properly.

Sampling systems fall into two broad categories—continuous and batch. Trego[1] describes a continuous LNG sampling system which is in operation at the LNG Terminal in Barcelona, Spain. He states that deviation between liquid samples taken upstream of a vaporizer and gas samples taken downstream of the vaporizer agree to within the error of the gas analysis (~ 0.5 to 0.9%). Cook[2] describes a batch sampling system; he reports[3] that the device gives good results for sampling LNG containing 95 mol % or more methane. However, the precision and accuracy have never been established quantitatively.

This paper describes a system for continuously sampling flowing LNG streams with a total uncertainty of ± 0.20% in the computed heating value. The system can be used in any LNG line where the pressure is at least 5 psi (32 kPa) above ambient conditions. The system design, dimensions and recommended ranges of operating variables are derived from a systematic study employing both laboratory and field tests. The laboratory work permitted rapid data accumulation under well controlled operating conditions using LNG-like mixtures of known composition. These tests considered 3 probes, 2 vaporizer designs and 10 operating variables. Sufficient data were taken to statistically establish the effect of each variable on the sampling precision and accuracy. Using the laboratory test results, a full scale sampling system was designed, built and tested aboard an LNG tanker and in the NBS flow facility.[4] Details and results of this work are presented elsewhere.[5]

SYSTEM DESCRIPTION

Fig. 1 shows a schematic of the full scale sampling system. All field tests were made with the sampling system having the dimensions given in Table 1. At this time it is not clear which of the dimensions are critical to the sampling system precision.

The sample is taken from the LNG line (in our tests a 3 in. (76 mm) pipe and flows through a side tap probe, past a stainless steel bellows block valve (T1) and through a 60 micron filter. A nitrogen purge line is attached to the system to inert the sampling system prior to startup and to back purge the filter if necessary. The LNG then flows through a stainless steel bellows needle valve (T2), which controls the sampling rate, and into the steam heated vaporizer. The vaporizer contains a coiled section of thin-walled stainless steel tubing and an impingement chamber. The impingement chamber causes a

TABLE 1—Dimensions of LNG sampling system (See Fig. 1 for system schematic)

Component	Length, inches (mm)	Outer Diameter, inches (mm)	Inner Diameter, inches (mm)
Line between test section & valve, T1	4.5 (114)	0.540 (13.7) (¼ in. Sch 80 pipe)	0.302 (7.67)
Line between valve, T1, and filter (contained a short radius 90-degree bend)	11 (279)	0.25 (6.4)	0.180 (4.57)
Line between filter and valve, T2	2 (51)	0.25 (6.4)	0.180 (4.57)
Line between valve, T2, and union at vaporizer	13.5 (343)	0.25 (6.4)	0.180 (4.57)
Vaporizer	36 (914)	0.13 (3.18)	0.101 (2.56)
Vaporizer steam casing (with flat welded ends)	10 (254)	6 (152)	5.5 (140)
Impingement chamber (with flat welded ends)	1.5 (38)	1.5 (38)	1.376 (34.95)
Accumulator	16 (406)	5.125 (130.2)	4.805 (122)

sudden change in the flow direction and speed to enhance vaporization of any entrained droplets. All of the cold lines, the steam lines and the vaporizer are insulated with fiberglass pipe insulation which is sealed with duct tape. After leaving the vaporizer, the sample goes to an accumulator. The accumulator acts as a time-averaging, or mixing, device to eliminate inhomogeneities caused by fractionation during vaporization. The homogeneous gas sample leaves the accumulator, passes through a manifold containing sample cylinders, a rotameter and a back pressure regulator before going to the vent system.

The sampling rate is set by adjusting the needle valve (T2) and the back pressure regulator. The back pressure regulator is extremely useful because it maintains a constant pressure in the sample cylinders.

TEST RESULTS

Fig. 2 shows the computed heating values for one series of tests made aboard the LNG tanker *El Paso Consolidated*. In these tests liquid samples were taken upstream of the shipboard steam vaporizer. Analyses of these samples were compared with those of gas samples taken from the completely vaporized stream. A laboratory gas chromatograph was used to determine the sample composition. The average heating value of the gas samples was 0.04% higher than that of the liquid samples. Also, the estimated standard deviation for both sets of samples was 0.04%. This precision is comparable to the estimated standard deviation of 0.05% in the heating value for gas analysis alone. A statistical analysis of computed liquid densities gave an estimated standard deviation of 0.02% for both the liquid and gas samples. This test shows that, within the precision of the gas analysis, samples taken from the liquid stream are indistinguish-able from the samples taken from the totally vaporized gas stream.

Table 2 lists the variables evaluated in the laboratory and field sampling tests and groups them according to their effect on sampling precision and accuracy. Each variable's effect on sampling precision was measured by repeated sampling under controlled conditions. The accuracy was determined in the laboratory tests by sampling mixtures of known composition. The only verification of accuracy in the field tests was made by comparing the liquid sample compositions with samples taken from the totally vaporized LNG stream. The test results indicated that for uninsulated liquid lines the heat leak causes back-flashing of nitrogen (and probably methane) which enriches the samples in the heavy (C_2^+) components. However, insulating the line with a $\frac{1}{2}$ to 1 inch (12 to 25 mm) thick layer of fiberglass sealed with duct tape is adequate to eliminate the heat leak problem. No other variable tested affected sampling accuracy. Therefore, by using insulated lines, the accuracy of the composition measurement depends only on the accuracy of the gas analysis.

Five variables were found to adversely affect sampling precision. Both laboratory and field tests showed that below a certain sampling rate, the sampling precision diminishes; this minimum sampling rate varied between various sampling systems. A mechanism for the sampling rate's importance is unknown. For the sampling system described here, the sampling rate should be greater than 20 standard liters per minute of gas.

Laboratory results clearly indicated that a small diameter tube vaporizer was better than a vaporizer with a large cross sectional area and that rapid sample vaporization gave the best results. However, there is no advantage in having the vaporizer outlet temperature above 100° F
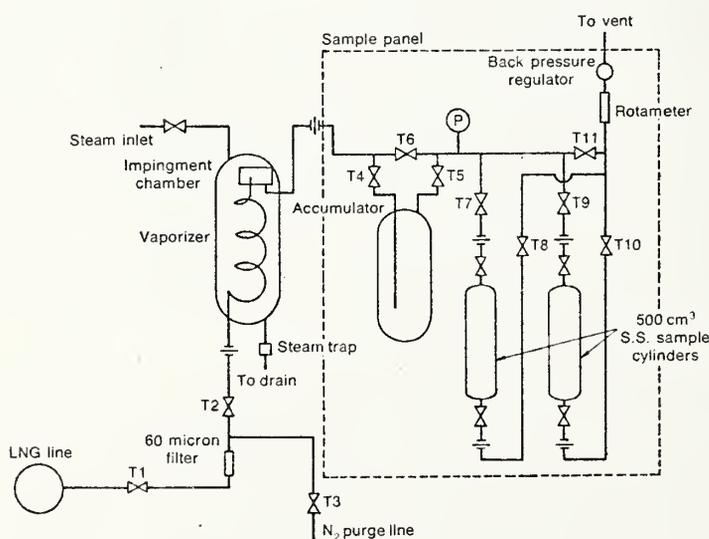

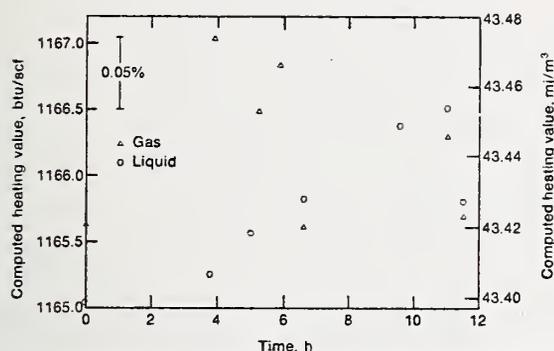**Fig. 1—LNG sampling system.**

LNG SAMPLING

Fig. 2—Computed real gas heating values of shipboard data.

TABLE 2—Variables evaluated for their effect on LNG sampling precision and accuracy

Variable effecting both sampling precision and accuracy:
  Heat leak to liquid sample line

Variables affecting sampling precision but not accuracy:
  Sampling rate
  Vaporizer design
  Time averaging the vaporized sample
  Sampling rate transients
  Probe

Variables not affecting sampling precision and accuracy:
  Temperature and pressure at the sampling point
  Pressure differential between the sampling point pressure and the equilibrium LNG pressure
  Flow rate past the sampling point
  Pressure drop in the liquid sample line between the sampling point and vaporizer
  Composition of the liquid being sampled

About the authors

W. R. PARRISH *conducts basic and applied experimental and theoretical research involving cryogenic systems for the National Bureau of Standards. He is a Ph.D. graduate in chemical engineering from the University of California, Berkeley. Dr. Parrish also has done post-doctoral work at University of Wisconsin, Madison. He is a member of AIChE.*

J. M. ARVIDSON *holds the B. S. degree in mechanical engineering from the University of Colorado. He is experienced in research in LNG metrology, mechanical properties of solids at low temperatures and pressure measurement studies at low temperatures. He is currently engaged in basic and applied experimental research in cryogenic systems. Mr. Arvidson is a member of Sigma Xi and the Instrument Society of America.*

J. F. LaBRECQUE *is a consultant to scientists and engineers on the use of statistics in the design and analysis of experiments at the National Bureau of Standards, Boulder, Colo. Dr. LaBrecque is a graduate of the University of Massachusetts (B.S.) and the State University of New York at Buffalo (Ph.D.). He is a member of the American Statistical Association.*

(38° C). Both steam and electrically heated vaporizers produce comparable results. An impingement chamber is unnecessary when using an electrically heated vaporizer. This is because the electrically heated unit vaporizes the sample under constant heat flux conditions. The steam vaporizer transfers heat with a constant wall temperature. This is less effective due to the film boiling.

The need to time-average the vaporized sample in an accumulator arises from fractionation during vaporization. The minimum residence time necessary to obtain precise results depended upon the sampling system; residence times of 45 to 120 seconds gave good results.

Field tests indicated that taking samples within 30 minutes of a major change in sampling rate diminishes sampling precision. However, minor fluctuations and slow drifts in sampling rates did not affect the results.

The side tap probe was found to be more reliable than an upstream facing pitot tube. For unknown reasons, the pitot tube occasionally gave erratic results.

The conclusions that certain variables did not affect sampling precision must be considered valid only over the ranges tested; however, this range usually included the typical operating ranges encountered during custody transfer.

There is no reason to expect the temperature and pressure to affect sampling precision provided the conditions are far from the critical point of the LNG.

At some low value the difference between the pressure of the sampled liquid and the saturation pressure of the LNG (i.e., subcooling) in combination with heat leak will adversely affect sampling precision; however, this effect was not found at a pressure differential of 3.9 psi (25 kPa) (this corresponds to ~ 0.5 K subcooling).

LNG flow rates corresponding to Reynolds numbers ranging between 1,500 and 50,000 did not affect sampling precision; it is unlikely that there would be any adverse effect on precision at higher Reynolds numbers.

The fact that a large pressure drop in the liquid sample line is unnecessary eliminates the need for a liquid flow control valve. This conclusion is known to be valid only when using tube vaporizers. However, the needle valve is useful in setting sampling rates.

Finally, there is no problem in sampling LNG mixtures which contain up to 0.15 percent C_6^+. The heavy components would cause problems if they raised the sample dewpoint temperature to near ambient temperature.

Additional work is underway to develop an improved vaporizer design which, hopefully, will eliminate the need for an accumulator. Also, additional tests are being made to determine the criterion for the minimum acceptable sampling rate. The goal is to provide general design and operating criteria for LNG sampling systems.

LITERATURE CITED

[1] Trego, J., "System samples LNG accurately," *Hydrocarbon Processing*, p. 83, April 1976.
[2] Cook, H. L., "Method and apparatus for sampling refrigerated volatile liquids," U. S. Patent No. 3,487,692, January 1970.
[3] Cook, H. L., Transco Co., Houston, private communication, May 1977.
[4] Mann, D. B., "Cryogenic flowmetering research at NBS," Cryogenics, Vol. 11, p. 179, 1971.
[5] Parrish, W. R., Arvidson, J. M., and LaBrecque, J. F., "Development and evaluation of an LNG Sampling Measurement System," NBSIR (to be published).

TEST OF DENSIMETERS FOR USE IN THE CUSTODY TRANSFER OF LNG

J. D. Siegwarth, J. F. LaBrecque and B. A. Younglove
National Bureau of Standards
Boulder, Colorado 80302

INTRODUCTION

The amount of liquefied natural gas (LNG) changing ownership, i.e., custody transfer, may be determined from the total volume of the liquid transferred and the density of the liquid. The density can be calculated from the temperature and composition or measured directly with a densimeter. Direct density measurements have the advantages that composition measurements are avoided and the density can be monitored continuously. Some commercial densimeters have been adapted for low temperature use. Before these densimeters are used in custody transfer measurements, it is necessary to establish whether their performance is adequate. Furthermore, methods must be developed to check accuracy and maintain performance in field use.

In order to assess the performance of densimeters for LNG custody transfer use, a density reference system (DRS) has been constructed at the Cryogenics Division facilities of the National Bureau of Standards.[1] Four commercial densimeters have been tested[2] to determine accuracy, precision and short-term reliability. The four densimeters include two vibrating-element types, one dielectric or capacitance type, and one Archimedes or displacement type. This program, sponsored at NBS by the American Gas Association, Inc., was conducted over a period of four years and considers densimeters that were commercially available at the start of the work.

THE DENSITY REFERENCE SYSTEM DESCRIPTION

The density reference system, shown schematically in Figure 1, consists of a vacuum-insulated, liquid-gas sample container of sufficient size and with sufficient access so that a number of commercial densimeters and a calibration densimeter can be installed at the same time. The calibration densimeter, built at NBS Boulder, is an Archimedes-type densimeter using a pure silicon single crystal for the displacement body. The density of silicon is relatively low and the density of pure single crystals of silicon is accurately known.[3] The silicon crystal is suspended on a wire from the pan arm of an electronic balance and is immersed in the fluid in question. In order to weigh the 127 g silicon crystal on the 0 to 20 g range (which can be read to 1 mg) a counter-balance is placed on the opposite arm. To eliminate the need to determine the mass of this counter weight, the silicon is weighed in the fluid, then disconnected. Then a reference mass, chosen so that it weighs on scale, is weighed. The equation for the fluid density contains only the mass of the silicon crystal, the density corrected for thermal contraction, the mass of the

reference weight, the electronic balance readings when the silicon crystal was weighed in the fluid, the balance reading with only the reference weight, and a small correction for the buoyancy effects on the reference mass from the gas in the balance space.

All four of the densimeters tested and the reference densimeter were installed and evaluated at the same time. Making the density tests simultaneously necessitated a large sample container. Not only does this method save time but it allows a cross-check between the densimeters. If one densimeter should give an erroneous density reading, the instrument at fault can be readily determined when the remainder show agreement.

The sample container, containing the test densimeters and the room-temperature electronic balance space, is connected in common through the tube containing the crystal suspension wire. Both containers are gas tight so the vapor pressure of the sample can be varied between 0 and 7 bars allowing a range of densities to be obtained with one fluid sample.

The sample holder and shield are cooled by flowing cold nitrogen gas or liquid through a coiled tube attached to the outside of the sample holder. These coils are used to cool the sample, and resistance heaters are used to heat it when changing temperatures between measurements. Each measurement is made with the sample and container as nearly as possible at isothermal conditions. During the period of time data are being recorded, the heat capacity of the sample fluid is used to keep the temperature nearly constant. The heat leak to the sample has been minimized by surrounding the sample container with a thermal shield. The shield temperature is maintained near that of the sample by controlling the flow of the nitrogen gas through the shield cooling coil. To obtain uniform temperature and density rapidly in the 14-liter vessel, a 5-cm diameter turbine pump is used to mix the sample. Liquid is circulated from the bottom to the top of the sample holder through 3.5-cm diameter tubes. The circulation rate is variable and is reduced during actual density measurements so that the densimeters are not disturbed. Temperature is measured near the bottom and at the top of the sample holder. The temperature differences, ΔT, from top to bottom of the sample holder were typically less than 0.1 K.

DENSITY REFERENCE SYSTEM ACCURACY

The random error associated with density measurements made using the DRS was obtained from least squares fits of the measured densities to a power series in temperature (T). A different fit was used for each of the various compositions. The estimated standard deviation for measurements made on the DRS is 0.065 kg/m^3. This is a standard deviation of less than 0.016% at the normal

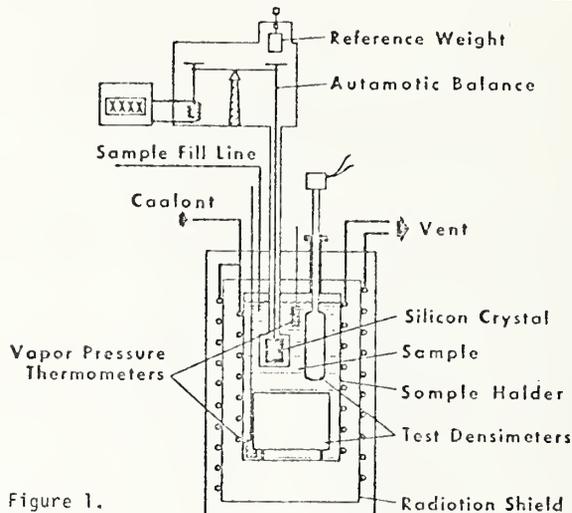## CRYOGENIC FLUIDS DENSITY REFERENCE SYSTEM

Figure 1.

boiling point of methane (422.63 kg/m³). The systematic error due to uncertainties in mass and temperature measurements is estimated to be 0.028%, while the uncertainty of a single density measurement by the DRS densimeter is estimated to be 0.076%. This is the sum of the systematic error and three times the estimated standard deviation.

Pure methane density measurements by the DRS densimeter agree with the densities calculated by Goodwin[5] to better than 0.03% over the temperature range from 110 to 126 K. The agreement between the methane densities determined by the DRS densimeter and those determined by Haynes-Hiza[6] is shown in Figure 2. The densities are compared through temperature measurements. The density difference in percent is shown as a function of the order of data acquisition. There is no evidence of a filling-to-filling shift in the density measurements, even though the DRS was brought to room temperature after each filling. The bias between the mean densities measured by the DRS densimeter and the Haynes-Hiza densities are less than 0.01%. The DRS is discussed in greater detail in Reference 1.

DESCRIPTION OF THE DENSIMETERS TESTED

Both vibrating-element densimeters determine fluid density by measuring a resonant frequency of a mechanically-vibrating element immersed in the fluid in question. Frequency is related to density as follows:

$$\rho = A + B/f^2, \qquad (1)$$

where f is the resonant frequency and A and B are constants. Since neither of these instruments had a suitable calibration for low-temperature low-density liquids, the resonant frequency rather than the density indication, was recorded using a frequency counter. The densimeters were calibrated using the density data from the DRS

densimeter and the corresponding frequencies to determine the constants A and B of Eq. (1). This equation was then used to study the precision, filling-to-filling offset and composition dependencies.

The capacitance densimeter actually measures the dielectric constant of the fluid in question. The dielectric constant is combined with a temperature measurement to give a density value. The calibration supplied with the instrument was used in the analysis of the density data.

The displacement densimeter determines density by measuring the buoyant force on a hollow float. The position of the float is sensed and the position is maintained by the interaction of the current in a coil on the float with the field of a permanent magnet. This current, and the temperature which is used to compensate for temperature dependence in the magnet, are combined to give a density. This instrument was factory calibrated. The factory calibration was used in the analysis of the density data.

DENSIMETER PERFORMANCE

Results of the density comparison measurements are shown in Figures 3 through 10. Five of the six fillings were pure methane and the sixth was an LNG-like mixture containing about 88-1/2% CH_4, 6-1/2% C_2H_6, 3% C_3H_8 and 2% nC_4H_{10}. Nitrogen was eventually added to two of the methane fillings and to the mixture filling as shown in table I.

The data presented in Figures 3 through 10 for the various densimeters is the percent difference between the density indicated by the densimeter under test and that measured by the DRS densimeter. The temperature range of the measurements was 108 to 130 K. In Figures 3, 5, 7 and 9
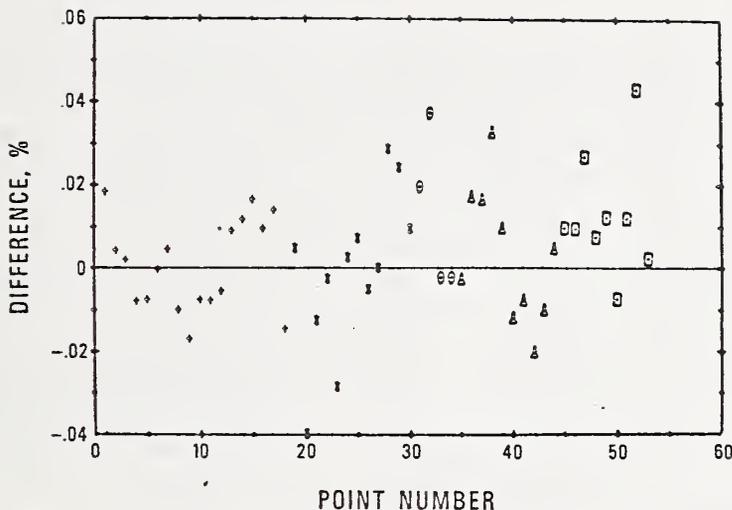
386

Figure 2. Haynes-Hiza densities compared to DRS densimeter for methane.

this density difference is shown for the methane fillings only and as a function of the order in which the data were acquired. The different symbols are for the different fillings.

Figures 4, 6, 8 and 10 show the density differences as a function of the density measured by the DRS densimeter. The different symbols are for the different compositions shown in table I.

Table I.

		Graph Symbol
1.	Methane	+
2.	Methane	+
	Methane + 1% nitrogen	θ
3.	Methane	+
4.	Methane	+
	Methane + 2% nitrogen	Δ
5.	Mixture	□
	Mixture + 2% nitrogen	Δ
6.	Methane	+

The results of the densimeter tests are reported in more detail in Reference 2.

Vibrating Cylinder Densimeter

In Figure 3 the percent density differences for pure methane, shown as a function of the order of the data acquisition, show a run-to-run shift of about ± 0.1%. The calibration of the densimeter was derived from these data. In Figure 4, the percent density differences for all the data are shown as a function of density. The density differences decrease slightly as the density increases for both the LNG densities and methane densities. The slope can be removed either by adding a temperature-dependent term or a 1/f-dependent term to Eq. (1). This instrument has sufficient precision to measure densities to within ± 0.1% with a proper calibration.

Vibrating Plate Densimeter

In Figure 5, the percent density differences for methane as a function of the data acquisition show filling-to-filling shifts of the order of ± 0.1%. The calibration of the densimeter was derived from these data.

The manufacturer's calibration was done at room temperature in heavy fluids and showed a 1.6% bias with measurements at cryogenic temperatures for these measurements. In Figure 6, the percent density differences as a function of the density are shown for all the data. Addition of nitrogen to the methane fillings produced a detectable offset in the densimeter reading. This densimeter has sufficient precision to measure density of these fluids to within ± 0.1% with the proper calibration.

Capacitance Densimeter

In Figure 7, the percent density differences for methane as a function of the order of data acquisition for the capacitance densimeter show filling-to-filling offsets of about ± 0.1%. The calibration supplied by the manufacturer was used for the data analysis and the disagreement between this densimeter and the DRS densimeter is 1% for methane.

The percent density differences as a function of the density are shown in Figure 8. The shift of the density reading with composition ranges from -2.4% for the LNG containing 2% N_2 filling to 1% for the pure methane fillings. These shifts are in reasonable agreement with the shifts calculated by Giarratano and Collier.[7] The density dependence of the density differences can presumably be removed by adjusting the calibration equation. These results indicate that the composition must be known to obtain the full precision of this densimeter.

387

Displacement Densimeter

In figure 9, the percent density differences for methane as a function of the order of data acquisition are shown for the displacement densimeter. For the analyses, the factory calibration was used. Data for the first, third and fourth methane fillings show no apparent shift in calibration. The calibration was adjusted for the fifth filling. The downward shift of the calibration in the second filling was accompanied by noise in the density readings. The DRS densimeter readings were also more noisy, though they showed no apparent calibration shift. The reason for the additional noise and calibration shift for the displacement densimeter is unknown. The factory calibration gave a density usually about 0.05% lower than the DRS densimeter reading.

The density differences as a function of density are shown in Figure 10 for all the data. The data below -0.08% are the data for the second CH_4 filling and the data for the subsequent addition of N_2. Even then, all the data are within the manufacturer's specified accuracy of $\pm$ 0.2%.

CONCLUSIONS

All the densimeters tested are sufficiently precise to use in LNG density measurements; although a composition input is required to get the best results from a capacitance densimeter. This work has not established the stability and reliability of these instruments over a long period of use in the field, but that could best be established by periodic review of densimeter performance in field use.

The most serious problem found is the lack of suitable calibration for low-temperature use. Only one densimeter was accurate to within the manufacturer's specified uncertainty and that instrument apparently could be used to a higher degree of accuracy with a better calibration.

The factory calibration and stability checks of these instruments might best be done by comparison measurements to a transfer standard or portable standard. Development of such standards will be the next phase in the continuation of this work.

REFERENCES

1. Siegwarth, J. D., Younglove, B. A. and LaBrecque, J. F., "Cryogenic Fluids Density Reference System: Provisional Accuracy Statement," NBS Tech. Note 698, (Oct. 1977).

2. Siegwarth, J. D., Younglove, B. A. and LaBrecque, J. F., "An Evaluation of Commercial Densimeters for Use in LNG," NBS Tech. Note 697 (Oct. 1977).

3. Bowman, H. A., Schoonover, R. M. and Jones, M. V., "Procedure for High Precision Density Determinations by Hydrostatic Weighing," J. Res., NBS C, 71C, 178 (1967).

4. Henins, I. and Bearden, J. A., "Silicon Crystal Determination of the Absolute Scale of X-Ray Wavelengths," Phys. Rev. 135, A890 (1964).

5. Goodwin, R. D., "The Thermophysical Properties of Methane, from 90 to 500 K at Pressures to 700 Bar," NBS Tech. Note 653 (Apr. 1974).

6. Haynes, W. M. and Hiza, M. J., "Measurements of Orthobaric Liquid Densities of Methane, Ethane, Propoane, Isobutane and Normal Butane," J. Chem. Thermodynamics 9, 179 (1977).

7. Giarratano, P. J. and Collier, R. S., "Evaluation of Capacitance Densitometry by Examination of the Relationships between Density, Dielectric Constant, Pressure and Temperature for LNG Mixtures," I and EC Process, Design and Development 16, 330 (July 1977).
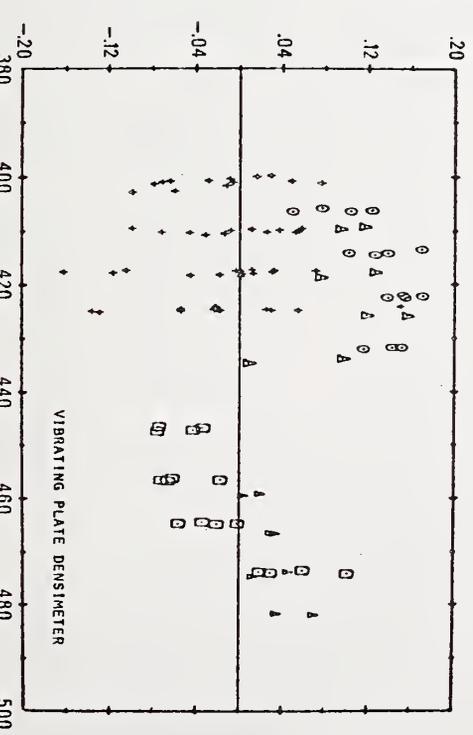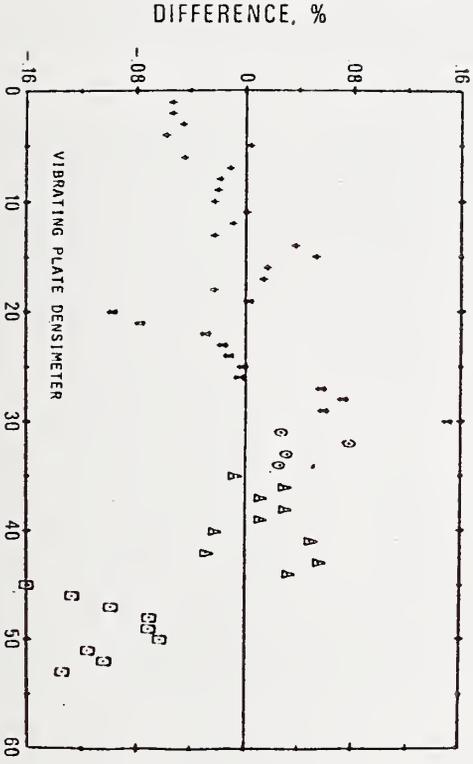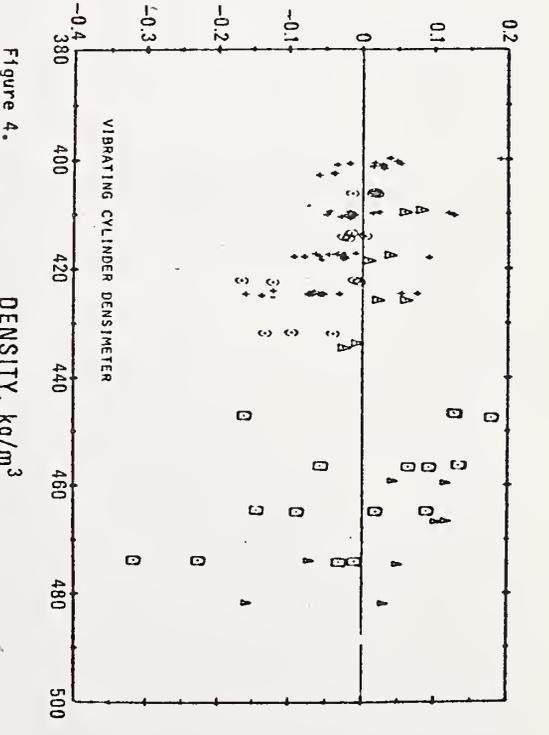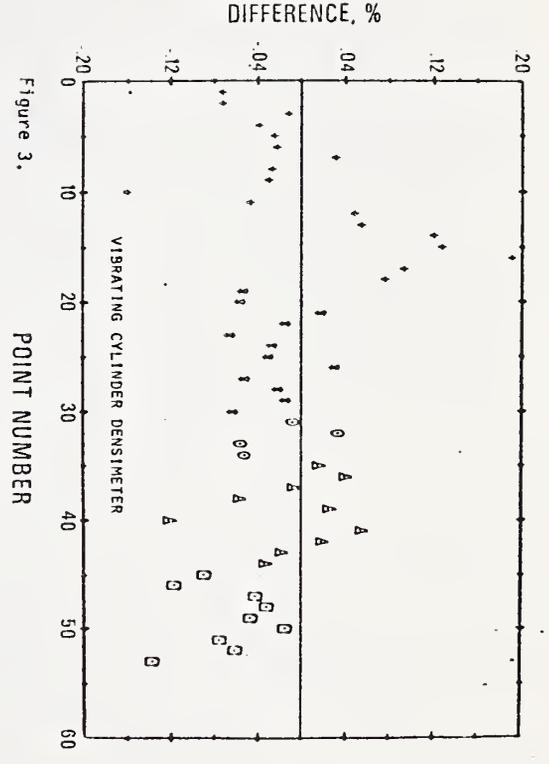
Figure 3. VIBRATING CYLINDER DENSIMETER
DIFFERENCE, % vs POINT NUMBER

Figure 4. VIBRATING CYLINDER DENSIMETER
DENSITY, kg/m³

Figure 5. VIBRATING PLATE DENSIMETER
DIFFERENCE, % vs POINT NUMBER

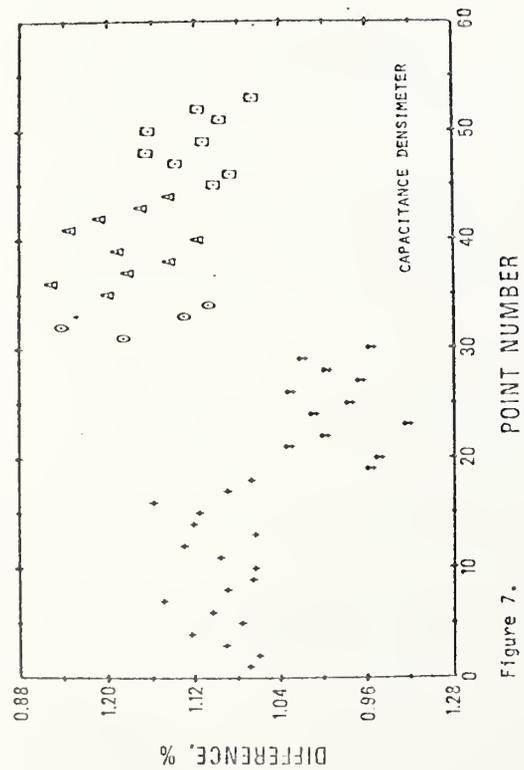Figure 6. VIBRATING PLATE DENSIMETER
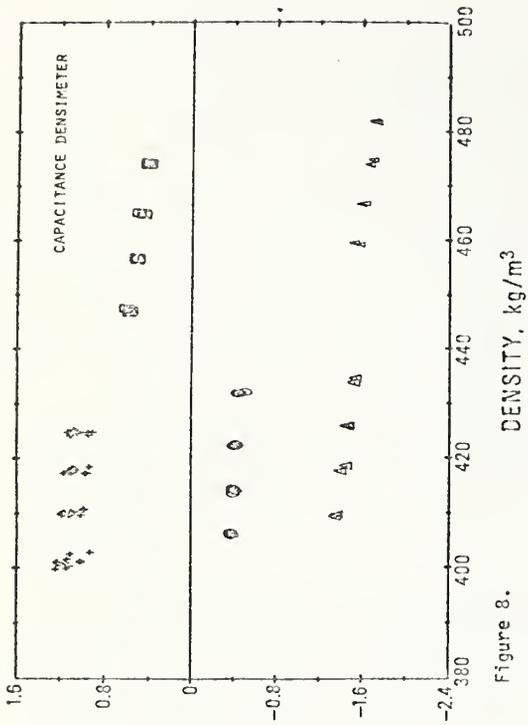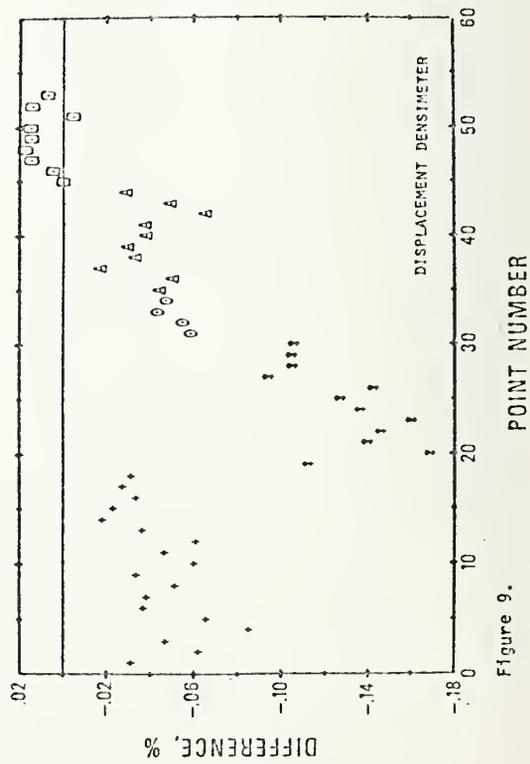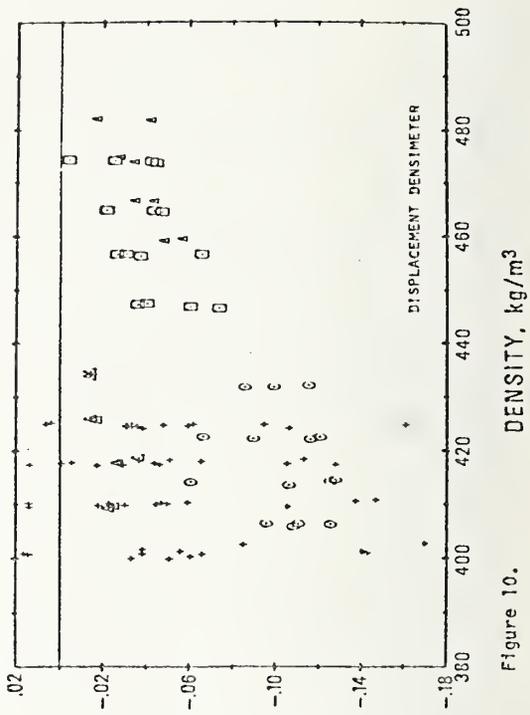DENSITY, kg/m³

Figure 7.

Figure 8.

Figure 9.

Figure 10.

390   F-6

Better LNG flow measurement sought

J. A. BRENNAN
National Bureau of Standards
Boulder, Colo.

WORK on improving LNG flow measurement is being done under the sponsorship of the Pipeline Research Committee of the American Gas Association. This includes development of a method of testing flowmeters for use in large-diameter LNG pipelines and on densitometers for use in conjunction with volumetric flowmeters to give mass-flow information.

Answers to two basic questions are being sought. One is whether water calibrations can be used to predict flowmeter performance in LNG service. The second is whether flowmeter performance in LNG measurement can be determined in facilities where LNG is totally vaporized and comparisons then made between the liquid and gas-flow measurements.

Affirmative answers to both questions would be indicated by computing an LNG meter factor based on a water calibration and then demonstrating good agreement between LNG flow measurements and the vaporized gas-flow measurements.

Based on the data obtained thus far,

it appears possible to answer the two basic questions affirmatively, provided uncertainties of about ±2% are tolerable. As more data are obtained on both liquid and gas-phase measurements, it may be possible to reduce the uncertainty. LNG flow measurement has the potential of being a much easier measurement to make than measurements with orifice flowmeters in the gas phase. This is possible since:
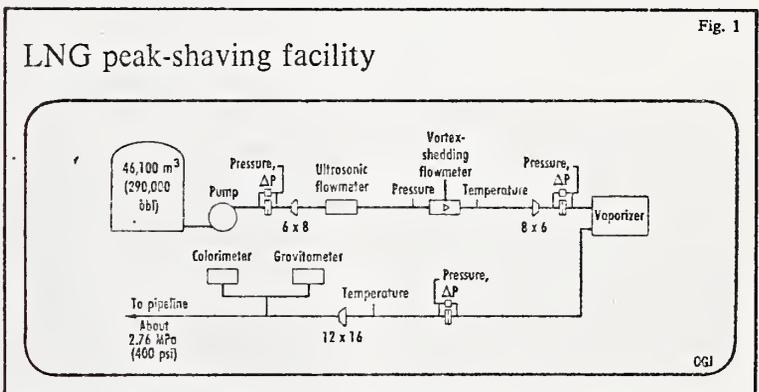
1. One liquid flowmeter has about three times the flow range of an orifice flowmeter.

2. Gas measurements are quite sensitive to pressure and temperature which can fluctuate broadly—18.9%/MPa (145 psi), and 0.18%/°C., respectively.

3. Liquid measurements are sensitive to temperature, but the temperature remains almost constant (0.35%/°C.).
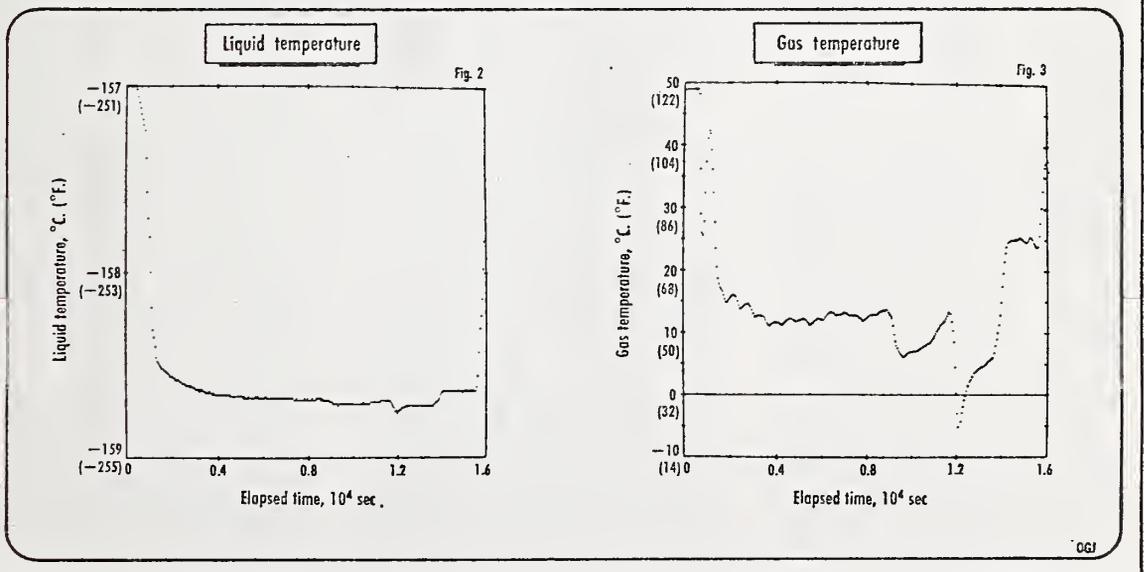
4. Liquid measurements are insensitive to pressure fluctuations—0.29%/MPa (145 psi).

Of course, good densitometers could eliminate the last three problems. There appears to be progress in these areas. The main problem remains in the proving of large LNG flowmeters. The work being done is a good start, but a much broader base is needed to
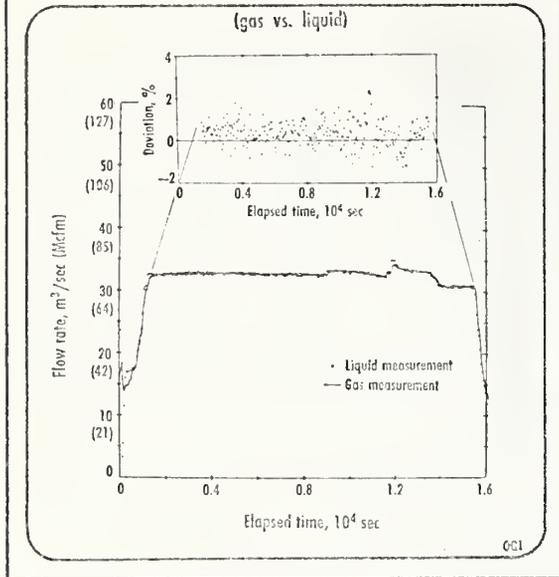

LNG peak-shaving facility

Fig. 1

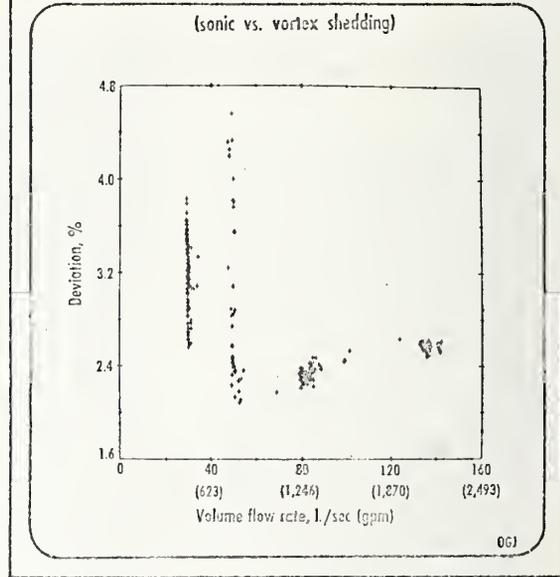
Temperature change vs. time

Figs. 2 and 3

Liquid temperature — Fig. 2

Gas temperature — Fig. 3

Flow-rate comparison Fig. 4

(gas vs. liquid)

Meter comparison Fig. 5

(sonic vs. vortex shedding)

predict meter performance with confidence.

Problems. There are two main problem areas associated with flow measurement of LNG. The first one is the lack of accurate calibration facilities—especially for large-diameter flowmeters. Presently, only two accurate cryogenic flow facilities are operating in the U.S. One is at the National Bureau of Standards (NBS). The other is at the Linde Div. of Union Carbide.[1][2]

Both facilities normally use liquid nitrogen as the test fluid, although other liquids are possible. There is also an LNG flow facility at NBS, but this facility is not of the same quality as the nitrogen facility and cannot be used for high-accuracy calibration work. All three facilities are limited to maximum flow rates of 13 or 19 l./sec (200 or 300 gpm).

The second major problem is the lack of information on surrogate fluid calibrations for the flowmeters presently being used in LNG. If it could be shown that accurate correction factors could be applied to meter factors determined from a water calibration to give the meter factor in LNG, then the need for large LNG flow facilities would not exist.

Unfortunately, there has not been enough work done in this area to establish the validity of such a procedure. This area is being investigated as part of the work described in this article.

Test procedure. To circumvent the lack of LNG flowmeter test facilities, an alternative procedure was established based on NBS's liquid-nitrogen flow facility at Boulder, Colo., and the water facility at Gaithersburg, Md.

Starting with small (2 and 4-in.) flowmeters that could be tested on both facilities, a relationship was determined for the change in meter factor from water to liquid nitrogen. The 4-in. flowmeter was then installed in an LNG peak-shaving facility where its measurements were compared with measurements made on the vaporized gas using conventional orifice flowmeters.

The flowmeter selected was a vortex-shedding type. The selection was based on an extensive flowmeter-evaluation program conducted at NBS, cosponsored by NBS and the Compressed Gas Association. Other flowmeters could have been selected. But, based on information available at the time on both flowmeter performance and potential problems associated with the measurement of LNG, the vortex-shedding flowmeter was selected as the one offering a good potential for success and a reasonable potential for scaling to large sizes.

Test installation. Little data were obtained on LNG with the 4-in. flowmeter because of the demand schedule on the peak-shaving facility. Very little control could be exercised over the test parameters since the facility had to operate on demand and at flow rates and time intervals specified by the need for gas at the time. This flow-

meter was half the size of the facility piping and could not be left installed during the high-demand portion of the sendout season.

The data obtained did not indicate any major difficulties with the procedures, however, so the 4-in. flowmeter was replaced with an 8-in. meter. This larger meter was the same size as the facility piping. Therefore, it did not restrict the sendout capacity and could be left installed throughout the season.

The size increase was a logical step to test the adequacy of the overall test procedure, also. It was also an important step since no cryogenic calibration was possible on the larger flowmeter—only a water calibration preceded the LNG testing.

Fig. 1 shows the layout of the LNG peak-shaving facility where the flowmeter testing was performed. This facility is owned by a private company which was testing a sonic flowmeter in the same LNG line.

As part of this program, data from both flowmeters were recorded simultaneously on magnetic tape. The temperature and pressure of the LNG were also recorded for calculating density.

During the first year of testing, some unexplained shifts occurred from one test to another.[3] No explanation for these shifts could be found so additional instrumentation was added to the gas-phase measurements to permit recording the flow data on magnetic tape.

Both liquid and gas measurements were then returned to NBS for analysis. Before the addition of the recordings on the gas phase, the information was manually read from facility circular-chart recordings.

Flow-rate computations. Liquid flow rates were computed from these equations:

$$Q_L = f/k \qquad (1)$$

$$Q_{GL} = Q_L \rho_L / \rho_G \qquad (2)$$

where:

Q_L = liquid flow rate, l./sec
f = flowmeter output, pulses/sec
k = meter factor computed from water calibration, pulses/l.
Q_{GL} = equivalent gas-flow rate, m³/sec
ρ_L = LNG density, kg/l.
ρ_G = vaporized gas density, kg/m³

LNG densities were calculated from the composition determined by gas analysis from a sample taken of the vaporized LNG using a computer program developed by McCarty.[4] Gas densities were calculated according to American Gas Association (AGA) recommended practices.[5]

Other than gas density, there are three critical parameters in these calculations: (1) meter factor, (2) gas composition, and (3) liquid temperature at the flowmeter. Pressure of the liquid at the flowmeter is of secondary importance. The meter factor was to be verified in this work.

Composition obviously depends on obtaining a representative sample and then analyzing it accurately. The subject of sampling, beyond the scope of this article, is an important consideration. A check on the composition determination was obtained by calculating the heating value and specific gravity of the gas from the analysis and comparing the result with the measured values from a calorimeter and gravitometer.

Both instruments require a representative sample. But, since the samples were continuous, taken from a different location, and used a different technique, any errors involved were probably different from those associated with the sample taken for the gas analysis. Since the two heating-value determinations agreed within the accuracy of the instrumentation, it was concluded that no large sampling errors were present.

Liquid densities are a strong function of temperature—about 0.35%/K. (or °C.)—but fortunately temperature is quite steady throughout a test. Fig. 2 shows the variation in liquid temperature over a 4-hr test interval. Other tests for longer periods and a large variation in flow rates had similar temperature traces.

Errors from this source can be made small by good installation and calibration techniques. To show more detail in Fig. 2, the start-up and shutdown were cut off at 116° K. (−251° F.).

Gas-flow rates were calculated according to Equation 3:[5]

$$Q_G = F_b F_r Y F_{pb} F_{tb} F_{tf} F_g F_{pv} F_m F_a F_e$$
$$(h_w \, p_f)^{\frac{1}{2}} \qquad (3)$$

where:

Q_G = orifice gas-flow rate
F_b = basic orifice factor
F_r = Reynolds number factor
Y = expansion factor
F_{pb} = pressure/base factor
F_{tb} = temperature-base factor
F_{tf} = flowing temperature factor
F_g = specific gravity factor
F_{pv} = supercompressibility factor
F_m = manometer factor
F_a = orifice thermal expansion factor
F_e = gauge-location factor
h_w = differential pressure
P_f = absolute static pressure

In Equation 3, several parameters are constant for a particular installation. Pressure and temperature parameters are not constant, however, and the calculation is quite sensitive to changes in them.

Fig. 3 shows the gas-temperature fluctuation during the same test as that in Fig. 1. This is a relatively steady temperature profile, too. When flow conditions were changing, the gas temperature would fluctuate over even wider ranges and on short time intervals.

The possibility for errors in calculating results from widely varying parameters is obviously increased and

The author . . .

James A. Brennan has been associated with the Cryogenics Division of the National Bureau of Standards for about 20 years. He currently is working on projects investigating instrumentation for use in measuring the heating value of LNG flowing in a pipeline and the use of transfer standards in the custody transfer of cryogenic liquids. Both projects involve measurements of flow, density, temperature, and pressure. Brennan's experience includes flow of cryogenic liquids into a vacuum, pipeline cool-down problems, and bearings for low-temperature applications. He is the author or coauthor of over 20 publications on cryogenic subjects, and holds a BS degree in mechanical engineering (1958) from the University of Colorado.

James A. Brennan

can be significant since a 1° C. error results in an 0.18% error in flow rate. Similar problems can exist with gas-pressure fluctuations where errors of 18.9%/MPa (145 psi) result from errors in pressure measurement.

During start-up, a high-temperature spike occurred. It has been deleted from Fig. 3 so the remainder of the test can be seen in more detail.

Fig. 4 compares flow rates determined with the 8-in. vortex-shedding flowmeter in LNG with a 9-in. orifice meter in a 16-in. pipe in vaporized gas. During this flow test, flow rate was relatively constant throughout the run. The comparison is within the measurement uncertainty of the two flow measurements except during start-up, shutdown, and the rate change just before 12,000 sec elapsed time.

Disagreement during changing flow rates is not considered serious since there effectively is a variable-capacity capacitance in the gas-phase portion of the system. During this test, only one orifice flowmeter was required.

Gas temperature and pressure were relatively steady. Therefore, the conditions for good comparisons were favorable.

During later tests, up to three orifice runs were required, and wide fluctuations occurred in gas temperature and pressure. Since the data analysis on the later tests is not yet complete, no definite statements are possible. But from a preliminary analysis, the comparison still looks to be within the experimental uncertainty.

At high flow rates, it appears the liquid measurements were consistently higher than the gas measurements. Possible explanations for this trend must await final data analysis. The deviation shown in Fig. 4 was calculated from Equation 4:

$$\text{Deviation (\%)} = (Q_{GL} - Q_G) \times 100/Q_G \qquad (4)$$

Fig. 5 shows a comparison of the two liquid flowmeters. The deviation shown is that of the sonic flowmeter from the vortex-shedding flowmeter. It was calculated from the equation,

$$\text{Deviation (\%)} = (Q_s - Q_{vs}) \times 100/Q_{vs} \qquad (5)$$

where:

Q_s = flow rate indicated by sonic flowmeter
Q_{vs} = flow rate indicated by vortex flowmeter

At flow rates above about 50 l./s (790 gpm), deviation between the two

flowmeters is nearly constant. At lower flow rates, the sonic flowmeter became erratic. The fact that the sonic flowmeter exhibited a positive deviation means that it indicates an even larger discrepancy when compared with the gas-flow measurements.

Since the sonic flowmeter was not originally part of this program, no history had been documented. So far as is known, no prior cryogenic flow data were obtained, and the meter factor was calculated by the manufacturer from dimensional and fluid-properties data. As more data are obtained, these calculations can obviously be refined.

Densitometers. An obvious improvement to this measurement method would be addition of a direct-reading densitometer. Several promising instruments are available. One has been used in flowing liquid nitrogen with encouraging results.[6] T h e densitometer was a vibrating-plate type.

Recently, that type, along with a vibrating-cylinder and a capacitance type, have been tested in nonflowing liquid methane and LNG-type mixtures. Both vibration types of densitometers have demonstrated ability to indicate densities to within about 1/4%.[7]

The capacitance densitometer also shows promise, provided the range of composition is known and does not fluctuate too much. All three types are suitable for in-line use in flowing streams, although the effect of fluid velocity is not well documented.

References

1. Close, D. L., "Cryogenic Flowmeters —Today," Cryogenics and Industrial Gases, Vol. 4, August 1969, pp. 19-23.

2. Dean, J. W., Brennan, J. A., and Mann, D. B., "Cryogenic Flow Research Facility of the National Bureau of Standards," Advances in Cryogenic Engineering, Vol. 14, 1968, pp. 299-305.

3. Brennan, J. A., LaBrecque, J. F., and Kneebone, C. H., "Progress Report on Cryogenic Flowmetering at the National Bureau of Standards," Instrumentation in the Cryogenic Industry, Vol. 1. Proceedings of the First Biennial Symposium on Cryogenic Instrumentation, 31st ISA Conference & Exhibit, Houston, Oct. 11-14, 1976.

4. McCarty, R. D., "A Comparison of Mathematical Models for the Prediction of LNG Densities," National Bureau of Standards Interagency Report 77-867, 1977.

5. Orifice Metering of Natural Gas Measurement Committee Report No. 3, American Gas Association, 1515 Wilson Blvd., Arlington, Va., 1969 Revision, 95 pp.

6. Brennan, J. A., Stokes, R. W., Kneebone, C. H., and Mann, D. B., "NBS-CGA Cryogenic Flow Measurement Program," ISA Transactions, Vol. 14, No. 3, 1975, pp. 237-247

7. Siegwarth, J. D., Younglove, B. A., and LaBrecque. J. F., "An Evaluation of Cryogenic Densimeters for Use in LNG," National Bureau of Standards Technical Note 697, July 1977.

NBS-114A (REV. 7-73)

U.S. DEPT. OF COMM. BIBLIOGRAPHIC DATA SHEET	1. PUBLICATION OR REPORT NO. NBSIR 78-894	2. Gov't Accession No.	3. Recipient's Accession No.
4. TITLE AND SUBTITLE LIQUEFIED NATURAL GAS RESEARCH AT THE NATIONAL BUREAU OF STANDARDS			5. Publication Date September 1978
			6. Performing Organization Code 736
7. AUTHOR(S) D. E. Diller, Editor			8. Performing Organ. Report No.
9. PERFORMING ORGANIZATION NAME AND ADDRESS NATIONAL BUREAU OF STANDARDS DEPARTMENT OF COMMERCE WASHINGTON, D.C. 20234			10. Project/Task/Work Unit No. 7360104
			11. Contract/Grant No.
12. Sponsoring Organization Name and Complete Address (Street, City, State, ZIP) See block 16 below.			13. Type of Report & Period Covered Semi-Annual Jan 1 – June 30, 1978
			14. Sponsoring Agency Code

15. SUPPLEMENTARY NOTES

16. ABSTRACT (A 200-word or less factual summary of most significant information. If document includes a significant bibliography or literature survey, mention it here.)

Thirty-one cost centers, supported by six other-agency sponsors in addition to NBS, provide the basis for liquefied natural gas (LNG) research at NBS. During this six-month reporting period the level of effort was over 20 man-years/year with funding expenditures of over $500,000. This integrated progress report, to be issued in January and July, is designed to:

1) provide all sponsoring agencies with a semi-annual report on the activities of their individual programs;

2) inform all sponsoring agencies on related research being conducted at the Thermophysical Properties Division;

3) provide a uniform reporting procedure which should maintain and improve communication while minimizing the time, effort and paperwork at the cost center level.

The contents of this report will augment the quarterly progress meetings of some sponsors, but will not necessarily replace such meetings. Distribution of this document is limited and intended primarily for the supporting agencies. Data or other information must be considered preliminary, subject to change and unpublished, and therefore not for citation in the open literature.

17. KEY WORDS (six to twelve entries; alphabetical order; capitalize only the first letter of the first key word unless a proper name; separated by semicolons)

Cryogenics; liquefied natural gas; measurement; methane; properties; research.

18. AVAILABILITY	☐ Unlimited	19. SECURITY CLASS (THIS REPORT) UNCLASSIFIED	21. NO. OF PAGES
☒ For Official Distribution. Do Not Release to NTIS			
☐ Order From Sup. of Doc., U.S. Government Printing Office Washington, D.C. 20402, SD Cat. No. C13		20. SECURITY CLASS (THIS PAGE)	22. Price
☐ Order From National Technical Information Service (NTIS) Springfield, Virginia 22151		UNCLASSIFIED	